Results in Engineering 26 (2025) 105257

Contents lists available at ScienceDirect

Results in Engineering

journal homepage: www.sciencedirect.com/journal/results-in-engineering

Review article

Advancements in corrosion studies and protective measures for copper and copper-based alloys in varied environmental conditions

Okpo O. Ekerenam [a,n,*], Alexander I. Ikeuba [b,n,q,*], Chigoziri N. Njoku [c,n,o], Demian I. Njoku [d,n,o], Wilfred Emori [e,n,*], Izuchukwu K. Nwokolo [n,q], Ini-Ibehe N. Etim [f,n,o,r], Bright O. Okonkwo [g,n], Inime I. Udoh [h,n,*], Enobong F. Daniel [i,n], Paul C. Uzoma [j,n,p], Bukola O. Awonusi [n], Sharafadeen K. Kolawole [k,n], Iniobong P. Etim [l,n], Olajire S. Olanrele [m,n]

[a] *Department of Biochemistry, School of Pure & Applied Sciences, Federal University of Technology, Ikot Abasi, P. M. B 1055, Uyo, Nigeria*
[b] *Department of Mechanical & Aerospace Engineering, Benjamin M. Statler College of Engineering & Mineral Resources, West Virginia University, Morgantown, WV 26506-6106, USA*
[c] *Environmental, Composite and Optimization Research Group, Department of Chemical Engineering, Federal University of Technology, PMB 1526 Owerri, Nigeria*
[d] *Department of Applied Science, School of Science and Technology, Hong Kong Metropolitan University, Hong Kong, SAR, China*
[e] *School of Materials Science and Engineering, Sichuan University of Science and Engineering, Zigong 643000, Sichuan, PR China*
[f] *Marine Chemistry and Corrosion Research Group, Department of Marine Science, Akwa Ibom State University, P. M. B. 1167, Uyo, Nigeria*
[g] *Institute of Corrosion Science and Technology, Guangzhou 510530, PR China*
[h] *School of Environmental and Chemical Engineering, Shenyang Ligong University, Shenyang 110159, PR China*
[i] *Shenyang National Laboratory for Materials Science, Institute of Metal Research, Chinese Academy of Sciences, Shenyang 110016, China*
[j] *ZJU-UIUC Institute, International Campus, Zhejiang University, Haining 314400, China*
[k] *Mechanical Engineering Department, School of Engineering and Technology, Federal Polytechnic, P.M.B 420 Offa, Nigeria*
[l] *Department of Physics, Faculty of Physical Sciences, University of Calabar, Calabar, Nigeria*
[m] *Department of Chemical Sciences, Mountain Top University, Ibafo, Ogun, Nigeria*
[n] *Nigerian Alumni Association of the Institute of Metal Research, Chinese Academy of Sciences (NAAIMCAS), Nigeria*
[o] *Africa Center of Excellence in Future Energies and Electrochemical Systems (ACEFUELS), Federal University of Technology, P.M.B. 1526, Owerri, Nigeria*
[p] *Department of Polymer and Textile Engineering, Federal University of Technology, P.M.B. 1526, Owerri, Nigeria*
[q] *Materials Chemistry Research Group, Department of Pure and Industrial Chemistry, University of Calabar, Calabar, Nigeria*
[r] *Key Laboratory of Advanced Marine Materials, Key Laboratory of Marine Environmental Corrosion and Bio-fouling, Institute of Oceanology, Chinese Academy of Sciences, Qingdao, 266071, PR China*

ARTICLE INFO

Keywords:
Copper alloys
materials degradation
failure analysis
stress corrosion cracking
microstructure
grain boundary
corrosion protection
surface modification

ABSTRACT

The continued utilization of copper and copper-based alloys is significantly threatened by various forms of corrosion that result from exposure to corrosive environments. Corrosion of copper and copper-based alloys such as brass, bronze, and cupronickel occurs when these materials are subjected to different environmental conditions, including moisture, pollutants, acids, and other reactive agents. Although copper and its alloys possess good natural resistance brought on by the development of a protective oxide layer, exposure to aggressive conditions, such as chlorides, pollutants, and mechanical stresses, can lead to corrosion problems. The development of surface films and the processes by which copper-based alloys corrode are covered in this thorough review. The main elements that affect how copper and copper-based alloys corrode are also highlighted. A significant focus of this review is on mitigation strategies to increase the lifespan of copper and copper-based alloys. Several methods have been summarized, with particular emphasis on the utilization of inhibitors and anticorrosion coatings. The use of inhibitors and anticorrosive coatings, including organic compounds, plant extracts, and polymers, has proven effective in enhancing copper and copper-based alloys resistance to corrosion, with inhibition efficiencies ranging from 80% to 95%. For example, an extract from *Pyracantha fortuneana* in 0.5 M H_2SO_4 achieved an inhibition effectiveness of 95% at an inhibitor concentration of 600 mg/L. The insights obtained from this review will inform future research initiatives and the application of copper and copper-based alloys across a variety of industries. The primary objective will be to develop copper alloys that possess self-

---

* Corresponding authors.

E-mail addresses: oekerenam@gmail.com (O.O. Ekerenam), ikeubaalexander@unical.edu.ng (A.I. Ikeuba), wemori@suse.edu.cn (W. Emori), inudoh@kt.dtu.dk (I.I. Udoh).

https://doi.org/10.1016/j.rineng.2025.105257
Received 14 February 2025; Received in revised form 30 April 2025; Accepted 7 May 2025

healing capabilities, as well as self-healing anticorrosion materials. Such advancements have the potential to represent a significant leap forward for critical applications in the aerospace, power plants and marine sectors, in addition to other high-temperature environments.

1. Introduction

Copper (Cu) and copper-based alloys are one of the significant categories of commercial metals. Among their many qualities are their exceptional corrosion resistance, superior strength and fatigue resistance, excellent electrical and thermal conductivity, and attractive look [1]. In the upcoming years, the global copper market is anticipated to rise significantly due to the growing need for creative and sustainable products as well as the increased acceptance of technology [2]. This demand is expected to be driven by the growth of renewable energy in addition to sectors such as electrical, electronic, construction, automobiles, power, marine, and oil and gas where copper and copper-based alloys are already highly utilized. These materials are utilized in the manufacture of solar panels and wind turbines as well as notable applications including surgical equipment and biological implants, heat exchanger tubes in flash systems in desalination plants, pipe systems in offshore platforms, and ships and power plants, and so on. The numerous important causes, such as growing consumer demand, technological developments, and changing customer preferences, are expected to drive the rising demand.

The widespread application of copper and copper-based alloys to fabricate structures and components commonly use in various sectors is as the result of their good machinability, increased electrical and thermal conductivities, antimicrobial and antibacterial activities, and biofouling resistance [3–7]. copper and copper-based alloys when exposed to aggressive environmental conditions are known to possess good resistance to corrosion because a protective corrosion product layer forms, which decreases ion diffusion and corrosion rates [8]. The protective layer of corrosion product developed on this materials after exposure to corrosive environment has been established to be a duplex layer consisting of a cupric hydroxyl chloride ($Cu_2(OH)_3Cl$) outer layer, covering a cuprous oxide (Cu_2O) inner layer that is compact, with the alloying elements added, the corrosion resistance is increased by filling cation vacancies [9–11]. Additionally, for copper and copper-based alloys exposed to atmosphere, the common term used to describe the mechanisms governing the development and expansion of corrosion products is "patina evolution" [12]. This development establishes the material's corrosion performance and surface appearance and is dependent on the current climate, environmental factors, and pollutant levels. The spontaneous formation of the surface film copper and copper-based alloys when exposed to corrosive environment is the first line of defense.

To enhance specific properties of metals such as Cu, alloying elements are frequently added in small amounts. Cu is alloyed to change color or gain or lose strength, hardness, electrical and thermal conductivity as well resistance corrosion. The resistance to corrosion of Copper-based alloys is found to be improved by the addition of alloying elements like Ni and Fe [13,14]. Copper-based alloys contain 1 – 2 % Fe which improve erosion and corrosion resistance (e.g., Cu-l0% Ni-2% Fe), UNS C70600 and Cu-30% Ni-30%- 1%Fe, UNS C7150011 [15,16]. In addition to copper-nickels, several alloys of Cu have been produced for various applications by incorporating of one or more alloying elements such as Zn (Brass), Zn and Pb (Leaded brass), Zn. Sn and Pb (Tin brasses), Cu, Al, Ni, Fe, Si and Sn (Aluminium bronzes), Cu, Si and Sn (Silicon bronzes), Cu, Zn, Mn, Fe and Pb (Manganese bronzes) and so on.

However, copper and copper-based alloys suffer premature failure due to corrosion which may be due to (1) material characteristics, including contaminants, grain boundary flaws, microstructure inhomogeneity, and alloying element segregation [17,18], and (2) environmental factors, such as water contamination from hydrogen sulfide ions [19], increased or disrupted flows [20,21]. Corrosion is a broad term for a deterioration process that metallic materials undergo when exposed to specific environmental factors [22]. This process involves chemical reactions that have the potential to drastically change the characteristics of the metallic material. The corrosion process electrochemically oxidizes metallic objects to produce ions, oxides, or other chemicals [23]. Corrosion can happen in a variety of environments and fluids, including acidic, alkaline, and aqueous solutions. Certain ions that are corrosive, such as halide ions and different ions that contain sulfur can also lessen the corrosion resistance of a material [24]. In general, corrosion shortens the material's service life and lowers its performance [25]. Corrosion causes significant losses in industries when it comes to the replacement and repair of various equipment and facilities. Corrosion costs are estimated to be approximately 3.5% of the GDP of wealthy countries [26]. Corrosion is therefore acknowledged as a significant issue that either directly or indirectly results in enormous financial losses [27].

There are several forms of corrosion of copper and copper-based alloys. One of the first known instances of corrosion of copper and copper-based alloys is stress corrosion cracking [1]. Atmospheric corrosion of copper and copper-based alloys used in architectural and artistic works is well documented [12]. It is also intimately linked to the visually attractive greenish patinas that are created after prolonged atmospheric exposure. The wealth of ancient artifacts made of copper offers an archive of stability overtime that helps confirm corrosion models for the long-term storage of radioactive waste. General, galvanic, and erosion-corrosion of copper and copper-based alloys are well documented.

To fully comprehend the corrosion of these alloys in aggressive environment and the implications of various factors (material and environmental) on the corrosion of copper and copper-based alloys in different environments, an assessment of existing literature becomes a necessity. In this in-depth review, the corrosion, factors influencing corrosion and mitigation strategies to elongate the service life of copper-based alloys are discussed. This review seeks to highlight how each factor influences the corrosion of copper-based alloys and the best mitigation approaches that can improve the performance and elongate the service life of the alloys. This comprehensive review will be of immersed benefit to beginners and seasoned researchers in related fields.

1.1. *Copper and copper-based alloys performance*

The unique capabilities of copper and copper-based alloys in comparison to other corrosion-resistant alloys can be partially explained by the Pourbaix diagram for the Cu-H_2O system at 25°C as shown in Fig. 1a. From the diagram, there exists a stable water domain between two dashed lines, a and b. It is evident that there is some overlap between the water's stability domain and the immunity domain of copper. It is obvious from this that copper will not corrode in water without oxygen. When some metals are exposed to a de-aerated atmosphere, corrosion occurs. Metal dissolution occurs in the anodic reaction, whereas the cathodic reaction involves the electrolyte evolving hydrogen gas. Nonetheless, the corrosion domains show that Cu is more prone to corrosion in the presence of oxygen. In particular, the reduction of oxygen to generate hydroxide ions is the main cathodic mechanism for Cu corrosion in aqueous systems. The numbers in the diagram that are circled show the existence of a chemical reaction and the activity of dissolved species, at which other numbers are used to represent the lines that were calculated.

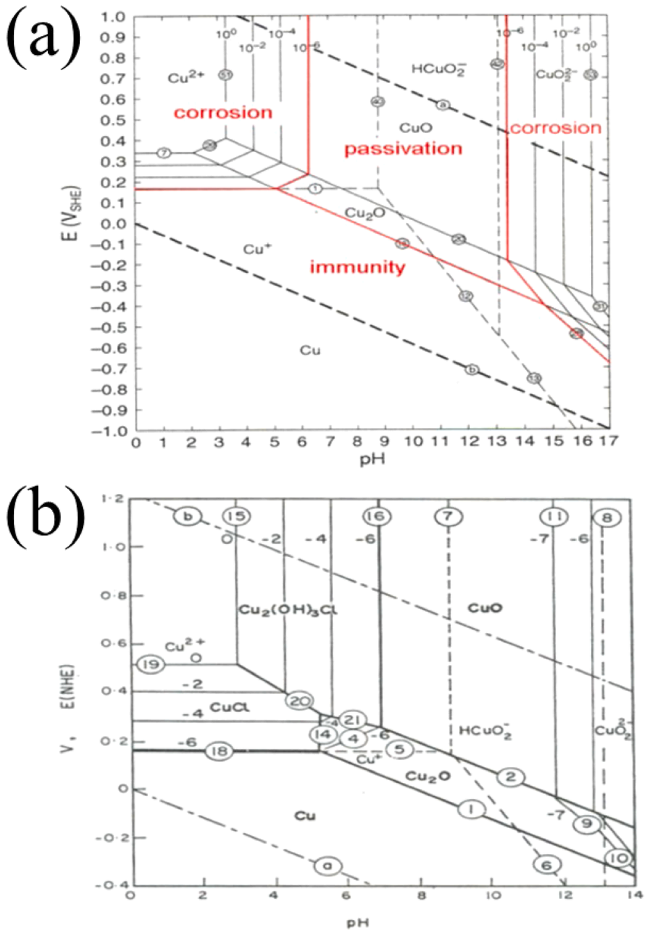

Fig. 1. Pourbaix diagram for (a) Cu-H_2O system at 25 °C [28] and (b) copper in seawater at 25 °C [29] and.

The Pourbaix diagram was also determined for copper in seawater at 25 °C as displayed in Fig. 1b. In contrast to Fig 1a, Fig. 1b examines the interactions between copper and water (H_2O) and chloride ions($Cl.^-$). Consequently, the diagram shows the presence of two new chemical species: $Cu_2(OH)_3Cl$ and CuCl. Moreover, because of these novel compositions, the range that each species lives in is distinct.

2. Surface film formation and failure mechanism of copper-based alloys

Copper and its alloys enjoy several beneficial properties including excellent mechanical properties, electrical conductivity, heightened corrosion resistance, and anti-biofouling properties. These have encouraged the application of copper and its alloys in several sectors such as in mechanical products (machine parts, pipes, bars, etc.), marine installations, energy and natural gas piping systems, and automotive and electrical devices. The inherent anti-corrosive properties of copper and its alloys rely on the formed protective oxide layer on its surface. It can form some sort of nonconductive layer or passive (oxide) protective film that can mitigate corrosion in the atmosphere and some aqueous environments [30]. However, in aggressive environments, the oxide is porous and not impermeable to the corrosive species. In an alkaline medium, Cu_2O can transform to $Cu(OH)_2$ in the porous layer which can be partially hydrated forming $Cu(OH)_4$ resulting in the destruction of the protective film [31]. In low pH or acidic environments, however, the protective oxide products (i.e. CuO and Cu_2O) are quite unstable and readily under dissolution to produce Cu(II). Furthermore, chloride ions ubiquitous in seawater are one of the most aggressive ions that destroy the protective layer in copper. The reaction of cuprous ions with chloride to form insoluble CuCl may occur. Thus, with the continued presence of chlorides, more of CuCl converts to a highly soluble $CuCl_2^-$ complexes which are further oxidized to $Cu_2Cl(OH)_3$, making copper dissolve. Consequently, the presence of chloride triggers copper corrosion even in neutral environments [32,33]. The general process of copper corrosion in different environments can be summarized in equations 1-10:

The oxide formation of copper in ambient environments follows:

$$2Cu + 1/2O_2 \rightarrow CuO \tag{1}$$

In chloride-rich environments:

$$Cu + 1/2Cl_2 \rightarrow CuCl \tag{2}$$

$$Cu_2O + Cl^- + 2H_2O \rightarrow Cu_2(OH)_3Cl + H^+ + 2e^- \tag{3}$$

In acid environments:

$$2CuO + HCl + H_2O \rightarrow Cu_2Cl(OH)_3 \tag{4}$$

$$3CuO + H_2O + SO_2 + 1/2O_2 \rightarrow CuSO_2.2Cu(OH)_2 \tag{5}$$

The general anodic process can be represented by:

$$Cu - 2e^- \rightarrow Cu^{2+} \tag{6}$$

The cathodic process can be represented in equations 7-10:

$$Cu + 2H_2O + 4e^- \rightarrow 4OH^- \tag{7}$$

During the oxygen reduction process, an indirect route can generate hydroperoxide (HO_2^-) as an intermediate following [34,35]:

$$O_2 + H_2O + HO_2^- + OH^- \tag{8}$$

$$HO_2^- + H_2O + 2e^- \rightarrow 3OH^- \tag{9}$$

During hydrogen evolution cathodic process:

$$2H^+ + 2e^- \rightarrow H_2 \tag{10}$$

In acidic systems, and even in saline environments, metals can induce hydrogen evolution by catalysing the hydrogen evolution cathodic route by reducing hydrogen protons (H^+) from the aqueous solution (water). This promotes crevice corrosion [34].

The microstructural details of the corrosion processes in copper-based alloys show the formation of various oxides when exposed to harsh environmental conditions. For example, beneath the rhythmic waves of the open sea, a cupronickel pipe lies still, its once gleaming surface starting to dull with age. Composed primarily of copper and nickel, this alloy was crafted for strength and is well-known for its remarkable resistance to the corrosive effects of the ocean. On contact with seawater, oxygen and moisture began to react with the copper atoms in the alloy leading to the formation of a thin, reddish, compact protective cuprous oxide (Cu_2O) as shown in equation below.

$$2Cu^+ + 1/2O_2 + H_2O \rightarrow Cu_2O + H^+ \tag{11}$$

Beside the copper atoms, nickel, the silent partner, also played its role: In alkaline and neutral water, nickel hydroxide is form.

$$Ni + H_2O \rightarrow Ni(OH)_2 \tag{12}$$

And in more oxidizing conditions:

$$2Ni + O_2 \rightarrow 2NiO \tag{13}$$

This NiO or $Ni(OH)_2$ layer intertwined with the copper oxide, creating a complex, multi-layered passive film, that grew and thickened with time, protecting the pipe like a second skin.

Increasing the nickel (Ni) content enhances the corrosion resistance of copper alloys. For instance, Cu-30Ni typically exhibits higher corrosion resistance than Cu-10Ni. However, when the nickel content exceeds

40%, any additional nickel can actually reduce corrosion resistance.

Iron (Fe) also contributes to corrosion resistance. A moderate Fe content of 0.5% to 2.0% helps refine the crystal structure and improve corrosion resistance by reducing defect concentration and increasing the compactness of the Cu_2O layer. However, if the Fe content surpasses this range, it can lead to the precipitation of Ni-Fe in the substrate, resulting in the formation of loose and porous oxide layers [36].

Within this metallic structure, subtle imperfections have emerged. Grain boundaries which minute seams between crystalline formations developed during the solidification process. Typically inactive, these boundaries now serve as susceptible channels through which chloride ions from seawater began to permeate. In specific regions, the addition of trace amounts of iron and manganese during the cooling process resulted in the precipitation of intermetallic particles, such as $FeNi_3$ and $CuFe_2$. These intermetallic particles functioned as cathodic islands, while the surrounding copper-rich matrix transitioned to an anodic state. This phenomenon led to the formation of micro-galvanic cells within the material.

Ma et al. [14] reported the existence $\gamma - \mathrm{FeOOH}$ throughout the corrosion product film of copper based alloy with it maximum concentration at the outer layer of the film. Iron dissolution (oxidation) proceeds at a significantly faster rate than copper in seawater during the initial stages of corrosion product formation as'

$$\mathrm{Fe} \rightarrow \mathrm{Fe}^{2+} + 2\mathrm{e}^{-} \tag{14}$$

Most of the oxidized Fe is converted into $\gamma - \mathrm{FeOOH}$ via the following reactions;

$$\mathrm{Fe}^{2+} + 2\mathrm{OH}^{-} \rightarrow \mathrm{Fe(OH)}_2 \tag{15}$$

$$\mathrm{Fe(OH)}_3 \rightarrow \mathrm{FeO} + \mathrm{H_2O} \tag{16}$$

$$\mathrm{Fe} + \mathrm{H_2O} \rightarrow \gamma - \mathrm{FeOOH} + \mathrm{H}^{+} + 2\mathrm{e}^{-} \tag{17}$$

The overall reaction for the formation of $\gamma - \mathrm{FeOOH}$ in the corrosion product film of copper-nickel alloy in seawater can be given as;

$$\mathrm{Fe} + 2\mathrm{H_2O} \rightarrow \gamma - \mathrm{FeOOH} + 3\mathrm{H}^{+} + 3\mathrm{e}^{-} \tag{18}$$

Consequently, iron gradually accumulates and becomes concentrated within the corrosion product film in the form of $\gamma - \mathrm{FeOOH}$, despite its status as a minor element within the alloy composition. The presence of metallic iron and also manganese in the corrosion product film of a copper-based alloy immersed in seawater is infrequently documented in the literature. Furthermore, the mechanism underlying reactions and formation remains unclear.

3. Corrosion forms of copper and copper-based alloys

3.1. *Corrosion of copper-based alloys in different environments*

Copper corrosion occurs readily in aggressive environments like seawater and humid, oxygen-rich climates. The chloride ions in seawater are especially corrosive to copper, accelerating deterioration [37]. This has led to a strong demand for economical, long-lasting anti-corrosion coatings. In marine settings, copper and its alloys develop a protective patina—a greenish-blue or brownish film—that shields the metal from further corrosion in chloride-rich conditions [38, 39]. Additionally, in neutral or slightly alkaline conditions (pH 8–12), copper exhibits notable resistance to corrosion [40]. However, in competitive media like seawater, copper experiences significant corrosion, especially in a 3.5 wt.% solution of NaCl, which mimics seawater salinity [11,41,42]. In this environment, chloride ions facilitate anodic and cathodic processes. The primary cathodic reaction involves oxygen reduction presented earlier.

Zhang *et al.* [43] examined how 70/30 copper-nickel alloy corroded in potassium permanganate, finding uniform corrosion at high concentrations. This study uses electrochemical methods (EIS, LPR) and array electrode techniques (WBE) to analyze B10 copper-nickel alloy weld joints in flowing seawater as displayed in Fig. 2a. SEM and EDS characterizations presented in Fig. 2b provided a macro and sub-micron perspective on corrosion across weld metal (WM), base metal (BM), and the heat-affected zone (HAZ). Results showed that corrosion rates of WM, BM, and HAZ decreased over time, with resistance ranking as WM > BM > HAZ. SEM and EDS revealed that accumulated corrosion products improved joint resistance over time. On a submicroscopic scale, WM acted as a cathode, mitigating corrosion under high flow rates in later stages. This work highlights the impacts of time and flow rate on corrosion in copper-nickel alloy seawater pipes, offering valuable insights into weld joint durability across scales.

Farro et al. [44] conducted a year-long study on early copper corrosion across different zones in Peruvian seawater and marine air, focusing on Salaverry Port. Key factors like oxygen content, chloride salinity, wetting-drying cycles, and wetness duration were found to strongly affect corrosion rates. The highest rate (0.071 mm/year) was observed at the tidal boundary. The atmospheric zone, however, had the lowest (0.016 mm/year), with the splash (0.025 mm/year) and immersion zones (0.032 mm/year) showing moderate rates, indicating less corrosive effects in these areas. The study also addressed the impact of increased port activity on copper corrosion, assessing electrolytic copper samples across different marine zones. Findings support strategies for corrosion prevention and maintenance of port structures, identifying the need for possible structural replacements. Factors such as oxygen availability in the immersion zone and chloride levels, wetness duration, and wetting-drying cycles in atmospheric and splash zones were noted as primary influences. Additionally, windborne sand, dredging, biomass accumulation, and oil residues further accelerated corrosion. Copper mass loss in the atmospheric zone followed a power law $C=At^n$ in relation to wetness time (t), with similar patterns observed in the splash zone, reflecting consistent corrosion behaviors across marine environments.

Wu et al. [45] studied the erosion-corrosion behavior of 90/10 and 70/30 copper–nickel tubes exposed to 1 wt% NaCl using a specially designed loop apparatus that better simulates industrial conditions than traditional methods. They aimed to determine the critical flow velocity (v-crit) for each alloy and study the corrosion resistance of the resulting films as shown in Fig. 3(a). Optimal corrosion resistance was observed at 1.5 m/s for the 90/10 alloy and 0.5 m/s for the 70/30 alloy. The critical flow velocity, marked by the formation of a continuous corrosion film, was 3–4 m/s for 90/10 and over 4.7 m/s for 70/30. In the 90/10 alloy, the film inhibited the cathodic oxygen reduction reaction, showing atypical passivation. Conversely, the 70/30 alloy film demonstrated traditional passivation, suppressing both anodic and cathodic reactions as shown in Fig. 3(a). This variation highlights distinct corrosion mechanisms across flow velocities and alloy types.

In another study, Cui et al. [46] examined how environmental factors impact the corrosion of B10 copper alloy, aiming to develop accelerated testing conditions that accurately represent real-world environments. Their three-part framework included experimental design, corrosion testing in both outdoor and laboratory settings, and verification of corrosion mechanism consistency. An L6 orthogonal design was used to test the effects of temperature, salinity, and dissolved oxygen in laboratory conditions, where H_2O_2 was added to seawater to accelerate corrosion. Comparisons with outdoor tests in natural seawater revealed similar corrosion mechanisms in both settings, reflected by comparable corrosion products, morphology, kinetics, and mechanical properties. The study also highlights limitations in laboratory-based simulations. Short-term tests often fail to significantly reduce testing durations, and translating lab results to outdoor environments remains challenging without quantitative models for environmental factors. Additionally, differences in corrosion products and morphology between natural and artificial seawater (NSW vs. ASW) point to possible variations in mechanisms, underscoring the need to combine outdoor and laboratory

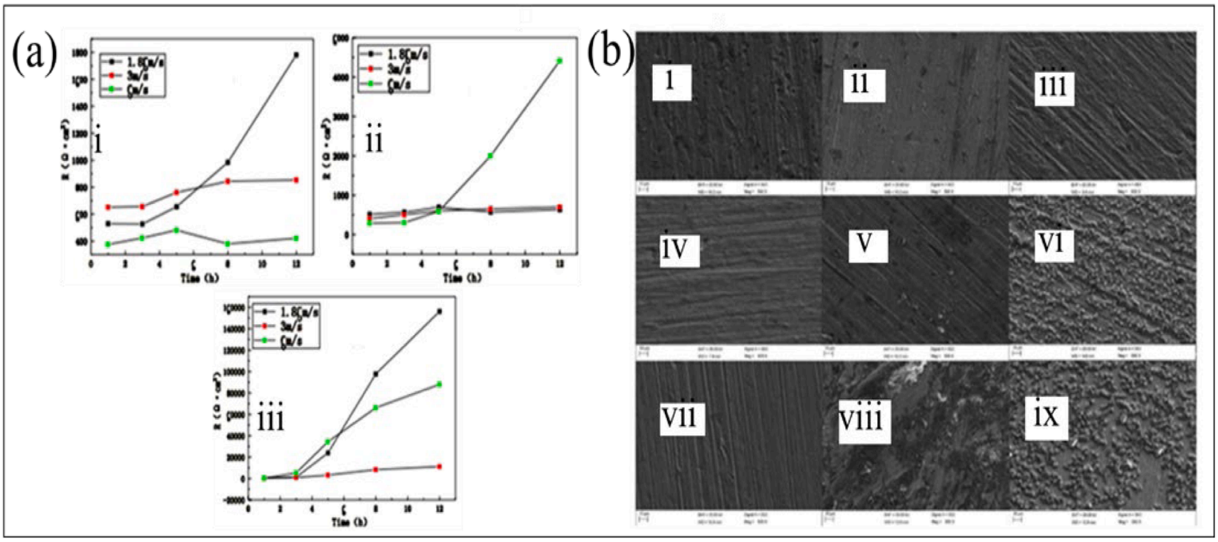

Fig. 2. (a) Comparison of overall impedance values of B10 Copper-Nickel Alloy Weld Joints in Flowing Seawater across three zones of welded joints under different flow rates (i) base metal (BM), (ii) heat-affected zone (HAZ), and (iii) weld metal (WM); (b) the SEM images illustrating the corrosion effects on each zone after 12 hours of seawater exposure at flow rates of (i-iii) 1.85 m/s, (iv-vi) 3 m/s, and (vii-ix) 6 m/s: for BM, HAZ,WM [43].

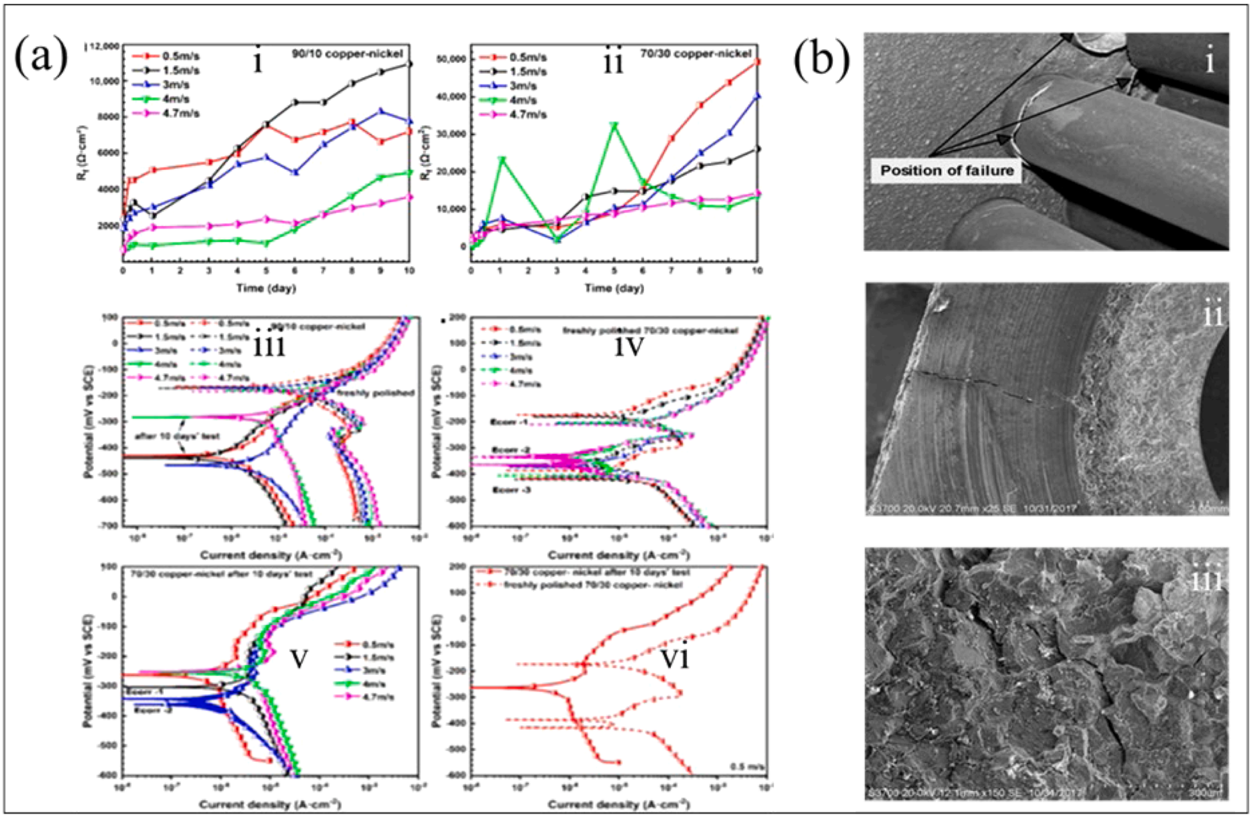

Fig. 3. (a) Film resistance evolution and potentiodynamic polarization curves for copper–nickel samples.The evolution of film resistance with erosion–corrosion time at various flow velocities for the 90/10 (a) and 70/30 (b) copper–nickel samples. Potentiodynamic polarization curves measured in a 1 wt% NaCl solution for both alloys: (c) 90/10 samples, freshly polished and after 10-day erosion–corrosion testing; (d) freshly polished 70/30 samples; (e) 70/30 samples post 10-day testing at various flow velocities; and (f) comparison between the 70/30 sample post-test at 0.5 m/s and its freshly polished counterpart [45], (b) (a) Failure of brass condenser tubes near joining location with backing plate [37]; (b) SEM morphology of fracture surface of entire brass nut entirety (c) fracture surface [59].

tests to ensure consistency.

3.2. *Stress corrosion cracking of copper-based alloys*

A significant failure mechanism affecting many technical materials, particularly copper-based (copper-based) alloys, is stress corrosion cracking (SSC). Tensile stress with a corrosive environment can cause a material to spontaneously and unexpectedly fail [47]. Because of their conductivity, strong mechanical qualities, and corrosion resistance, copper-based alloys are widely utilized in various industries, including plumbing, maritime, electrical, and automotive [48–50]. Although copper-based alloys offer numerous advantages, they can occasionally experience SCC, which can lead to significant financial losses and safety concerns. To guarantee the durability and dependability of components manufactured from copper-based alloys, it is essential to comprehend the elements that lead to SCC in these alloys, the conditions that encourage it, and the techniques to reduce it. The influencing variables and notable instances associated with the SCC of copper-based alloys are discussed as follows.

3.2.1. Factors Influencing SCC in copper-based Alloys

3.2.1.1. Alloy composition. Impurities and alloying elements have serious influence in SCC of copper-based alloys. Lead and bismuth are examples of impurities that might raise the risk of SCC. The low melting points of lead and bismuth prevent them from dissolving readily in most alloys. They separate at grain boundaries and may result in embrittlement, which makes the alloy more susceptible to SCC and potentially deteriorates the material [51]. Copper and zinc alloys like brass can experience a type of corrosion known as dezincification, in which zinc is extracted from the alloy in a targeted manner. As a result, the material may become weaker and more vulnerable to SCC [52,53]. Anargh et al. [54] examined the stress corrosion cracking resistance of copper-based alloys with appropriate weight percentages of copper (Cu), nickel (Ni), and tin (Sn). When the samples were heat treated, they noticed that the dendritic structure had totally gone after solutionization and aging. Stress corrosion cracking (SCC) was most common in normal bronze, and it was linked to the production of oxide layers, in accordance with the passive film rupture theory. In contrast, only internal cracks were discovered in the spinodal alloys. These cracks were connected to the presence of pits and burrs in the alloy.

Another compositional parameter that influences SCC of copper-based alloy is grain structure. Fine-grained structures are typically more resistant to SCC than coarse-grained structures because they can prevent the propagation of cracks [55,56]. The absence of grain boundaries in a coarse-grained structure result in a reduced barrier that hinders the propagation of cracks. Given that a crack can spread farther into the material once it begins, there is a possibility that it may lead to SCC [57].

3.2.1.2. Environmental conditions. Corrosive media can initiate and accelerate SCC in copper-based alloys. Ammonia, nitrate, and sulfide ions are common media that can stimulate SCC in copper-based alloys. For instance, brass is particularly susceptible to ammonia-induced SCC [58]. Studies have indicated that SCC exposure can result in the corrosion of brass fittings and other components. Bobić et al. [37] investigated the breakdown of a brass condenser tube at a Serbian thermal power plant. Results indicate that SCC in brass is caused by the presence of nitrogen and ammonia compounds on the inner tubes and fracture surfaces. The brass condenser tubes failure close to the connecting point with the backing plate is depicted in Fig. 3b.

Chen and colleagues examined the cracking of a brass connection nut in a circuit breaker located in a power substation. It was observed that stress concentration and stress corrosion were the main causes of the fracture, with poor mechanical characteristics accelerating the onset of SCC. Numerous techniques were used, including energy spectrum analysis, chemical composition analysis, numerical simulation, fracture morphology analysis (see Fig. 3b), microstructure analysis, and macro-morphology inspection [59]. Tensile stress together with a corrosive environment causes SCC, which leads to an unanticipated material failure. By inducing dezincification-selective leaching of zinc from the alloy, nitrate ions can exacerbate SCC in brass by weakening the material. Through the selective removal of zinc from the alloy, this procedure leaves the brass structure weaker and more porous, making it more prone to SCC. Fernández & Alvarez examined the anodic activity and SCC vulnerability of pure copper and four α-brasses of various zinc alloy concentrations in a 1 M solution of $NaNO_3$. SCC was observed when the potential was equal to or greater than a critical value (Ec), suggesting the same mechanism should operate in sodium nitrate, sodium nitrite, and copper (II) nitrate solutions. The fracture surface of the specimens (as seen in Figure 3) showed the fractographic characteristics typical of cleavage-like transgranular SCC [60].

SCC in brass can be caused by sulfide ions, in industrial and marine environments. The formation of copper sulfide coatings on the brass surface can embrittle the material and promote sulfide SCC. Brass intergranular-stress corrosion in an H_2S environment was investigated using the density functional theory and computational tensile test [61]. The findings demonstrated that although the segregation of Zn atoms promotes H atom penetration and weakens the metallic bond strength, the grain boundary structure makes it easier for H_2S and broken-down corrosive ions to adsorb. Ammonia is another media that accelerate SCC in copper-based alloys. When ammonia or ammonium compounds are present, zinc amine complexes are created, which degrades the material. Qiao and Luo [62] used Mode III loading to investigate the SCC of brass in an ammonia solution. The findings indicated that SCC occurred on primary stress planes with small shear loads but not on the main stress plane. It was also demonstrated that ammonia content affected fracture behavior, with low concentrations resulting in various degrees of cracks on 45^o planes. In a study conducted by Davalos-Monteiro [63], the SCC of brass in varying ammonia environments was analyzed by optical and scanning electron microscopy techniques. The results (refer to Fig. 4a) demonstrated that the corrosion is more severe in ammonia vapour, and corrosion increases with increased concentrations of ammonia and copper ions. Habib & Husain [64] conducted a stress corrosion study on copper-nickel alloys in sulfide -polluted seawater to determine their susceptibility to SCC at moderate temperatures. The experiments, which compared ultimate tensile stress, elongation, and time to failure, were carried out in a slow strain machine. The study confirmed SCC and fracture mode through metallographic techniques and scanning electron microscopy examination of failed samples.

Stress corrosion cracking in copper-nickel alloys can be brought on by sulfide ions. Copper sulfide is created when sulfide ions react with the alloy, causing embrittlement and fracture. Embrittlement can result from this compound building up at grain borders and other important locations. Under tensile stress, the embrittled areas are more prone to fracture. For instance, some researchers previously examined the impact of variables on the corrosion mechanism of two copper/nickel alloys, CA706 and CA715, in seawater. The results showed that sulfide in seawater prevent the development of a protective corrosion product, while simultaneous exposure to sulfide and oxygen accelerates the corrosion. A qualitative model was developed to explain this uniform corrosion mechanism in different seawater environments [65]. Additionally, to understand how sulfide aids in the development of films and the alloy's dissolution when sulfuric acid, sodium sulfate, and sodium chloride are present. Al-Kharafi et al. [66] reported that the presence of sulfide ions increased the corrosion rate relative to electrolytes solution without sulfides. The highest corrosion rate was observed in 0.58 M NaCl and 0.58 M NaCl + 0.1 M Na_2SO_4 containing 20 ppm sulphide. Torchio [67] investigated the corrosion-induced cracking of aluminium brass in non-ammoniacal acidic chloride solutions. The maximum transgranular penetration intensity was found in synthetic seawater, sodium chloride, and tri-sodium citrate solutions. The findings indicate that elevated levels of Arsenic (As) and Phosphorus (P) in the alloy significantly influence the morphology and intensity of the corrosion process. Furthermore, using energy dispersion of X-ray analysis, studies by Lin & Zhao [68] investigated the corrosion resistance of aluminum brass tubes and plates exposed to seawater for four years. Results show general and pitting corrosion, with localized corrosion caused by marine organisms (barnacles). Aluminium brass has exceptional resistance to corrosion but high antifouling susceptibility due to forming a dense

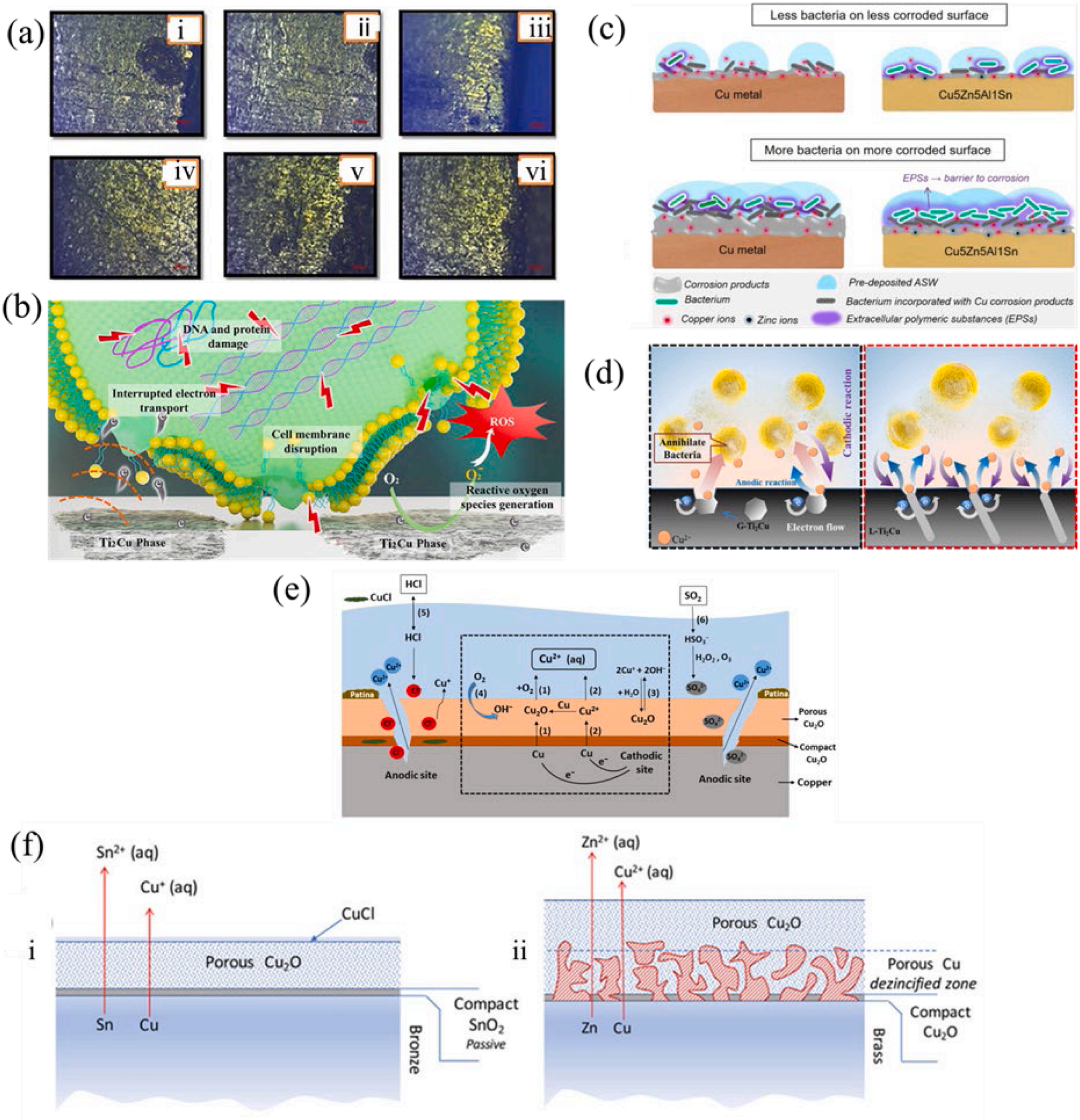

Fig. 4. (a) Optical microscopy images of exposed sample showing evidence of cracking on the surface [63]; (b) shewanella algae and its biofilm depicting the anti-bacterial activities [80]; (c) scheme showing the dominance of microorganisms, EPSs and corrosion products on Cu alloy and $Cu_5Zn_5Al_1Sn$ at various levels of corrosion [84]; (d) schematic illustration of Cu ion release due to micro-galvanic corrosion of Ti-Cu alloy in medical applications: G-Ti_2copper and L-Ti_2Cu [86]; (e) schematic representation of the atmospheric corrosion mechanism of Cu [87]; (f) formation mechanism of Cu–Sn/SnO_2/Cu_2O electrolyte interface (I,) Cu–Zn alloy hypothetical dezincification structure (ii) [88].

Cu_2O surface film with AI and Zn.

Another environmental factor that influences SCC of copper-based alloys is pH. Acidity and alkalinity can facilitate SCC process in copper-based alloy. A pH of neutrality usually results in less aggression. Both acidic (low pH) and alkaline (high pH) environments can initiate SCC process in copper-based alloys. While alkaline conditions can result in localized corrosion and the destabilization of protective coatings [69, 70], acidic conditions can increase corrosivity and produce hydrogen embrittlement. Due to their disruption of the alloy's surface integrity and promotion of crack initiation and propagation, both extremes increase the chance of SCC [53].

3.3. *Microbiological induced corrosion (MIC) of copper-based alloys*

Microbiologically influenced corrosion (MIC) denotes the breakdown of structures associated with microorganism proliferation. These destructions have caused economic loss by collapsing structures, roads, and bridges, damage to metals, and destroying its functionality. It has been reported that the effect of MIC contributes about 20 % of global corrosion costs and more than 50 % of oil pipeline issues [71]. Some key metals prone to MIC effects are copper-based alloys [72,73], aluminum [74,75] and carbon steel [76,77]. Generally, the MIC related to copper-based alloys is unique because of its characteristic mechanism and the proliferation of microorganisms [71]. Many microorganisms are associated with biocorrosion and play key roles in the deterioration of structures [78,79]. For instance, the biocorrosion of copper-based alloys in some unique environments has led to high-maintenance repairs. Most of the notable microorganisms associated with the MIC of copper-based alloys are Shewanella algae [80], Escherichia coli [81], Desulfovibrio desulfuricans [82], and Staphylococcus aureus [83]. A typical feature of microorganisms involved in MIC is shown in Fig. 4a. According to the illustration in Fig 4b, the anti-bacterial function was primarily due to the reactive oxygen species (ROS) rise influenced by the nano Ti_2Cu phase. Notable mechanisms linked with biocorrosion exist, depicting how the microorganism affects the destruction of structures.

It is pertinent to understand the mechanism of MIC in copper-based alloys, especially when choosing an alloy for building and construction. Several mechanisms exist showing how microbial proliferation could influence the breakdown of concrete structures in several environments [80]. Chang et al. [84] demonstrated the interaction between Cu, air corrosion and $Cu_5Zn_5Al_1Sn$ antibacterial efficacy under high-touch simulations. Fig. 4c demonstrates the total interaction between corrosion products, EPSs, and bacteria on $Cu_5Zn_5Al_1Sn$. Furthermore, the EPS shielded bacteria from dissolved Cu-ions and improved surface barrier qualities against corrosive products, whereas corrosion products could encourage the adhesion of bacteria to surfaces. Additionally, a finding from Ingo et al. [85] presented the corrosion mechanism of copper-based alloys. In this case, the naturally occurring corrosion products were created on historical artifacts made of Cu after prolonged contact with seawater. The bronze artifacts included pieces of priceless images and other objects that had been recovered several decades earlier from various seabeds along the Mediterranean coast of Italy. The results demonstrated that the alloy material was severely corroded in the media, and they also showed that the primary hazardous corrosive source was derived from chlorine. In the deeper layers of the patina, chlorine was found as CuCl, which caused the periodic and frequently unabated Cu degradation phenomena known as bronze disease when combined with moisture and oxygen. The obtained corrosion products were $PbCO_3$, and $CaCO_3$, which is probably because saltwater has a far higher concentration of CO_2 than freshwater does [85].

Many case studies of MIC in Cu-alloys in different applications have been reported [89,90]. For instance, the deterioration of metal was observed in medical applications [86]. It was shown that a greater percentage of Cu ions were found at the surface of the Ti-Cu alloys due to the discharge of Cu ions into the environment. The body gradient's driving tendency decreased as the concentration of Cu ions gradually increased. Furthermore, the body's metabolism would lessen the local build-up of Cu ions and accelerate the concentration gradient's decline. In biological settings, Ti-Cu alloys exhibited biological electrochemical corrosion in addition to releasing Cu ions to suppress microorganisms. Different micro galvanic corrosion electric field distributions were formed by the α-Ti and Ti_2Cu, due to their distinct distributions and morphologies. As seen in Fig 4d, the corrosive electric environment caused Cu ions to travel in the bacterial solution, significantly enhancing their participation in the antibacterial process [86].

A study by García-Mintegui et al. [91] showed the stenting applications of Zn-Mg and Zn-Cu alloys: mechanical characterization at the nanoscale to biocompatibility and in vitro degradation. To identify the ideal alloy composition for stent performance, the work examined the mechanical characteristics, biocompatibility, and biodegradability of Zn-copper and Zn-Mg alloys. Microstructure, nanoindentation measurements were evaluated to assess the mechanical characteristics at the nanoscale in relation to the alloying-induced alterations in Zn. The processes of biodegradation were examined and linked to mechanical efficacy, microstructure, and bacterial/cell response. The microstructure of zinc was improved by the input of either Cu or Mg alloying elements, which also enhanced yield strength and ultimate tensile strength in proportion to the volume percentage of secondary stages. Interestingly, Zn-Mg had excellent degrading stability in Hanks' solution and exhibited greater yield and ultimate tensile strengths. Zn-Cu alloys had an antibacterial activity against *S. aureus* that was regulated through diffusion and contact processes. The material's type and extent of deterioration both affected biocompatibility. An overview of recent findings related to MIC using Cu alloys in different environments is given in the Table 1

3.4. *Atmospheric corrosion of copper and copper-based alloys*

One of the most prevailing forms of corrosion is atmospheric corrosion, which affects materials exposed to the atmosphere but not completely submerged in a liquid. Despite being frequently considered resistant to air corrosion, copper and copper-based alloys are nevertheless prone to deterioration over time, particularly in contaminated environments. The structural integrity and usefulness of copper and copper-based alloys are significantly impacted by atmospheric corrosion [107]. Environmental factors like humidity, temperature, air pollution, time of wetness of the metal and atmospheric salinity influence atmospheric corrosion. In air pollution, pollutant gases such as SO_2, nitrogen oxides (NO_x), and chloride ions further exacerbate this corrosion process. It has been reported that the extent of influence of these factors on the corrosion characteristics of materials varies across different geographical locations [108,109]. The presence of O_2, humidity, chloride ions, and SO_2 is identified as the main contributors to atmospheric corrosion of copper and copper-based alloys [107,110].

Chlorides originating from marine environments, predominantly in the form of aerosols, come into contact with metal surfaces, thereby actively engaging in corrosion processes. Moreover, road deicers, coal combustion, municipal incineration, and bleaching facilities within the pulp and paper sector are significant sources of chlorides [107,108]. SO_2 stands out as the most significant gaseous precursor in industrial and urban environments. It originates from both human activities and natural processes, such as emissions from the petrochemical, metal, paper, and other industries, as well as the burning of fossil fuels like coal and crude oil. Once SO_2 is absorbed into the moisture layer, it oxidizes to form sulfites and sulfates, which acidify the electrolyte layer, thereby enhancing its corrosive properties. Chlorides and SO_2 exhibit high corrosivity due to their ease of incorporation into the moisture layers that form on metals [107,111].

Nitrogen oxides (NO_x), primarily generated by energy production and road traffic, have become increasingly significant as corrosive agents. Although, compared to sulfur or chloride molecules, NO_2 is less aggressive, it synergizes with SO_2 to exacerbate the corrosion of various metals. In recent decades, the concentration of SO_2 in various industrial and urban regions of developed nations has significantly decreased, while NO_2 emissions have consistently risen [107]. Another potentially hostile atmospheric agent is ozone, though it is relatively less important [112]. Creating effective preventative and mitigation solutions requires a complete comprehension of the mechanisms and processes associated with the atmospheric corrosion of copper and copper-based alloys.

3.4.1. *Mechanism of Atmospheric Corrosion*

Atmospheric corrosion of copper and copper-based alloys occurs through a complex process involving environmental factors, material properties, and electrochemical reactions. The interaction between the metal surface and atmospheric elements, mainly O_2, H_2O, and pollutants like SO_2, chlorides, and NO_x, causes atmospheric corrosion of copper and copper-based alloys. The combination of the generation chemical reaction and the protective properties of the copper oxide influence the distribution of the corrosion products formed on the copper surface. Understanding the mechanisms behind the corrosion of copper and copper alloys is crucial for numerous modern uses, including microelectronics and canisters used for storing nuclear wastes. In these situations, the extremely long lifetimes required or the little material present may harm even minimal corrosion rates. In other cases, a regulated corrosion rate can be required for uses like the purposeful

Table 1
Overview of recent findings related to MIC using Cu alloys in different environments.

Types of copper alloy	Test environments	Test methods	Key corrosion rate parameters	Findings	Ref.
Pure T2 Cu plate (Cu > 99.9 wt.%)	Simulated oilfield-produced water	SRB Cell counts, weight loss tests, electrochemical measurements, surface morphology, pit analysis	Weight loss, corrosion potential, corrosion current density	Inhibition efficiency of up to 89 % was reported. SRB biofilms accelerated the corrosion of pure Cu by secreting metabolites such as H_2S, which induced severe pitting and localized corrosion.	[92]
CuZnNi alloy	Marine environment	Antimicrobial tests, electrochemical analyses	Electrochemistry analyses	The corrosion rate was reduced from 0.0177 to 0.0021 mm/year. The CuZnNi alloy was effective in inactivating microorganisms on its surface	[93]
90/10 Cu-Ni	Anaerobic aqueous environments	Electrochemical measurements, Atomic adsorption measurements	Charge-transfer resistance, weight loss	SRB accelerates Cu corrosion by producing H_2S	[94]
Metallic Cu	Health care and Contaminated environments	Antimicrobial efficacy tests, inductively coupled mass spectroscopy (IC-MS)	Electrochemical measurements	99.9 % reduction rate was reported. Cu demonstrated high and rapid microbial efficacy against pathogens.	[95]
CuZn metal	Abiotic seawater and SRB media	Wettability and surface morphology characterization, SRB settlement analysis	Scanning Kelvin probe technique	The slippery liquid-infused porous surface affords high protection and inhibits abiotic and microbe-induced corrosion.	[96]
90/10 Cu-Ni and 70-30 Cu-Ni alloys	Power plant cooling water system	Corrosion and biofouling test	Heat exchanger fouling from corrosion products	Cu-Ni alloys are important in shipbuilding due to their resistance to seawater biofouling and corrosion.	[97]
2205 Cu-bearing duplex stainless steel	API RP-38 medium containing SRB	Microstructure, electrochemical measurements	LPR, OCP and pit depth	The duplex steel without Cu exhibited MIC resistance	[98]
Ti-5Cu alloy	Marine environment	Electrochemical techniques and surface analyses	Electrochemical and biofilm measurements	Pitting corrosion of the metal reduced from 3.1 ± 0.6 μm to 2.0 ± 0.4 μm.	[99]
B30 Cu-Ni alloy	Seawater simulated media	Kinetic potential anodic polarization curves	Maximum pit depth, EIS test	The occurrence of *P. aeruginosa* enhanced the breakdown of the passivation film	[100]
Cu_2O/Cu	Solar environment	Antibacterial and photocatalytic coating tests	Bacterial inhibition kinetics	A new highly efficient antimicrobial coating was developed	[101]
Cu-bearing steel	NS4 solution with SRB	Thermo-mechanical process, pit density, and LPR	Average pith and maximum pit depth	The pitting corrosion resistance of 1% Cu steel in as-aged media was better than X80 material	[102]
Ti-Cu alloy	Metallic biomaterial field	Surface roughness test, ion release	Microhardness, and corrosion resistance rate	The gradient nanostructured surface was developed on the alloy through surface ultrasonic rolling method	[103]
Pure Cu (99 %)	Seawater environment	FE-SEM, XPS, EDS	Corrosion potential, Corrosion current density	Corrosion inhibition efficiency of about 95.16 %. The coating enhances atmospheric corrosion inhibition performance.	[104]
Cu-Ti alloys	Wastewater pipelines	XRD, Mass variation, Dynamic modulus of elasticity	Antimicrobial corrosion test	The mortar mixed with $Cu_{50}Ti_{50}$ showed excellent resistance compared with MIC.	[105]
Cu bearing alloys	Natural gas transmission pipelines	Thermal spray, microstructural test, LPR, OCP	Antimicrobial corrosion test	Cu-based alloy influenced by the thermal spray had an excellent effect in mitigating MIC in natural gas pipelines	[106]

discharge of Cu ions as a biocide or the dealloying process that creates nanoporous materials.

The nobility of Cu typically positions it as the leading cathode in interactions with other metallic substances, accentuating the significance of its cathodic properties. In the corrosion process of Cu, the reduction of oxygen via a four-electron mechanism stands out as the predominant cathodic reaction [113].

$$O_2 + 2H_2O + 4e^- \rightarrow 4OH^- \tag{19}$$

Pure Copper: When exposed to the atmosphere, copper reacts with oxygen to form cuprite (copper (I) oxide or Cu_2O). Cu_2O can further oxidize to copper (II) oxide (CuO). Because the Cu (I) ion is only weakly soluble in aqueous solution, the main insoluble result during Cu corrosion is a thin, protective oxide layer of Cu_2O whereas Cu (II) ions are the predominant soluble species. Cu (I) becomes more soluble and dominates the solution when chloride ions or other complexing agents are present [114].

Early research by Ives and Rawson [115] proposed a two-layer structure for the cuprite (Cu_2O) film, with a porous outer layer and a compact interior layer (Fig. 4 (e)). The dense inner layer of Cu_2O helps protect the copper substrate by preventing further oxidation and corrosion of the copper ions. However, the outer layer is porous, which allows oxygen and water to penetrate, leaving the copper substrate exposed to corrosion. Additionally, harmful substances, including chloride and sulfate ions, can infiltrate the pores and defects present in the outer layer. This infiltration accelerates the corrosion process and facilitates the release of by-products from the copper substrate. The literature presents two proposed mechanisms for the dissolution of copper and the formation of an oxide layer: the one-electron mechanism and the two-electron mechanism. In the one-electron mechanism (mechanism (6) in Fig. 4 (e)), weakly soluble cuprite (Cu_2O) is formed step-by-step, and then cuprite is oxidized to produce soluble Cu (II) species:

$$2Cu + H_2O \rightarrow Cu_2O + 2H^+ + 2e^- \tag{20}$$

$$Cu_2O + 2H^+ \rightarrow 2Cu^{2+} + H_2O + 2e^- \tag{21}$$

The two-electron mechanism (mechanism (7) in Fig. 4 (e)), includes Cu^{2+} being directly formed, followed by a comproportionation reaction between Cu (0) and Cu (II) to form the slightly soluble Cu_2O [88];

$$Cu \rightarrow Cu^{2+} + 2e^- \tag{22}$$

$$Cu + Cu^{2+} + H_2O \rightarrow Cu_2O + 2H^+ \tag{23}$$

According to the initial model introduced by Ives and Rawson [115], copper dissolution was linked to the oxidation of the Cu_2O layer found on the external surface, as demonstrated in reaction (3) in Fig. 3e. Conversely, alternative studies by different researchers attribute the dissolution of copper to the solubility characteristics of Cu_2O, depicted in reaction (4) in Fig. 4 (e)). These mechanisms illustrate the complex processes involved in copper corrosion and copper film formation.

In chloride environment, Cl^- can infiltrate the Cu_2O film as interstitial ions due to their smaller ionic radius. Chlorine is introduced into the liquid-phase area by absorbing gaseous HCl or settling sea-salt particles or precipitation. When Cl^- enters the Cu_2O film, in order to preserve electrical neutrality, additional Cu^+ ions are created. The formation of CuCl (nantokite) occurs through the interaction between Cu^+ ions and Cl^-, which subsequently serves as a nucleation site to form a stable $Cu_2Cl(OH)_3$ (atacamite) through multiple successive dissolution-ion pairing-precipitation processes (mechanism (5) in Fig. 4e). Atacamite is the main component of chloride-rich corrosion products of copper patina [116].

The corrosion of copper may result from the influence of both oxidized and reduced forms of sulfur, wherein atmospheric SO_2 acts as the primary agent. The dissolved SO_2 in the atmosphere hydrolyzes to bisulfite ions (HSO_3^-), which are easily transformed to sulfate ions (SO_4^{2-}) by ozone, hydrogen peroxide, or transition metal ions which are all expected in the aqueous surface of the copper layer. After SO_4^{2-} is formed or integrated into the aqueous layer, it can be used in a catalytic process leading to brochantite formation. This process may involve PbO, derived either from the atmospheric oxidation of lead-containing compounds or from the corrosion of lead-based materials. PbO acts as a catalyst by promoting the oxidation of copper ions from Cu^+ to Cu^{2+}, which is essential for the formation of brochantite ($Cu_4SO_4(OH)_6$). Under sufficiently acidic conditions, this may also result in the formation of an unstable intermediate, posnjakite ($Cu_4SO_4(OH)_6{\cdot}H_2O$) (mechanism (6) in Fig. 4e) [112]. Brochantite is a stable compound classified as a mixed sulfate-hydroxide salt of Cu. This substance consistently emerges as the predominant constituent within the green patina developed by copper through prolonged interaction with the atmosphere.

Alloying effects: The Sn in Cu-Sn alloys (bronze) can improve corrosion resistance by forming a tin oxide layer [117]. The primary difference from pure copper corrosion is that the porous cuprite (Cu_2O) layer is separated by an inner cassiterite (SnO_2) layer from the bulk alloy, providing better protection to the metallic substrate (Fig. 4f). The substantial difference in standard Gibbs energies—519 kJ/mol for SnO_2 compared to 146 kJ/mol for Cu_2O, results in the preferential formation of the SnO_2 layer over the Cu_2O layer. Furthermore, the SnO_2 layer demonstrates stability across a broad pH range and is incorporated within the cuprous layer. As the outermost oxide layer dissolves and the primary oxide layer spreads inward toward the bulk, Cu is released into the electrolyte [118]. Thus, the initial step in the corrosion of bronze is SnO_2 layer formation.

$$Sn + 2H_2O \rightarrow 2SnO_2 + 4H^+ + 4e^- \tag{24}$$

For Cu-Zn alloys (brass), the dezincification of the alloy is usually observed (Fig. 4f (ii)). The mechanism and characterization of the dezincification structure have been investigated extensively in the past and reported in the literature [88,119]. The scenario is most straightforward in acidic media, where minimal oxide formation occurs. However, even with a decreased corrosion rate, more severe dezincification can be seen in a neutral electrolyte [120]. This is due to the development of a multilayered dezincification structure, which consists of a Zn-depleted layer and a layer of corrosion products made up of Zn and Cu compounds. The composition and structure of this altered layer fluctuate depending on the testing conditions, as well as the chemical composition of the alloy and the electrolyte used. Typically, the predominant species forming this layer of corrosion products include Cu_2O, CuO, $Cu(OH)_2$, ZnO, and $Zn(OH)_2$ [121,122].

4. Factors influencing the corrosion of copper-based alloys

4.1. Effect of Microstructure

Generally, it is a well-established knowledge that the understanding of the microscopic nature of a material gives a better description of the holistic property and behavior of the material in macroscopic scale, especially during its industrial applications [123–125]. Thus, this section will review the microstructure influence on the corrosion potential of copper-based alloys. In dealing with microstructure, several aspects will be considered in this review such as grain sizes and orientation, phases present and presence of inclusions.

4.1.1. Effect of grain sizes and orientation

Grain size and orientation is an important aspect of microstructural studies in copper-based alloys. Thus, their effects on the dissolution performance of copper-based alloys have been investigated till date [126,127]. For instance, Kosac et al. [128] studied the influence of crystal orientation and grain size on different grades of Cu alloys such as Cu-sheet, 99.99 % oxygen-free Cu (Cu-OF), electroplated Cu (99.95 %) on glass-fibre circuit board substrate (Cu-EP), and Cu wires from phosphorous deoxidized Cu. In their study, Cu-OF was found to have the largest crystal grain size of up to 150 µm, as shown in Fig. 5a, crystal grains of size 5 – 20 µm were noted for Cu wire and Cu-EP had the smallest value. In relation to their respective corrosion resistance, the Cu-OF with the largest grain size had the highest polarization resistance when compared to the Cu wire and others with smaller grain sizes, as shown in Fig. 6a. Furthermore, in a related study, Gao et al. [129] observed that microstructure variation such as, variation in grain orientation and presence of pore defects induced by the increase of dislocation density and vacancies arising from the influence of thickness reduction in the alloy, affected the resistance to corrosion of the studied CuZn alloy in a negative way.

4.1.2. Effect of phases present

Just like the grain size and orientation, phases present in copper-based alloys has an effect on their corrosion performance. In a study conducted by Filippo et al. [130], it was observed that the precipitation of martensitic phase on the grain boundaries of Cu-Zn-Al shape memory alloy led to an intense localized corrosion attack around the martensitic lamella. As a result, areas exhibiting a higher fraction of martensite along the grain boundary display increased susceptibility to the overall corrosion of the alloy under study.

4.1.3. Effect of inclusions

Inclusions are usually found in copper-based alloys in different sizes and compositions. Some studies have shown that either of the size or the composition can affect the corrosion characteristics of copper alloy. Chang et al. [131] noted that the Cu alloy containing inclusions in varying sizes, population density and compositions, reflected different corrosion behavior on exposure to a corrosive environment. In their study, the most common inclusion was O, then Sb, Pb, As and other minor elements like Fe, Ni, and Sn. Moreover, they found out that the larger inclusions are more noble than Cu matrix (as shown in Fig. 5 b), thus inducing a micro-galvanic corrosion effect that aggravated the overall corrosion of its containing alloy, as presented in Fig. 6 b.

4.2. Effect of Alloying Elements

The implication of alloying elements in the corrosion of copper-based alloys is extensively reported [132–136]. Such studies include the corrosion resistance of as-cast Al-Si-Cu alloy being enhanced by proper Zn addition [137]. Kong et al. [138] studied the influence of beryllium and tin on the dissolution of copper alloy and reported that after a 12-month exposure, the dissolution rate for QBe2 (about 15.5 g/(m2•y)) was less than pure Cu (roughly 42.2 g/(m2•y)) or QSn6.5-0.1 (roughly 38.1 g/(m2•y)), suggesting that the inclusion of beryllium improved corrosion resistance. It was also reported that by alloying with magnesium, Al-Cu-Mn alloys could become harder and more resistant to corrosion [139].

A typical example showed that Zn, Ni, and Al additions to Cu result in certain properties that are significant for various applications. For example, the combined influence of the effects of alloying components in Cu alloys in Cl- environments was investigated by Badawy and co-workers [13]. The goal was to look at how two alloying elements with

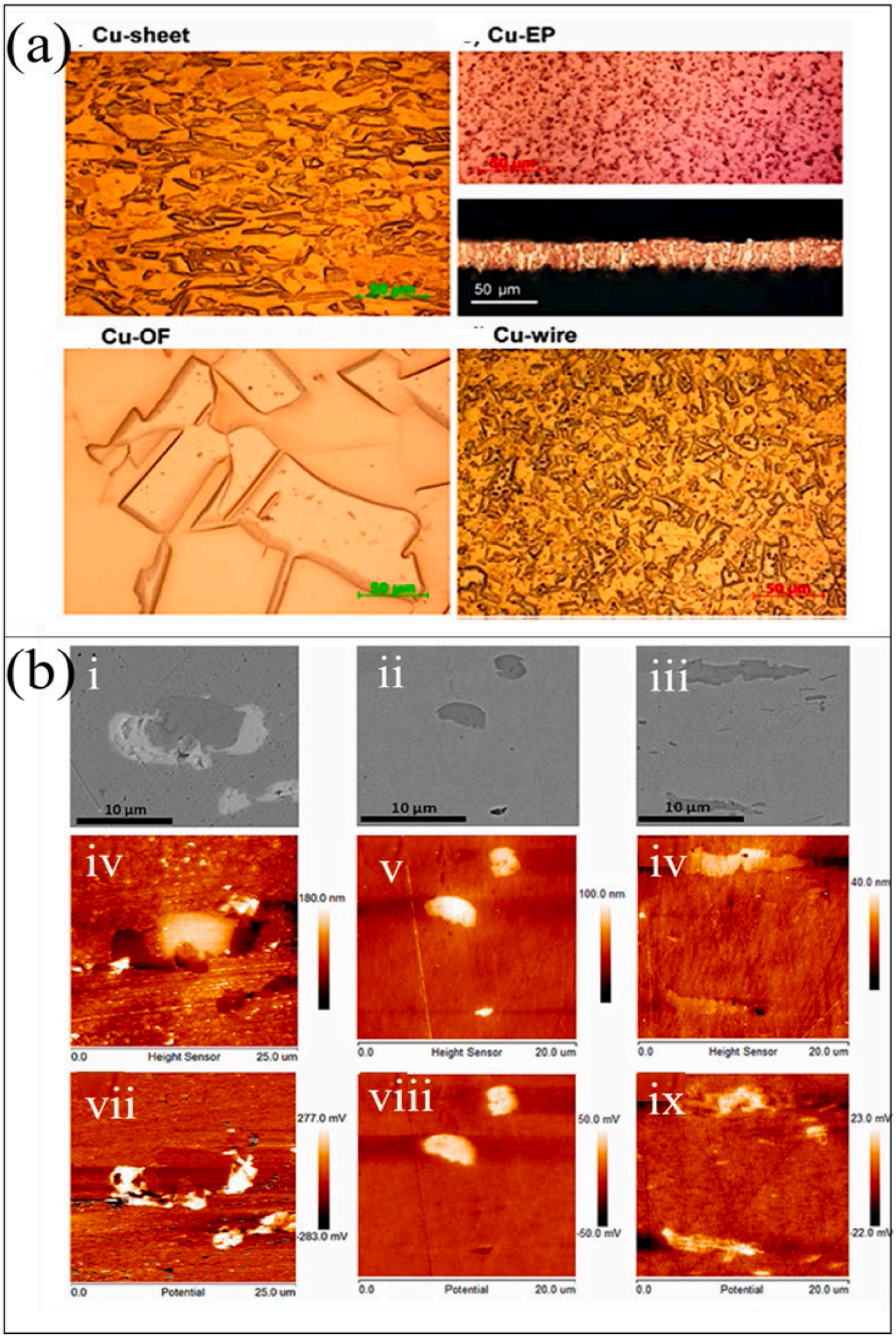

Fig. 5. (a) Microstructures of the different forms of copper: Cu-sheet, Cu-OF, Cu-EP, and Cu-wire. Adapted from reference [128]; (b) SKPFM imaging of the potentials of various inclusion sites and their surrounding Cu matrix sites. Adapted from reference [131].

Cu affected each other and how these alloys behaved electrochemically in solutions containing chloride, by employing Cu-10Ni-10Zn, Cu-10Al-10Ni, and Cu-10Al-10Zn where the two alloying elements have similar percentages, and the Cu ratio is maintained. When the Cu-10Ni-10Zn alloy was electrochemically compared to the Cu-10Al-10Ni and Cu-10Al-10Zn, it was found to be more stable and safe to use in neutral solutions containing chloride. It was noted that the Cu-10Al-10Zn alloy corrodes at a rate that is over thirty times faster than the Cu-10Ni-10Zn alloy. Compared to the other two alloys, the protective film generated on the Cu-10Ni-10Zn alloy had a greater thickness and corrosion resistance and was recommended for the setup that produces sulfate and chloride from concentrated marine solutions.

Similarly, Nady et al. [140], investigated Cu-10Ni-10Zn Cu-10Al-10Zn and Cu-10Al-10Ni corrosion performance in sulfate environments. The potentiodynamic polarization curves of all three alloys are shown in Fig. 6 c. These curves were recorded 60 minutes after the electrode was immersed in aerated, stagnant 0.5 M Na_2SO_4 solution at 25°C at a pH of 7. The Cu-10Al-10Zn and Cu-10Al-10Ni exhibit an anodic current plateau, which may indicate a passivation step caused by the presence of Al. Alloys containing Al appear to corrode at a slower rate than those containing both Ni and Zn. Therefore, according to polarization studies, the Cu-10Al-10Ni in this solution has a lower rate of

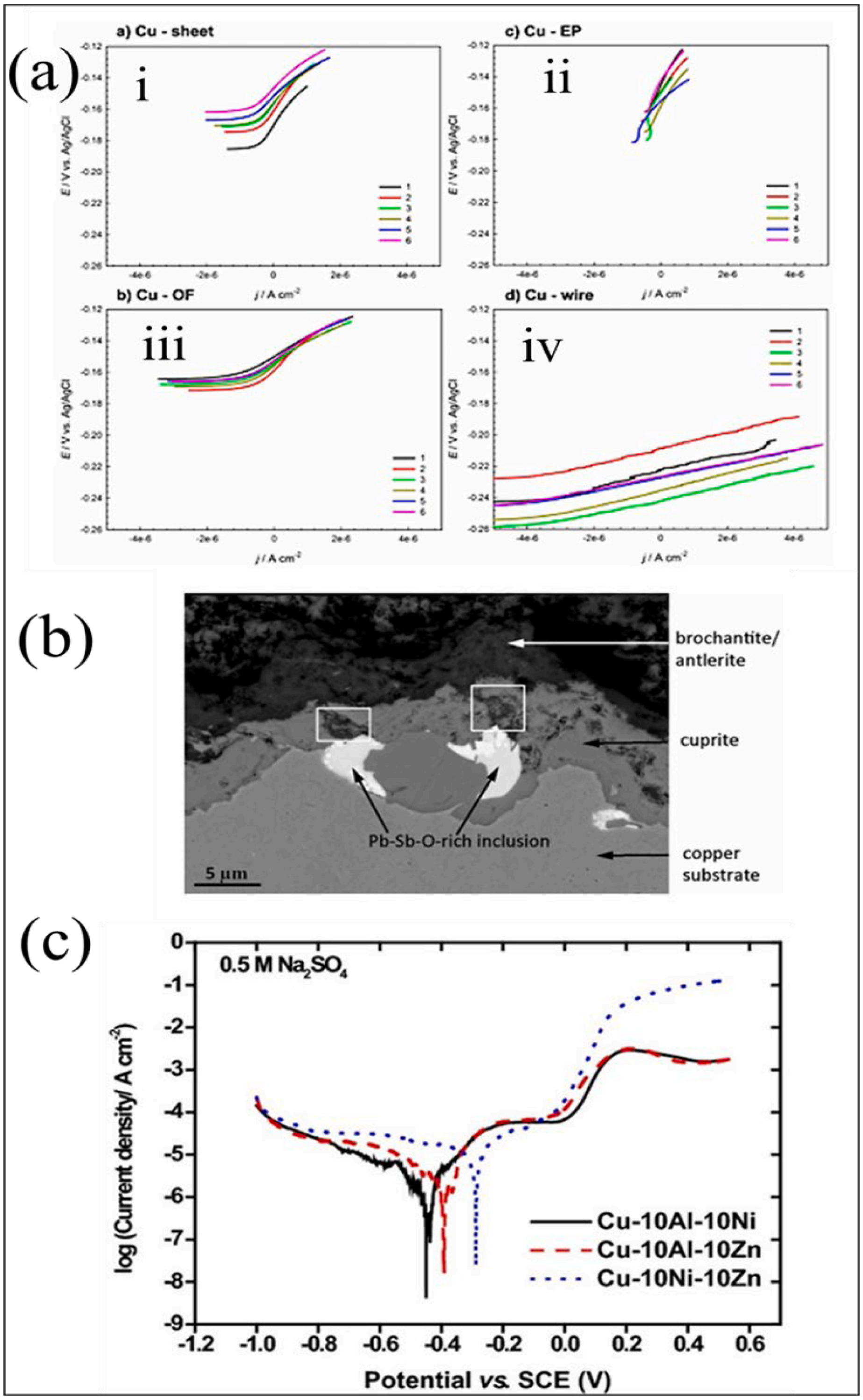

Fig. 6. (a) Replicate measurements of linear polarisation on (i) Cu-sheet, (ii) Cu-OF, (ii) Cu-EP and (iv) Cu-wire in 0.1 M NaCl. Adapted from reference [129]; (b) SEM image of the exposed Cu alloy showing the inclusion sites and the aggravated corrosion around its surrounding owing to galvanic corrosion. Adapted from reference [131]; (c) Potentiodynamic polarization of the various Cu alloys under investigation following 60 minutes immersion in a 0.5 M Na2SO4 solution at 25°C [140]; (f) Surface morphologies of Al-Cu (i-ii) and Al-Cu-Mg-Ag (iii-iv) alloys after immersion in 0.6 M NaCl solution for 24 hours and the corrosion products were removed and typical cycle polarization curves of the alloys (v) Al-copper and (vi) Al-Cu-Mg-Ag following different periods of immersion in a 0.6 M NaCl solution [141]; (g) (i) Surface morphology of the Zn-Cu alloys after immersion under dynamic conditions [142], (ii) the failed HA177-2 alloy tubes with corrosion perforations and distributions of the seawater velocity along the outside of multi-heat exchanger tubes [143], (iii) Erosion-corrosion damage mechanism transition map showing the transition from dissolution/passivation dominated to erosion-dissolution/passivation dominated [144].

dissolution compared to Cu-10Al-10Zn and Cu-10Ni-10Zn. It was discovered that the dissolution resistance is increased by the addition of Al and Ni. The findings lead to the Cu-10Al-10Ni alloy being suggested for use in the industrial production of sodium sulfate.

Also, due to the likelihood of pitting corrosion occurring close to constituent particles, coarse constituent particles negatively impact the resistance of Al-Cu alloys to corrosion. For example, using electrochemical and in situ observations, Wang et al. [141] investigated the combined impact of Mg and Ag additions on the localized corrosion of Al-Cu alloys bearing high Cu content. Samples of Al-Cu-Mg-Ag and Al-Cu alloys were exposed to a 0.6 M NaCl solution. In Fig. 7 a (i – iv) the degree of localized dissolution of Al-Cu [Fig. 7 a (i and ii)] and Al-Cu-Mg-Ag [(Fig. 7 a (iii and iv)] alloys, as well as the surface features following a 24-hour exposure to 0.6 M NaCl solution and after removal of corrosion products, are shown for comparison. Given that the cavity sizes are comparable to those of the respective particles in the two alloys, it is possible that Al_2Cu particles had a role in the cavity creation. On the corroded saAl-Cu alloy, lingering Al_2Cu particles are seen in addition to a high number of cavities. In Al-Cu-Mg-Ag alloy, on the other hand, only a few cavities are visible, and the majority of the Al_2Cu component particles are still in the matrix. Typical cyclic polarization curves of the alloys Al-Cu-Mg-Ag and Al-Cu following immersion at different times are shown in Fig. 7 [a (v and vi)], respectively. Given that the two alloys are prone to pitting corrosion during the early stages of corrosion. With increase in immersion time, the development of a protective oxide layer of corrosion products is likely the cause of the E_{corr} of the two alloys becoming more negative and the quasi-passive behavior of the polarization curves. The E_{pit} values seem approximately constant, implying the oxide layer composition essentially stays the same. However, the authors obtained values for ΔE ($\Delta E = E_{corr}$ - E_{prot}) which can be used to determine pitting corrosion quantitatively. Therefore, the findings demonstrate that compared to Al-Cu alloy, Al-Cu-Mg-Ag is less vulnerable to pitting corrosion.

4.3. *Effect of interface parameters (Eg. flow velocity and erosion-corrosion on copper and copper-based alloys)*

Erosion-corrosion has been considered the primary factor responsible for flow components like pumps, pipelines, heat exchangers, impellers, etc. This phenomenon can be attributed to the widely recognized interactions between mechanical erosion and corrosion that arise from the relative motion between a fluid and a solid surface [145]. Besides the nature of the engineering material, fluid-related factors such as flow velocity, flow regime, impact angle, liquid corrosivity, etc. are known to significantly influence erosion-corrosion [146]. Cu is widely used to construct tubing for heating, air conditioning, refrigeration, and water distribution systems where it works in flowing fluid and, hence, undergoes erosion-corrosion [147,148]. For instance, Wu et al. [143] investigated the premature perforation and leakages in HA177-2 Cu alloy tubes employed at a low-temperature. Interestingly, HA177-2 alloys are preferred because of their good conductivity, good anticorrosion properties, and low cost. Their study identified that the failure of the tube was due to a combination of stress cracking and pitting corrosion, which were caused by high fluid pressure and contaminated seawater. Notably, the failure was characterized by corrosion pits that concentrated in a specific strip on the upper part of the tubes as shown in Fig. 7 b (ii).

Luo and co-workers [149] proved that while ZHMn55-3-1 Cu alloy exhibited good anticorrosion behavior in stagnant seawater, the rate of erosion-corrosion increased with increasing flow velocity. They confirmed that an increase in the flow velocity can lead to enhanced diffusion of O_2 and Cl_2 species onto the surface of the material, accelerating both the anodic and cathodic processes, and limiting the corrosion resistance of the alloy. Zhang et al. [142] evaluated the effect of dynamic flowing conditions on the biocorrosion behavior of Zn-Cu alloys at high flow rates. As seen in Fig. 7 b (i), they proved that a higher flow rate largely accelerated the erosion and corrosion process of the alloy. Also, the finite element analysis model used to study the influence of shear stress and flow rates showed that the greater the flow quantities, the higher the shear stress and flow rates and the higher the rate of corrosion. Three factors were suggested to influence this behavior. Firstly, the high-speed fluid flows can grind out the protective corrosion product films on metal surfaces [Fig. 7 b (iii)]. Secondly, an increase in the flow-induced shear forces can enhance local concentrations of oxygen or other corrosive species. Lastly, fluid shear forces may trigger local strains and stresses on metal surfaces that change

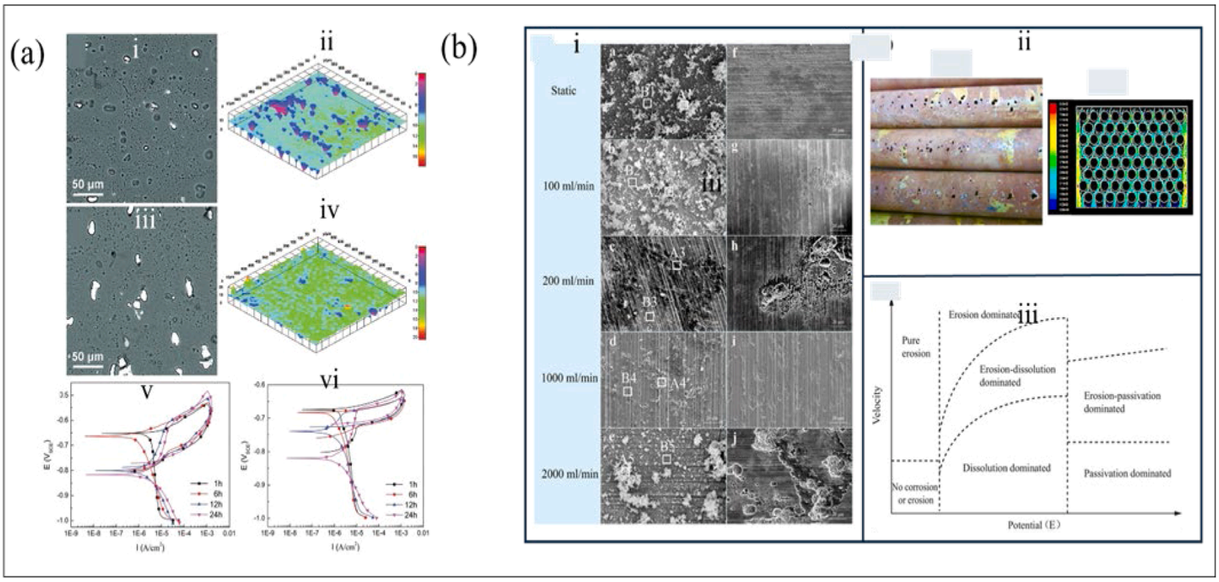

Fig. 7. (a) Surface morphologies of Al-Cu (i-ii) and Al-Cu-Mg-Ag (iii-iv) alloys after immersion in 0.6 M NaCl solution for 24 hours and the corrosion products were removed and typical cycle polarization curves of the alloys (v) Al-copper and (vi) Al-Cu-Mg-Ag following different periods of immersion in a 0.6 M NaCl solution [141]; (b) (i) Surface morphology of the Zn-Cu alloys after immersion under dynamic conditions [142], (ii) the failed HA177-2 alloy tubes with corrosion perforations and distributions of the seawater velocity along the outside of multi-heat exchanger tubes [143], (iii) Erosion-corrosion damage mechanism transition map showing the transition from dissolution/passivation dominated to erosion-dissolution/passivation dominated [144].

microstructures influencing corrosion susceptibility and rates. Their suggestions rightly correlate with conclusions made by Wang et al. [150]; that shear stress can quicken the overall corrosion rate due to the increment in mechanical force and mass transfer. It can also increase the localized corrosion coverage ratios, the thickness of the uniform corrosion layer and the rate of evacuation of corrosion pits.

In 1995, Stack used a plot of velocity vs potential to explain the degradation mechanism map of erosion-corrosion as shown in Fig. 7 (b) [144]. The plot provides a means of grouping the damage mechanisms, showing the transition to the localized corrosion coverage ratios from dissolution/passivation dominated which relates to the degree of severity of the damage. Furthermore, Stack's illustrations proved that the erosion-corrosion shows a critical damage phenomenon. Critical damage phenomenon occurs when the corrosion products films on a material are broken as a result of the fluid's impact energy and thereafter removed by fluid erosion. Cu alloys have been reported to show a critical damage phenomenon when undergoing erosion-corrosion [146,151]. Several reports have presented a critical damage phenomenon as a function of critical flow velocity [152]. Cu has been proven to be prone to a critical surface shear stress in a hydrodynamic system where the corrosion product films are peeled off and an accelerated corrosion action is triggered [153–155].

As explained by Wang et al. [146], critical flow velocity phenomenon for erosion-corrosion largely rely on the corrosion film. In the case of passive films, the phenomenon relies on the interplay between erosion-influenced de-passivation and re-passivation. The critical flow velocity phenomenon happens when the rate of re-passivation is slower than the rate of de-passivation. The stress-bearing capability adsorbed inhibitor and corrosion product films control the critical flow velocity for erosion-corrosion. When both the corrosion product films and the inhibitor films are broken, the damage of the erosion-corrosion is well pronounced, resulting in the critical flow velocity phenomenon. Mass loss, surface roughness, and electrochemical measurements are the three main reliable techniques for quantitatively determining the critical flow velocity encountered in erosion-corrosion [146,156]. Both the mass loss and surface roughness measurement methods are time-consuming and, therefore not used for quick measurements of the critical flow velocity [146].

4.4. *Effect of production methods*

The production methods of copper-based alloys significantly impact their corrosion behavior. These methods can be classified into three stages: processing, heat treatment and surface treatment. The processing techniques include casting, forging, rolling and extrusion; heat treatment covers the annealing, quenching and tempering processes, while surface treatment involves passivation, coating and electroplating. Only the processing methods are discussed in detail.

Casting in copper-based alloy production refers to the process of melting copper along with other metals (like tin, zinc, or aluminium) to create a molten alloy, which is then poured into a mould to solidify into a specific shape. This method is widely used in manufacturing various copper-based components, including pipes, fittings, electrical connectors, and art pieces. The most commonly used casting methods are sand, no-bake, die, shell, permanent mould, plaster, investment, centrifugal, etc. [157,158]. Although different casting methods can be employed based on the product's size, shape, and technical requirements, each has its advantages and disadvantages. Casting of copper presents various challenges, such as surface cracking, porosity problems, and the formation of internal cavities. On the one hand, sand casting, the most economical casting method, can lead to higher porosity and inclusions, which may act as corrosion initiation sites, whereas die casting (where the molten alloy is forced into a metal mould under high pressure, allowing for precise and high-volume production) provides a more homogeneous microstructure with fewer defects, improving corrosion resistance. A study showed that the corrosion resistance of all copper-based alloys in the permanent mould-cast condition was better than those in the sand-cast condition due to lower porosity [159]. Olga and Panayota [160] studied the influence of archaeometallurgical copper alloy castings microstructure towards corrosion evolution and reported an extended progression of the dealloying mechanism in casting features at the mid-term corrosion stage.

Forging in copper alloy production is a manufacturing process where a copper alloy is heated and then shaped by applying compressive forces, typically through hammering, pressing, or rolling. It is employed in the production of high-performance copper-based alloy components like gears, shafts, fittings, and connectors that require high strength, durability, and reliability. This process refines the metal grain structure, resulting in a product with enhanced mechanical properties. Some standard forging processes are open-die, closed-die, hot and cold forging. The advantages of forging include increased mechanical strength, reduced defect and enhanced surface finish, which enhances the corrosion resistance of copper-based alloys. Generally, forging improves the corrosion resistance of copper-based alloys by creating a more uniform and defect-free structure. Still, it must be carefully controlled to avoid adverse effects like stress corrosion cracking, which can be introduced as a result of residual stresses into the material due to the plastic deformation and rapid cooling, galvanic corrosion, which may arise from increased uneven distribution of alloying elements and other surface defects.

Rolling is a metalworking process in which a copper alloy is passed through many rollers to decrease its thickness, change its shape, or improve its mechanical properties. It is widely used to produce sheets, strips, plates, rods, and other copper-based alloy products. Rolling can be done at various temperatures and is typically classified as hot rolling or cold rolling, depending on the temperature relative to the material's recrystallization point. This process can positively and negatively impact the corrosion behaviour of copper alloys. When properly controlled and combined with post-processing treatments, rolling can improve the corrosion resistance of copper-based alloys, for many industrial applications. Zeng et al. studied the mechanical properties, corrosion behaviour and microstructural evolution of as-cast, as-annealed, and hot-rolled Cu-9Al-10Ni-4Fe-1.2 Mn. They found that rolling not only increases the hardness, elongation and strength of the alloy but also improves its corrosion resistance [161].

Extrusion is another process employed in the production of copper and its alloy. It is used to manufacture long, continuous sections with uniform cross-sectional profiles. It offers efficiency, versatility in shaping, and excellent mechanical properties, making it ideal for producing tubes, rods, bars, and complex profiles. The types of extrusion commonly used include hot, cold, direct, and indirect. Specifically, cold extrusion results in grain elongation along the direction of extrusion, potentially improving resistance to uniform corrosion due to the refined and aligned grain structure. However, cold extrusion can introduce significant work hardening into the copper-based alloy, increasing its strength and introducing residual stresses. These tensile stresses can increase the susceptibility to stress corrosion cracking (SCC), especially in environments containing chlorides or other corrosive agents. For hot-extruded materials, the thermal processes involved typically relieve internal stresses, reducing the risk of SCC. The high temperatures in hot extrusion can also cause surface oxidation and oxide scaling. If not cleaned or pickled after extrusion, uneven or porous oxide scales can cause pitting or crevice corrosion

Karthik and his colleagues [48], conducted a study on the morphological behavior of Cu–Sn, Cu–Sn–Ti, and Cu–Sn–Zn alloys throughout various manufacturing processes. Their research identified that factors such as grain size, grain distribution, heat treatment, morphological behavior, and the formation of intermediate phases significantly affect the properties of copper-based alloys. They further concluded that alterations in microstructure, which result from different manufacturing techniques, heat treatments, and the incorporation of alloying elements, can enhance both the mechanical and thermal properties of these alloys.

In summary, the production methods of copper-based alloys play an important role in determining their corrosion behaviour. Casting, forging, rolling, and extrusion influence the microstructure and defect density, which in turn affect the material's corrosion resistance. Heat treatments and surface treatments can further modify these properties to enhance performance. Understanding these relationships is essential for selecting and processing copper-based alloys for optimal corrosion resistance in specific applications.

4.5. Effect of chloride ions

The dissolution characteristics of copper-based alloys have been thoroughly researched in chloride environments in a variety of experimental methods to understand the stress corrosion cracking, dealloying, pitting, and passivation. It is pertinent to note that the dissolution behavior of copper-based alloys is pH dependent according to the Pourbaix diagrams (Fig. 9b) which describe the system thermodynamics based on the E-pH relationship [162,163]. For instance, Alfantazi et al. [162], studied commercial alloys with the nominal compositions of Cu–30Ni (Cu–Ni), 90Cu–8Al–2Fe (Cu–Al), and Cu–30Zn (Cu–Zn), using potentiodynamic polarization at pH 6.5 and pH 10. The alloys displayed passive properties at pH 10 (buffered)in contrast to pH 6, indicating pH's sensitive role in the dissolution characteristics of Copper-based alloys. However, beyond the breakdown potential, there was a sharp

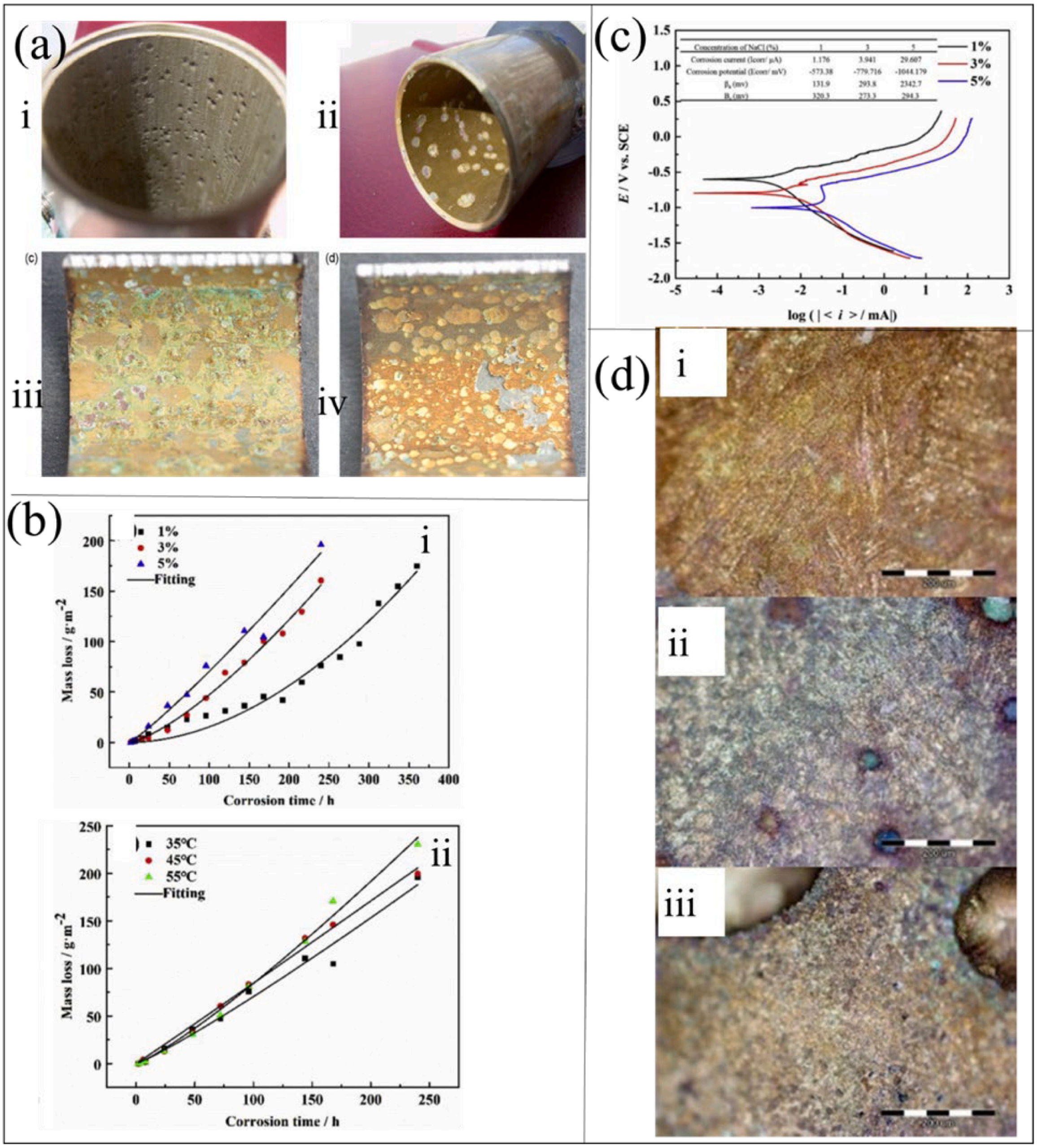

Fig. 8. (ai) CuNi 70/30 specimens, mechanically cleaned and exposed for 280 days in the chlorinated test line followed by 1 month in the non-chlorinated line, (aii) CuNi 70/30 specimen of "new" tube (that never operated in the condenser), after 1 month of exposure to seawater in the non-chlorinated line, (aiii) The inner surface of CuNi 70/30 condenser tube that operated with non-chlorinated water, (aiv) The inner surface of CuNi 70/30 condenser tube operated with non-chlorinated water [172]; (bi) Relation between mass loss and salt fog corrosion time for DCIC under 35 °C and (ii) different temperatures under 5 wt% NaCl [174]; (c) Potentiodynamic polarization curve of CueAl after salt fog corrosion for DCIC (Inset: parameters extracted from the measurements under DCIC [174]; (d) Optical micrographs of the CuAlNi alloy surfaces after the potentiodynamic polarization in the (i) 0.1% (ii) 0.9% and (iii) 1.5% NaCl solution [175].

increase in current density. The Cu–Zn alloys demonstrated the largest possible range of passivity. In another study, the two brasses were investigated in a buffered NaCl solution by Morales et al. [164] using the cyclic voltammetry technique. It was revealed that a compacted film of Cu_2O and ZnO xH_2O was responsible for the passivation of brass. However, pitting corrosion occurred as the potential became more anodic

Ismail et al. [16] probed the pitting of Cu–38Zn with varying concentrations of Cl^- ions from 0.01 M to 0.6 M. The polarization curves of the test solution indicated a shift in the breakdown potential to potentials that were more positive as chloride ions increased. It was seen that as the potential became more positive, pitting occurred due to film breakdown. Cu-Ni alloys are thought to be superior to the majority of other copper alloys because of their ability to withstand corrosion in maritime environments. Sham El-Din et al. [165] investigated the dissolution behavior of copper, three brasses, and zinc, in 0.1 M solutions of neutral Cl-, NO3-, and SO4. The OCP were similar for brass and copper compared to zinc. Milošev [166], investigated the degradation of passive films on 90Cu–10Ni in borate-buffered NaCl solutions. Their findings demonstrated that pitting corrosion, a type of film breakdown, took place and that a rise in NaCl content caused the detrimental breakdown potential to become more negative. The dependence of the corrosion characteristic and features of alloys on pH in NaCl solutions has also been noted for a variety of industrial alloys such as Al and Zn-containing alloys [167–171].

4.5.1. Specific case studies of the impact of chloride ions on copper-based alloys

4.5.1.1. Salt and exposure time. Cristiani et al. [172] investigated the influence of chlorides on Cu/Ni 70/30 condenser tubing. Interestingly, the results indicated that the development of a barrier film on the copper-based alloy is facilitated by short chlorination additions of 0.4 mg/L–0.8 mg/l of chloride solutions for 0.5–1 h several times a day. This layer, when properly built, can greatly decelerate localized corrosion even in situations when the saltwater gets extremely hostile, like when biofouling develops. Fig. 8 (a) shows the inner surface CuNi 70/30 condenser tube under different experimental chlorination conditions.

It is observed that in Fig 8 a (ii), the surface manifested passivation with a brown corrosion layer the visible “old” preformed localized corrosions sites formed before initial chlorination. In Fig 8 a (ii), shining metal red oxides inside the corrosion spots are seen. In Fig. 8 a (iii), purple–greenish deposits were seen inside the tubercles and localized

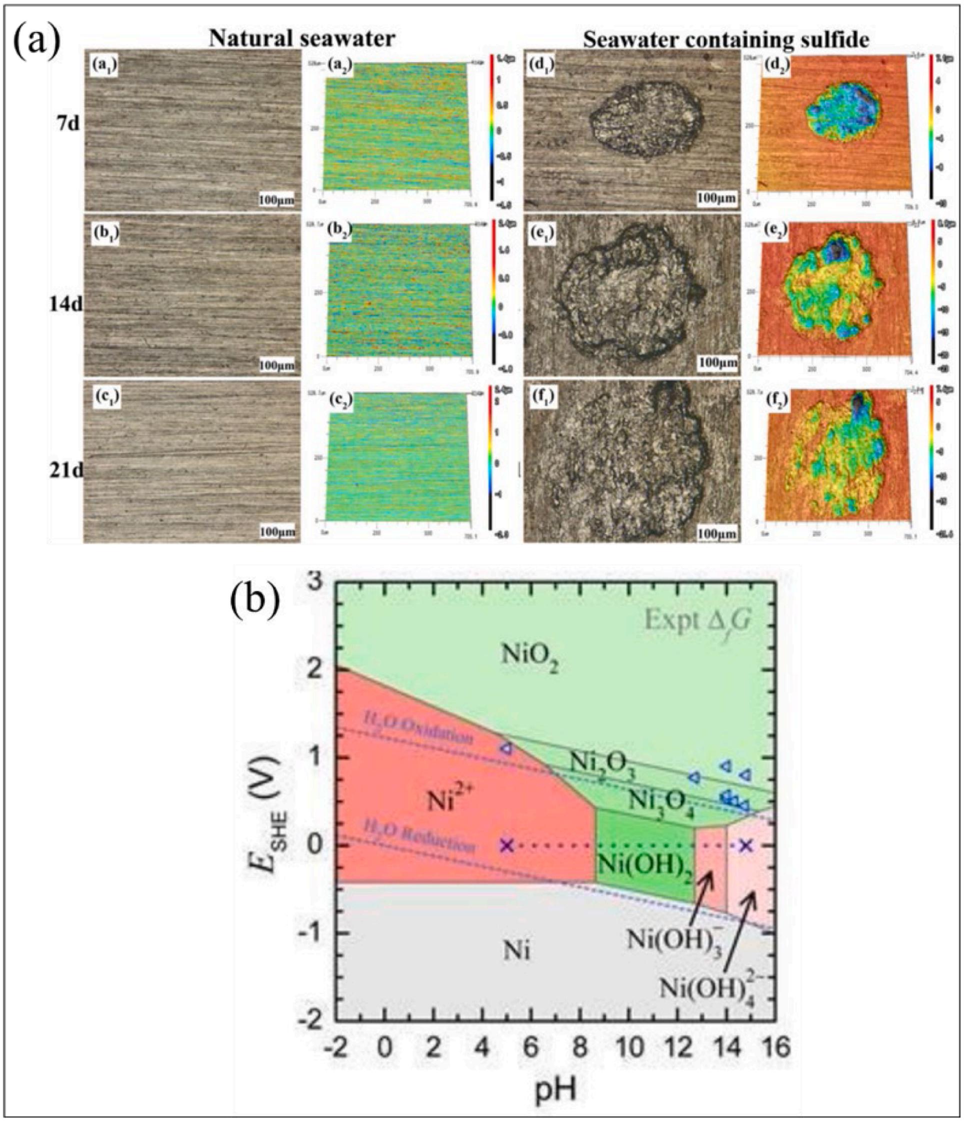

Fig. 9. (a) Surface morphologies and 3D profiles of the 70/30 copper-nickel alloy after immersion in natural seawater and seawater containing sulfide for different times [190]; (b) The Pourbaix diagram of nickel hydroxide, showing pH-EMF (V) vs. standard hydrogen electrode (SHE) [191].

attacks were observed. In Fig. 8 a (iv), the exfoliation of a thin film and localized attacks beneath the obvious crusts. These results indicate that chloride ions greatly impact the corrosion behavior of CuNi alloys.

4.5.1.2. Salt concentration and pH. Khan and Patil [173] investigated the combined effect of Cl- and pH on the dissolution of Cu-10Ni alloy. These alloys are widely employed in heat exchangers owing to superior thermal conductivity and corrosion resistance. The resistance to corrosion is linked to the protective Cu_2O film. However, a less protective $CuCl_2^-$ can also occur in the presence of different concentrations of H^+, OH^-, and Cl^- ions. When these two coexist, the corrosion behavior is greatly impacted. The corrosion of CuNi alloys is pH sensitive according to Pourbaix diagrams (Fig. 9b). The results of the anodic polarization tests at pH 6 and 8 for saltwater with different NaCl concentrations are shown in Table 2. The current density i_{corr} increases with an increase in Cl^- concentration. The term “critical current density and passivation current density” refers to both the pseudo-passive potential (i_{ppp}) and critical-pseudo-passive current (i_{cpp}). The term "Epseudo-passive potential" (E_{ppp}) refers to the comparable passive potential. The values of these parameters are presented in Table 2 which shows that as Cl^- concentration increases, anodic acidity increases and then decreases for pH values. Conversely, the maximum anodic current density at pH 6 in the 2.5% NaCl solution, and the maximum at pH 8 in the 1.5% NaCl solution indicating that there is a threshold for the effect of chlorides in the anodic activity. In the framework of the Tafel theory, β is the symmetry factor obtained from the Tafel equation. The symmetry factor is a theoretical concept, and its value cannot be determined experimentally. It related to the shape of the Gibbs energy barrier between the initial and final states of a process. It is the ratio of the effect of an applied potential on the standard electrochemical Gibbs energy of activation to that on the standard electrochemical Gibbs energy of the reaction. Higher values of β may comparatively indicate higher charge transfer processes.

4.5.1.3. Salt and Temperature. Zhang et al. [174], reported the influence of Cl^- ion concentration and temperature on the dissolution of Cu–Al composite plates in salt fog environments. It was seen that corrosion predominantly occurred along the diffusion zones composed of Al_4Cu_9, AlCu, and Al_2Cu, respectively. The kinetic constant was observed to increase by about 31% with the increase in the concentration of NaCl to 3% which manifested in the form of increased mass loss. Fig. 8 (b) is a plot of mass loss versus corrosion rate in a salt fog environment under 35°C under different chloride ion concentrations (DCIC) and different temperatures with 5 wt% NaCl. Table 3 also indicates that the kinetic constant depend on temperature. It was observed to increase and then decrease with the rise in temperature, and the high value was recorded at 45°C.

The electrochemical results testing indicate that a rise in the Cl^- ion concentration raises the disolution rate of Cu-Al composite plates. Fig. 8 (c) is the polarization curve of Cu-Al after salt fog corrosion for DCIC. The anodic and cathodic current densities dropped with the drop in the concentration of NaCl which translates to a lower corrosion rate with the decrease in chloride concentration.

Table 2
Electrochemical parameters derived from anodic polarization plots of CuNi alloy in NaCl solutions [173].

Parameter	pH	Percentage of NaCl				
		0.5	1.5	2.5	3.5	4.5
$E_{corr-anodic}$ (mV)	6	-220	-286.05	-232.6	-253.8	-265.15
	8	-175.29	-270.13	-212.79	-306.71	-252.37
E_{ppp} (mV)	6	37.78	-4.90-1	-1.31	-29.49	-42.59
	8	1.11	-19.59	-19.79	-18.87	-36.39
I_{cpp} (mA/cm^2)	6	2.13	5.67	6.50	8.43	11.37
	8	2.34	7.10	7.18	9.53	13.86
I_{ppp} (mA/cm^2)	6	1.37	1.34	1.70	2.28	4.47
	8	1.05	1.02	1.07	2.47	2.29
β (mV)	6	82.04	110.3	74.70	76.17	65.35
	8	75.08	117.54	58.55	109	61.35
$I_{corr-anodic}$ (mA/cm^2)	6	1.35	5.43	7.66	7.29	3.84
	8	4.20	8.96	3.49	7.15	3.56

Table 3
Kinetic rate constants of the materials exposed to salt fog environment [174].

Material	NaCl (wt%)	Kinetic laws: $W=a.t^b$ [W(g.m^{-2}).t(h)]		
		35 ^{0}C	45 ^{0}C	55 ^{0}C
Cu-Al	1	$2.7\times10^{-3}t^{1.875}$	-	-
	3	$8.6\times10^{-2}t^{1.368}$	-	-
	5	$4.0\times10^{-1}t^{1.123}$	$7.8\times10^{-1}t^{1.016}$	$3.6\times10^{-1}t^{1.185}$

4.5.1.4. Salt and Morphology. Vrsalović et al. [175], evaluated the effect of Cl^- concentration from 0.1 - 1.5 % on the electrochemical characteristics of the CuAlNi Alloy. The surface morphology of the alloys after electrochemical tests are shown in Fig. 8 (d). It is observed that pitting was absent at 0.1% Cl solution, but was visible at higher chloride concentrations. The EDS indicated the abundance of Cu_2O, and Al_2O_3 on the alloy surface. The presence of Al_2O_3 as a major component of corrosion has been reported elsewhere [176–179]. The SEM morphological observations were in tandem with the electrochemical results. The highest spread of pits on CuAlNi alloy surface was at 0.9% Cl- solution and the largest pit diameter was at 1.5% Cl- solution.

Overall, it is observed that the amount of chloride ions can have pronounced effects on the dissolution characteristics of copper-based alloys which impact other parameters such as electrochemical behavior, pH, dissolution kinetics, and morphology among others. An increase in exposure time leads to an increase in the impact of chloride ions on the alloy. And a rise in Cl^- ion concentration was found to generally have the following effects: an increase in electrochemical activity, an increase in kinetic rate constants, and increased pitting features on the alloy. Factors such as temperature and pH (depending on the Pourbaix diagram) were found to greatly impact the effect of the increase in chloride ions on copper-based alloys.

4.6. Effects of sulfide and ammonia contaminants

Copper-based alloys are extensively utilized in seawater systems for a range of applications, including heat exchangers, pumps, valves, pipes, and fasteners. The selection of specific alloys, such as CuNi alloys (e.g., CuNi10Fe1Mn) or nickel aluminum bronzes is often determined by the required mechanical properties for each application. Despite the recent introduction of alternative materials that exhibit enhanced characteristics such as nickel-based alloys, stainless steels, and titanium, copper alloys continue to be widely implemented owing to their established reliability and effectiveness in marine environments. However, copper-based alloys are susceptible to specific forms of corrosion.in contaminated environments, notably; localized corrosion can arise from sulfide contamination [180–184]. Furthermore, crevice corrosion is frequently observed in valve and flange assemblies [185–187]. There have also been documented instances of stress corrosion cracking occurring in seawater that is subject to varying levels of ammonia pollution [188].

In their study of the corrosion behavior of high strength C71500 Cu-Ni alloy pipe, Gao et al. Gao et al. [189], found that alloy exhibits activation polarization at all test conditions. Surface morphological analysis indicated that the corrosion products exhibit a protective effect, which resulted in the cessation of the diffusion process. In contrast, EIS revealed that only the capacitive reactance arc persists with prolonged immersion time. Furthermore, the introduction of a high concentration of Na_2S facilitated the formation of Cu_2S, and acceleration of the redox process, thereby enhancing the rate of corrosion. Li et al. [190], conducted a comprehensive investigation into the impact of sulfides on the pitting corrosion behavior and film chemistry of 70/30 copper-nickel alloys in aerated seawater, utilizing electrochemical measurement techniques. The findings indicated that the presence of sulfides in seawater impairs the formation of corrosion products and morphology. As a result, the corrosion product film exhibits a double-layer structure, comprising a loose and porous outer layer that contains sulfides and a dense inner layer which was noted to be ineffective in mitigating corrosion; instead, it exacerbates the development of pitting corrosion, as demonstrated in Fig. 9 (a).

A number of studies have probed the effect of sulfide on the corrosion behavior of copper and copper-based alloys when subjected to sulfide-contaminated seawater. However, the literature reveals a lack of consensus regarding the findings. The prevailing consensus among the majority of authors [189,190,192–195] is that copper and copper-based alloys experience increased corrosion when exposed to sulfide-polluted seawater. However, a minority of studies [196,197] have suggested that the corrosion rate of Cu- alloys diminishes as sulfide concentration increases in seawater with relatively high flow rates. These researchers attribute this phenomenon to the development of a copper sulfide layer that thickens over time, which serves as a physical barrier that mitigates further corrosion of the base material. Recent study by Ekerenam et al. [19] under dynamic flow conditions seems to be in agreement with the report of the minority that increasing sulfide concentration reduces the corrosion rate of copper based alloy in sulfide contaminated simulated seawater at static flow condition.

Sulfur can be derived from various sources, including industrial wastewater pollution, biodegradation processes, and the reduction activities of sulfate-reducing bacteria. Sulfide ions (S^{2-}) significantly enhance the corrosion sensitivity of copper. When sulfide reacts with copper ions (Cu^{+}), it produces copper(I) sulfide (Cu_2S), which exhibits properties of hardness, brittleness, and porosity. These attributes render it a non-protective corrosion product layer, particularly in the context of seawater flow. Furthermore, sulfide can also interact with nickel (Ni) to form non-protective nickel sulfide (Ni_2S). The specific formation processes for copper-sulfur (Cu-S) and nickel-sulfur (Ni-S) compounds are elaborated upon as follows [198];

$$Cu + HS^{-} \rightarrow Cu(HS^{-})_{ads} \tag{25}$$

$$Cu(HS^{-})_{ad} \rightarrow Cu(HS) + e^{-} \tag{26}$$

$$Cu(HS) \rightarrow Cu^{+} + HS^{-} \tag{27}$$

$$2Cu^{+} + HS^{-} + OH^{-} \rightarrow Cu_2S\downarrow + H_2O \tag{28}$$

$$2Cu^{+} + S^{2-} \rightarrow Cu_2S\downarrow \tag{29}$$

$$Ni + HS^{-} \rightarrow Ni(HS^{-})_{ads} \tag{30}$$

$$Ni(HS^{-})_{ads} + Ni(HS)^{+} + 2e^{-} \tag{31}$$

$$Ni(HS)^{+} \rightarrow Ni^{2+} + HS^{-} \tag{32}$$

$$Ni^{2+} + HS^{-} + OH^{-} \rightarrow (NiS)\downarrow + H_2O \tag{33}$$

$$Ni^{2+} + S^{2-} \rightarrow NiS\downarrow \tag{34}$$

The electrochemistry of copper in NH_3-containing environments is critical to many industrial applications, including the cleaning of copper surfaces, the etching of printed circuit boards, and the electrodeposition of Cu. Furthermore, a comprehensive understanding of this behavior is essential for analyzing corrosion processes in Cu alloys. The thermodynamics of the $Cu–NH_3–H_2O$ system has been explored by multiple researchers, contributing valuable insights to this field of study [199–203]. Recent discussions have highlighted the controversy surrounding the stability regions of Cu (II) oxide and Cu (I) oxide. The findings have been discussed by Tromans [204], who noted that ammonia exhibits an activity greater than one in concentrated solutions. This phenomenon slightly alters the stability domains of copper species in the potential-pH diagrams Additionally, Halpern [205], examined the corrosion rate of Cu in NH_3 proposed the following reaction::

$$Cu + 4NH_3\ 1/2O_2\ H_2O \rightarrow Cu(NH_3)_4^{2+} + 2OH^{-} \tag{35}$$

The process likely commenced with a very thin oxide film, san activation complex comprising $NH_3–Cu^{2+}–O^{2-}$. Sedzimir [206] investigated the impact of temperature and NH_3 concentration on corrosion rates utilizing a rotating disk method and thus;

$$Cu + Cu(NH_3)_4^{2+} \rightarrow 2Cu(NH_3)_2^{+} \tag{36}$$

It was concluded that NH_3 concentration did not affect the rate of the surface reaction. Khobotova et al. [207–209], conducted extensive research on the products of the positive-going and chemical dissolution of copper in a $Cu(NH_3)_4Cl_2$ medium. They observed various corrosion products, including CuCl, Cu_2O, $Cu(OH)_2$, and CuO.

The corrosion of Cu alloys is significantly affected by the presence of sulfide and ammonia contaminants in the environment. These pollutants can increase corrosion by interacting with the metal surface and forming various corrosion products, such as copper sulfides and copper ammonia complexes. Understanding and addressing the impact of these contaminants is essential for ensuring the longevity of copper and copper-based alloys in various applications.

4.7. *Effect of Biofouling*

Biofouling is the process by which living organisms aggregate on surfaces exposed to water, leading to notable economic, structural, and microbial challenges on various structures such as ship hulls, piers, oil rigs, power plants, pipelines, water treatment plants, and medical equipment [210]. Consequently impairing their operational efficiency, and thereby, causing significant financial repercussions [211]. Issues arising from biofouling, such as heightened corrosion, greater biomass accumulation, elevated drag resistance, the introduction of non-native species, reduced water flow, and decreased oxygen levels, are frequently documented within the aquaculture and maritime sectors [212,213]. The regulation of bacterial adherence and subsequent biofilm development can be attained through various approaches, contingent upon the surrounding circumstances and the specific field of use. Predominant methods employed for biofilm regulation typically revolve around the application of antimicrobial agents, including the utilization of biocides and disinfectants (for surface applications) or the administration of antibiotics (for biofilms associated with healthcare settings).

Copper-based alloys possess an extensive history of demonstrating favorable corrosion and fouling resistance in maritime environments, with a proven track record dating back to the 18th century [214]. Bulow reported that minor adjustments to some copper alloys by including or removing additional elements can significantly impact their ability to resist corrosion when exposed to unpolluted seawater currents [215]. Biofouling poses a significant challenge to mariculture in tropical waters. Santos et al demonstrated the effectiveness of copper alloy metal as an antifouling agent in tropical waters in comparison to nylon meshs and monofilaments in an experimental period of 150 days [216]. The results of the seven and eight-year use of a 90/10 copper-nickel alloy were reported to have better corrosion resistance than copper while having similar biofouling resistance in offshore structures and boat hulls [217].

Metallic copper or copper alloys are popularly used in plumbing systems. Water distribution systems for drinking (DWDS) lacks microbiological safety [218], as a result of the ability of microorganisms to colonize DWDS and form biofilms. Copper has been employed in potable water systems on a global scale, with several studies focusing on assessing its antimicrobial characteristics and its role in biofilm development within drinking water distribution systems (DWDS) [219–223]. In addition, Silhan et al. evaluated DW biofilm formation and reported that the 58-day biofilms formed at 15°C on Cu pipes had lower density biofilms in comparison to medium-density polyethylene (PE) pipes, galvanized steel (GS) and cross-linked polyethylene (PEX). Moreover, they provided evidence indicating that the viability of E. coli within biofilms formed on copper piping exhibited a decreased rate compared to that on polyethylene [224].

Based on the physiological functions and advantages associated with copper and its alloys, researchers have directed their attention toward creating innovative biomaterials containing copper. These materials demonstrate distinctive qualities in safeguarding the cardiovascular system, facilitating the mending of bone fractures, and demonstrating antimicrobial properties. The antimicrobial qualities of Cu are widely acknowledged within the scientific community, leading to heightened enthusiasm for utilizing these materials in medical devices [225]. For instance, Ti-Cu alloy dental implants were also found to demonstrate good antimicrobial functions [226,227]. Also, Bergemann et al showed the efficacy of TiCuN coated orthopedic implants in killing *S. epidermidis* strains within 24 hours of incubation [228]. Furthermore, Lemraski et al investigated the antimicrobial efficiency of PVA/CS/Cu-NPs fibres fabricated through electrospinning against both gram-negative and gram-positive bacterial strains. The nanofibers exhibited notable antimicrobial efficacy towards Bacillus cereus, *E. coli, S. aureus,* and *Pseudomonas aeruginosa* [229]. In a clinical study, Mohammady et al. explored the microbial load on Cu-coated and non-coated Cu surfaces within a typical ICU setting. The findings revealed a 96% reduction in bacterial burden on copper-coated surfaces that had frequent contact, compared to the control surfaces [230].

The formation of biofouling in cooling water systems poses a significant challenge for industries by causing corrosion, diminishing heat transfer efficiency, and elevating pressure drop [231]. The existence of biofilms within cooling towers has the potential to serve as a reservoir for environmental pathogens, thereby posing a significant public health threat. Cu alloys are extensively utilized in various industrial sectors, particularly in heating and cooling systems, owing to their remarkable attributes including high conductivity, corrosion resistance, mechanical malleability, and the antimicrobial and antibiofilm properties associated with copper. Li et al. reported that copper material was less prone to degradation in the presence of microorganisms than MS1010 in a cooling water environment [232]. Several studies have introduced novel approaches for integrating copper into heat exchangers and cooling systems, aiming to mitigate biofouling and its associated drawbacks [233,234]. The impact of copper materials on the prevention of bacterial adhesion and the retardation of biofilm formation is undeniable.

5. The mitigation strategies to elongate copper-based alloys

5.1. Corrosion mitigation techniques for copper-based alloy

Over the years, several mitigation techniques have been employed to elongate the service life of copper and copper-based alloys. These techniques will be highlighted in this section as presented in Fig. 10 below.

5.1.1. Alloying

Alloying is a fundamental approach to enhancing the resistance to corrosion of copper-based alloys. By adding specific elements, such as tin, aluminum, or nickel, the corrosion behavior of the base copper alloy can be significantly improved. Bronze, primarily composed of copper and tin, is one of the oldest and most widely used copper alloys. Tin improves the corrosion resistance of copper by promoting the development of a stable oxide layer on the surface, which acts as a shielding barrier. Bronze alloys are particularly resistant to corrosion in marine and industrial environments, making them ideal for applications such as ship propellers, bearings, and sculptures [235,236]. Aluminum bronze alloys contain aluminum as the primary alloying element, which significantly enhances corrosion resistance, particularly in aggressive environments like seawater and acidic conditions. The aluminum in the alloy forms a protective aluminum oxide layer on the surface, which is highly resistant to corrosion [236,237]. Cupronickel alloys, typically containing 10-30% nickel, are known for their excellent corrosion resistance, especially in seawater environments. The nickel content in these alloys enhances their resistance to chloride-induced corrosion, making them ideal for marine applications such as ship hulls, offshore platforms, and desalination plants [238,239].

Recent advancements in metallurgy have led to the development of high-performance copper alloys with enhanced corrosion resistance. These alloys often contain a combination of elements, such as chromium, zirconium, and beryllium, which provide superior resistance to corrosion, wear, and high temperatures. These alloys are used in demanding applications, such as aerospace, power generation, and chemical processing [240,241].

5.1.2. Surface Modification

Surface modification techniques, such as passivation, ion implantation, and laser treatment, can significantly enhance the corrosion

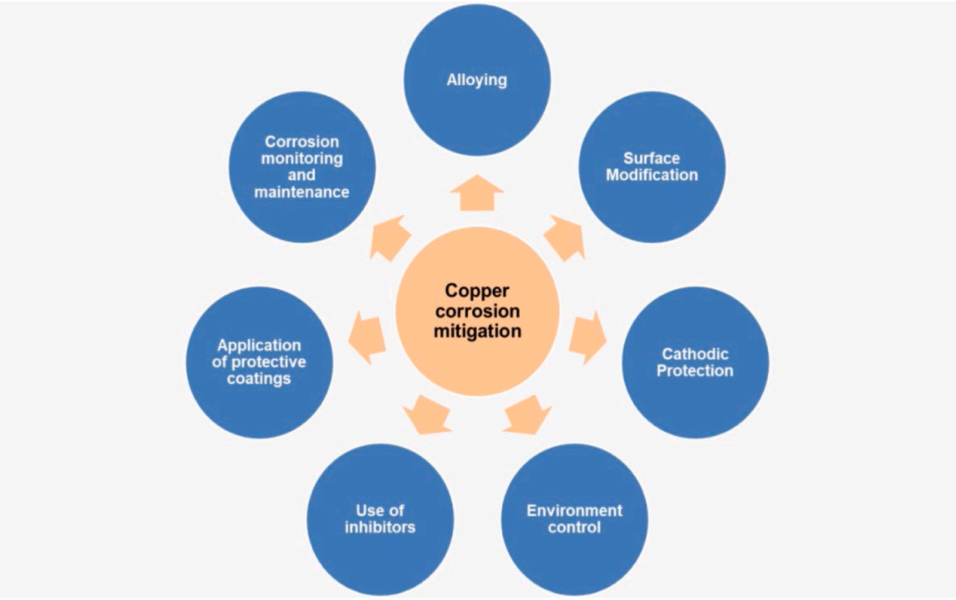

Fig. 10. Copper and copper alloys corrosion mitigation strategies.

resistance of copper-based alloys by altering the surface properties of the material. Passivation involves treating the copper alloy surface with oxidizing agents, such as nitric acid, to form a thin, protective oxide layer. This layer significantly reduces the metal's reactivity, preventing further oxidation and corrosion. Passivation is commonly used in stainless steels and is also effective for certain copper alloys, particularly in electronics and architectural applications [235,241]. Ion implantation is a surface modification technique that involves bombarding the metal surface with high-energy ions, which penetrate the surface and modify its properties. This technique can improve the hardness, wear resistance, and corrosion resistance of copper alloys by altering the surface composition and structure. Ion implantation is particularly effective in enhancing the performance of copper alloys in aggressive environments, such as in aerospace and medical devices [237,238]. Laser surface treatment involves using a high-energy laser beam to melt and rapidly solidify the surface of the metal. This process can refine the microstructure, eliminate surface defects, and enhance the corrosion resistance of copper alloys. Laser treatment is particularly effective for improving the performance of copper alloys in high-temperature and corrosive environments [240,242].

5.1.3. Cathodic Protection

Cathodic protection is a widely used method to control the corrosion of copper-based alloys, particularly in marine and underground applications. This method involves making the copper alloy the cathode of an electrochemical cell, thereby preventing it from corroding. Types of cathodic protection includes, sacrificial anode, impressed current, galvanic coupling and design considerations. In sacrificial anode cathodic protection, a more anodic metal, like zinc or magnesium, is connected to the copper alloy. The sacrificial anode corrodes preferentially, protecting the copper alloy from corrosion. This method is commonly used in pipelines, ship hulls, and offshore structures [236,243]. Impressed current cathodic protection involves applying an external current to the copper alloy, making it the cathode. This method is used when sacrificial anodes are not sufficient to provide the required level of protection, particularly in large structures such as bridges and storage tanks [240,244]. Galvanic coupling is a technique where a copper alloy is electrically connected to a more anodic metal, such as zinc, to protect it from corrosion. This approach is commonly used in electrical connectors and marine applications [237,245]. The design of cathodic protection systems for copper-based alloys requires careful consideration of various factors, including the type of alloy, environmental conditions, and specific application. For instance, in marine environments, the resistivity of seawater, the presence of biofouling, and the accessibility of the structure must be taken into account [238,243].

5.1.4. Environmental control

Controlling the environment surrounding copper-based alloys remarkably decreases the risk of corrosion. This includes managing factors such as humidity, temperature, and exposure to corrosive agents. In environments where copper alloys are exposed to high humidity and temperature, such as in tropical or industrial settings, controlling these factors is crucial to preventing corrosion. Dehumidification, air conditioning, and the use of desiccants are effective methods for reducing humidity levels, thereby minimizing the risk of corrosion [246,247]. Controlling the chemical environment, such as the concentration and pH of corrosive agents, is essential for preventing the corrosion of copper alloys. For example, in cooling water systems, maintaining the pH within an optimal range and using corrosion inhibitors can significantly drop the dissolution rate of copper condenser tubes [238,244]. In certain industrial processes, such as heat treatment and welding, using a protective atmosphere, such as argon or nitrogen, can prevent the oxidation and corrosion of copper alloys. In particular, applications where the presence of oxygen or moisture can lead to rapid degradation of the material [235,248]. Adhering to environmental regulations and standards is crucial for ensuring the long-term protection of copper alloys. These regulations often specify limits on the exposure of copper alloys to corrosive agents, such as sulfur compounds and chlorides, and require the implementation of corrosion control measures [240,241].

5.1.5. Use of inhibitors

Corrosion inhibitors are chemicals that, when introduced to the environment, can significantly reduce the corrosion rate of copper and copper-based alloys. These inhibitors function by forming a protective barrier on the metal surface. There are two main classes of inhibitor which are organic and inorganic inhibitors. Traditional inhibitors, particularly those that contain heavy metals such as chromium and lead, present substantial risks to both environmental integrity and public health. These substances are highly toxic and have the potential to bioaccumulate in living organisms, leading to serious health issues for humans, including respiratory problems and an increased risk of cancer, as well as harmful effects on ecosystems, such as damage to aquatic life and soil health.

In response to these pressing concerns, researchers are increasingly focused on the development and exploration of "green" or sustainable corrosion inhibitors. These innovative alternatives are often derived from natural sources or synthesized in a way that minimizes their environmental impact. Green inhibitors are typically less toxic and biodegradable, significantly reducing the risk of pollution and harm to human health and the environment [249–254]. By prioritizing these safer options, industries can effectively combat corrosion while embracing a more sustainable and environmentally responsible approach to infrastructure maintenance.

Organic inhibitors, such as benzotriazole (BTA) and imidazoles, are widely used to protect copper and its alloys in various environments. BTA is particularly effective in preventing the tarnishing and pitting of copper in environments containing chlorides and other halides [241,244]. Inorganic inhibitors, such as phosphates and molybdates, also play a crucial role in corrosion mitigation. These inhibitors can precipitate as insoluble compounds on the metal surface, providing a barrier that limits the access of corrosive species. Phosphates, for example, are commonly used in cooling water systems to prevent the corrosion of copper condenser tubes [235,247]. In some cases, the combination of inorganic and organic inhibitors can provide enhanced protection against corrosion. For instance, the combination of BTA and phosphate inhibitors has been shown to offer superior protection for copper alloys in both neutral and acidic environments [255,256].

5.1.6. Application of protective coatings

Applying protective coatings is a widely used method to enhance the corrosion resistance of Cu-alloys. Coatings act as a physical barrier, blocking the interaction between the metal surface and the corrosive environment. Various types of coatings such as metallic, organic, conversion and Nano coatings have been explore in the protection of copper and copper-based alloys. Metallic coatings, such as tin, zinc, and nickel, are commonly applied to copper alloys to improve their corrosion resistance. Tin coatings are particularly effective in preventing the tarnishing of copper in air and are widely used in the food and beverage industry. Nickel coatings provide excellent resistance to oxidation and wear, making them suitable for harsh industrial environments [238,243]. Organic coatings, such as epoxy, polyurethane, and acrylic, provide good corrosion protection by forming a continuous, adherent layer over the metal surface. These coatings are often used in combination with primers and sealers to enhance their adhesion and durability. Epoxy coatings, in particular, are known for their excellent chemical resistance and are widely used in marine and industrial applications [240,245]. Conversion coatings involve chemically treating the metal surface to form a protective layer that enhances corrosion resistance. Chromate conversion coatings, for example, are commonly used to protect copper alloys in aerospace and military applications. These coatings not only provide corrosion resistance but also improve the adhesion of subsequent paint layers [237]. Recent advancements in nanotechnology have led to the development of nanocoatings that offer superior corrosion protection. These coatings typically consist of nanoparticles embedded in a polymer matrix, which provides a dense, impermeable barrier against corrosive agents. Nanocoatings are particularly effective in protecting copper alloys in aggressive environments, such as marine and industrial settings [242,257]. With reported reduction in inhibition efficiency of most inhibitors and anticorrosive coating materials with increasing temperature, research focus is gradually shifting to thermally stable coatings. In their research on the corrosion of copper and copper alloys in seawater, coated with hydrothermal carbon through electrochemical methods, Gan et al. [258] reported that the carbon-rich layer, measuring 120 μm in thickness, exhibits considerable corrosion resistance. The application of this carbonized coating notably decreases the corrosion current and shifts the corrosion potentials to a range of 0.05–0.1 V. Furthermore, the hydrothermally produced carbon layer functions as a passivation coating for both pure copper and copper alloys, thereby effectively reducing their corrosion rates in seawater environments.

5.1.7. *Corrosion monitoring and maintenance*

Regular monitoring and maintenance are essential components of a comprehensive corrosion mitigation strategy. These practices ensure the early detection of corrosion and allow for timely interventions to prevent further damage. Corrosion monitoring techniques include electrochemical methods, such as linear polarization resistance (LPR), electrochemical impedance spectroscopy (EIS), ultrasonic testing, eddy current testing and radography. These techniques can provide valuable information about the corrosion rate, the effectiveness of corrosion inhibitors, and the condition of protective coatings. Regular monitoring allows for the early detection of corrosion and timely maintenance to prevent further degradation [245,257] Predictive maintenance involves using data from corrosion monitoring to predict when maintenance should be performed to prevent failures. This approach is particularly useful in critical applications, such as power generation, oil and gas production, and aerospace, where unexpected failures can have severe consequences. Predictive methods can help optimize maintenance schedules, reduce downtime, and extend the service life of copper-based alloys [242,244].

Regular inspection and cleaning are vital for maintaining the corrosion resistance of copper-based alloys. Inspections can identify early signs of corrosion, such as pitting, discoloration, or coating degradation, allowing for timely repairs. Cleaning removes corrosive agents, such as chloride salts or sulfur compounds, from the metal surface, reducing the risk of corrosion. In marine environments, regular cleaning is particularly important to prevent biofouling, which can create localized aggressive environments and accelerate corrosion [238, 243]. When corrosion is detected, repair and recoating are often necessary to restore the protective properties of the metal. This may involve removing corroded material, applying a new protective coating, or replacing sacrificial anodes in cathodic protection systems. The choice of repair method depends on the extent of the corrosion, the type of alloy, and the operating environment. Recoating with high-performance coatings, such as epoxy or polyurethane, can provide long-term protection and extend the service life of the copper alloy [244].

5.2. *Corrosion inhibitors for copper in chloride and other corrosive media*

To extend the service life of copper and its alloys, corrosion inhibitors need to block the anodic and cathodic processes. Aside from protective coatings and/or anodic/cathodic protection techniques, the mitigation of copper's corrosion process has mainly involved using corrosion-inhibiting agents [259]. The most effective inhibiting agents for copper corrosion is benzotriazole (BTA) and its derivatives. BTA is a heterocyclic organic compound synthesized via the reaction of ortho-phenylenediamine acetic acid and sodium nitrite [260]. These compounds are attractive because they are reasonably soluble in water to a level; that can support effective corrosion inhibition properties. In addition, benzotriazole is only slightly toxic indicating minimal environmental hazard. Considering the multidimensional corrosion process of copper, a compound with multipurpose anticorrosion ability would be able to function in diverse situations. BTA conformation in aqueous solution depends on the pH of the medium according to equations 19-20. Thus, in near neutral or minimal acidic pH, the compound exists in the undissociated form as BTAH, whereas in low pH (acidic environments) the protonated form dominates (BTAH2+); whilst at alkaline pH the negatively charged form (BTA-) predominates. The possible protonation of BTA in low pH is consistent with the mechanism put forward previously by Njoku et al. [261–263]. Fig. 11 demonstrates the protonation and various natures of chemical interactions or complexes between copper and benzotriazole which served as a model for the interaction of all the related compounds leading to the protection of Cu.

$$\mathrm{BTAH_2^+} \leftrightarrow \mathrm{BTAH} + \mathrm{H^+},\ \mathrm{pK_1} \sim 1 \tag{37}$$

$$\mathrm{BTAH} \leftrightarrow \mathrm{BTA^-} + \mathrm{H^+},\ \mathrm{pK_2} = 8.2 \tag{38}$$

Thus, the corrosion protection efficacy of BTA can be related to the complex formation (Cu(I)–BTAH) following the reactions (39) and (40) [259]:

$$\mathrm{Cu_{(s)}} + \mathrm{BTAH_{(aq)}} \rightarrow \mathrm{Cu : BTAH_{(ads)}} + \mathrm{H^+} \tag{39}$$

$$\mathrm{Cu : BTAH_{(ads)}} \rightarrow \mathrm{Cu(I) - BTA(s)} + \mathrm{H^+_{(aq)}} + \mathrm{e-} \tag{40}$$

However, it has been posited that if the plane of the Cu(I)BTA surface complex is aligned parallel to the Cu surface, the protection of Cu is based mainly on the d of a Cu(I)BTA surface complex film other than the chemisorbed BTAH film [260]. Generally, the adsorption of an inhibitor film (organic) on any metal surface is accompanied by displacing a proportional water molecule previously adsorbed following the reaction [264]:

$$\mathrm{Inh_{sol}} + \mathrm{xH_2O_{ads}} \rightarrow \mathrm{Inh_{ads}} + \mathrm{xH_2O_{sol}} \tag{41}$$

where x describes the number of water molecules displaced by a molecule of inhibitor species adsorbed [264]. The protonated BTA molecules could adsorb electronically in low pH following equations 42-43.

$$\mathrm{Cu} \rightarrow \mathrm{Cu^{2+}} + 2\mathrm{e^-} \tag{42}$$

$$\mathrm{Cu^{2+}} + \mathrm{Inh_{ads}} \rightarrow \mathrm{(Cu - Inh)^{2+}_{ads}} \tag{43}$$

Furthermore, it has been widely reported that N, S, O, P and double bonds in a conjugated system in organic molecules contribute to the inhibition performance of organic molecules [265,266]. Thus, to advance the development of BTA-based inhibitors, derivatives with different groups have been studied over the years as corrosion inhibition of Cu. In this regard derivatives of BTA and other related compounds have been investigated as corrosion inhibitors for copper. For instance, the report of Tasic and Milan [267] investigated benzotriazole and its derivatives, namely, 5-methyl- 1H-benzotriazole (MBTAH) and 5-chloro-1H-benzotriazole as corrosion in an acidic sulfate medium. Following the previous reviews [259,260], modification and substitution can improve the performance of BTA as a corrosion inhibitor of copper and its alloys. Fig. 12 shows some typical structures of BTA and related compounds that have been investigated as corrosion inhibitors for copper in different mediums.

Given this, several kinds of corrosion inhibitors have been proposed for the protection of copper ranging from inorganic [276,277], organic [30], green [278], polymeric [279] and even natural products [280]. Table 4 collected the various inhibitors that have been reported in recent years for copper and copper based alloys protection including the nature of copper and the environments highlighting the heightened achievements in copper corrosion inhibition.

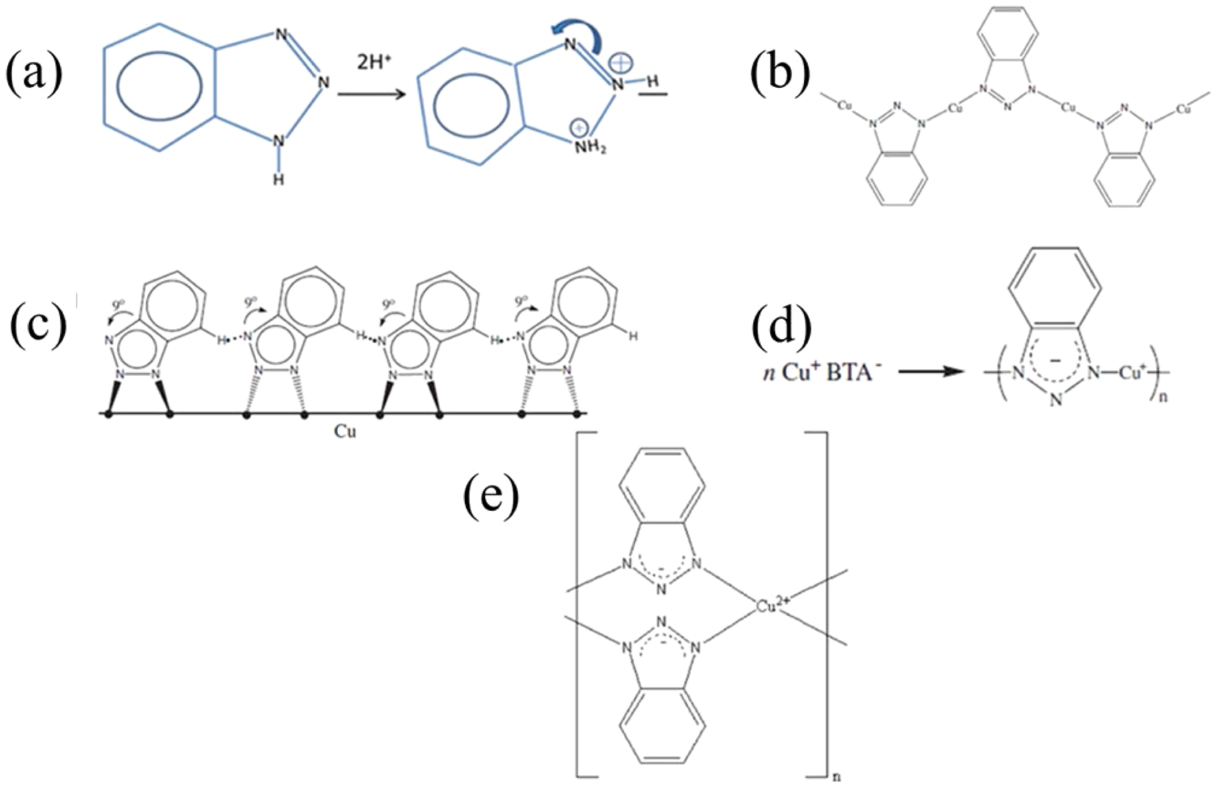

Fig. 11. The protonation of BTA in an acidic environment as proposed by Njoku et al. [261–263], copper-BTAH complex structure, the structure of the first chemisorbed BTA layer on copper, and the Cu(II)(BTAH)$_2$ structure as collated by Finšgar, and Milošev [260].

Computational studies in the last decades have been employed to study how organic inhibitors interact with metal surfaces, which is essential for predicting their protection efficiency at the atomic level. Rahimi et al. [281] have utilized DFT (density functional theory) and MDS (molecular dynamics simulation) to understand the copper corrosion protection potentials of several oxalohydrazide and the methylated structures. Exploring MDS on the various derivatives of the xalohydrazide on the Cu (111) surface reveals how the degree of methylation influences the adsorption orientation and the stable parallel adsorption mode. The data reveal that derivatives with highly parallel adsorption orientation on the Cu surface exhibit the strongest adsorption. As shown in Fig. 13, the adsorption orientation of oxalohydrazide derivatives on the Cu(III) surface is associated with their interaction energy. Compounds oriented in a parallel fashion (Fig. 13a) exhibit higher interaction energy values compared to those oriented perpendicularly (Fig. 13b). The values collated in Fig. 13c provide the corresponding interaction energies, indicating that the nature and degree of adsorption orientation, as computed by MDS, are linked to the interaction energy, while the interaction energy is linked to the inherent inhibition efficiency. Going further, Mahamdi et al. [282] employed MDS and DFT to appraise and propose the corrosion inhibition mechanism of copper in saline environments, utilizing coating films derived from chitosan and chitosan Schiff base. The studies reveal that the incorporation of $SrTiO_3$ (STO) ceramic nanoparticles into matrices of epichlorohydrin-crosslinked chitosan-salicylaldehyde Schiff base (CS-S-Ep) to yield CS-S-Ep-STO nanocomposite showed enhanced adsorption energy, which is attributed to the inclusion of oxygen and nitrogen heteroatoms, such as -C=N-, -C-O-, -OH and SrTiO3 groups on the composite. In another calculation, quantum chemical calculations enabled the investigation of the corrosion inhibition of 2-mercaptobenzothiazole (MBT) on copper, where the surface was locally de-passivated [283]. The computational studies reveal that the partially oxide-covered sites are the most reactive sites on the copper surface, which are charged and susceptible to interacting with the inhibitor. The MBT forms a covalent interaction with the charged, partially oxide-covered sites on both the surface and edges of the copper via both intact and dissociative adsorption modes. Intact adsorption occurs when unsaturated oxygen is present, while dissociative adsorption readily takes place in the presence of doubly unsaturated oxygen at the oxide edges [283]. In another investigation, DFT and MDS were adopted to divulge the inhibition mechanisms of triazole derivatives on copper [284]. The computational analysis reveals how the lone electron pair orbitals of O, N, and S atoms in triazole inhibitor derivatives hybridize with the Cu-d orbital to form covalent bonds. This enhances the adsorption passivation action, predicting the effectiveness of each inhibitor as a corrosion inhibitor at the atomic level. DFT, MDS, and Monte Carlo simulations provide an innovative approach for efficiently selecting inhibitors. Thus, with the successes recorded with computational studies including DFT and MDS, several researchers have integrated computational data to study the corrosion inhibition of copper in various media [285,286].

5.3. Anticorrosion coatings for the protection of copper and copper-based alloys

The application of corrosion inhibitors, anticorrosion coatings, and molecular passivators are some of the recent techniques developed for the corrosion protection of copper alloys. We will critically examine the use of anticorrosion coatings in this subsection. Since the onset of corrosion begins when metallic surfaces directly interact with corrosion-promoting species, like oxygen, moisture, and ions of sulfur and chlorine, the most efficient way of discouraging and impeding such interactions is the use of barriers (e.g. anticorrosion coatings and films) on metal surfaces [31]. The barriers function by significantly blocking/impeding the diffusion of the corrosion-promoting species, thereby controlling the rate of metal corrosion [306]. A pictorial depiction of this strategy is illustrated in Fig. 14 (a) where Bai et al. [307] fabricated a dual purpose coating, called (PNCA), by modifying the surface of nickel-copper alloy (NCA) with perfluorodecyltrimethoxysilane for the

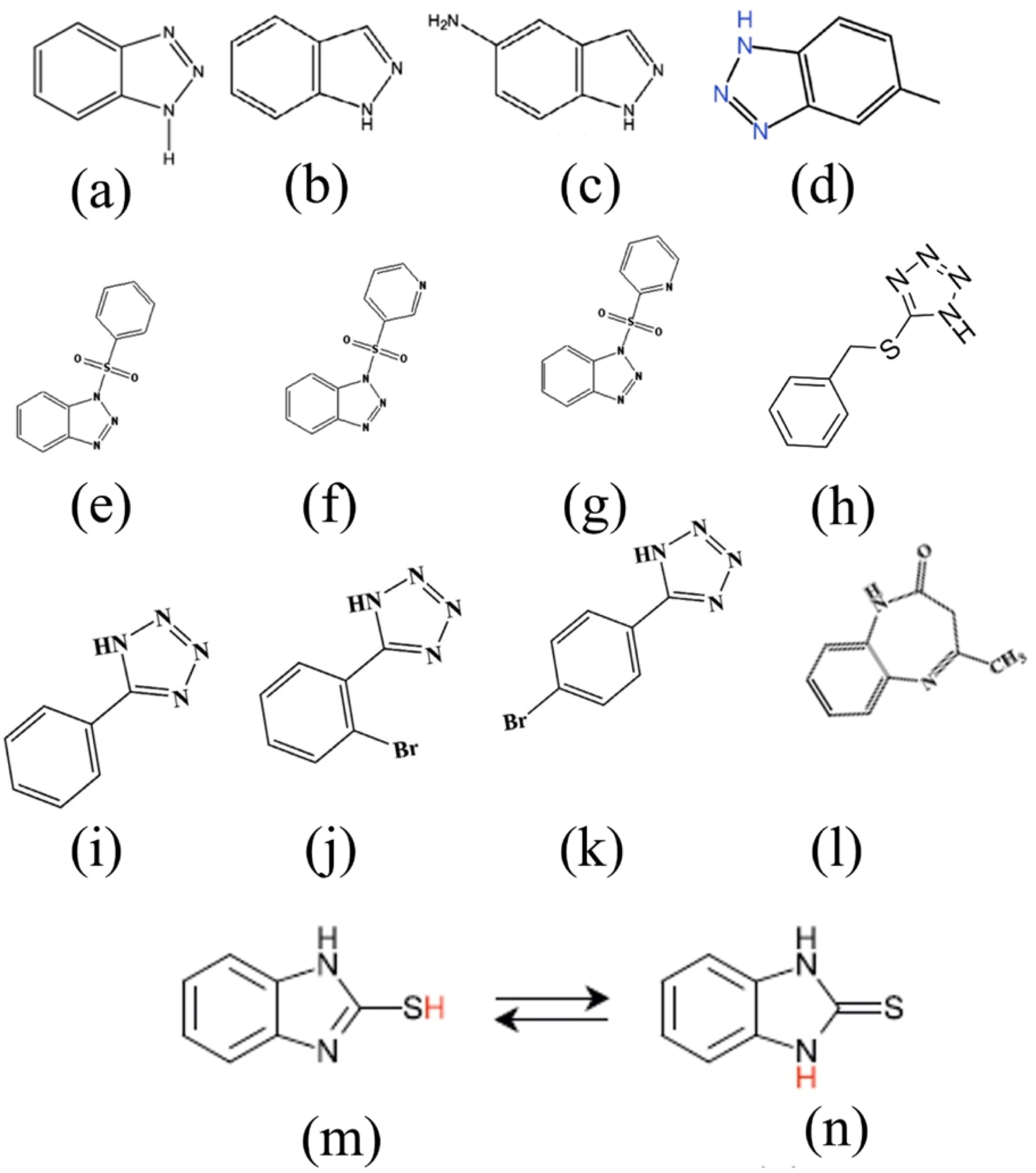

Fig. 12. BTA and related compounds used for copper protection in different environments (a) benzotriazole used for copper protection inflow conditions [268], (b-c) indazole derivative for protection of copper in 3.0% NaCl solution [269], (d) 5-Methyl(1H)benzotriazole adsorption on the copper surface [270], (f-g)1-(Phenylsulfonyl)-1H-benzotriazole (f), 1-(3-Pyridinylsulfonyl)-1H-benzotriazole (f) and 1-(2-Pyridinylsulfonyl)-1H-benzotriazole (g) as corrosion protection of copper in varied concentrations of 1M HNO_3 [271], (h) 5-(3-Aminophenyl)tetrazole as corrosion of Cu–Ni (90/10) alloy in seawater [272], (i-k) 5-Phenyltetrazole (i), 5-(2-Bromophenyl)-1H-Tetrazole (j), 5-(4-Bromophenyl)-2H-Tetrazole (k) as inhibitors for copper in 0.5 M H_2SO_4 [273]. (l) benzodiazepine as efficient corrosion inhibitor for copper in 3.5% NaCl solution [274], (m-n) benzimidazole (m), and 2- mercaptobenzimidazole (n) as corrosion inhibitor of copper that bond stronger to the surface and display weaker tendency to form soluble complexes with hydrated copper (II) ion [275].

protection of brass, an alloy of copper.

As previously stated, anticorrosion coatings establish physical barriers on metal surfaces, thereby providing effective protection against aggressive contaminants present in their immediate environments. This is a crucial method for preventing corrosion, and there have been significant advancements in materials science of copper following the use of advanced coating materials to protect copper against corrosion. These materials comprise a wide variety of choices, such as graphene, conductive polymers, and inorganic materials (including nitrides, oxides, and carbides). Table 5 summarizes some of the notable results obtained for the fabrication of anticorrosion coatings on copper-based substrates. This growing diversity of coating materials has presented new opportunities to improve the protectability of copper against corrosion, and they have shown tremendous potentials in a number of industrial applications.

Moreover, the use of organic polymers like epoxy resin is a common method for preventing corrosion of metal substrates. Conducting polymers with specific electrical conductivity can facilitate the creation of passivation layers on metal surfaces through their oxidative properties, unlike traditional organic coatings that primarily act as physical

Table 4
The collection of different inhibitors for copper corrosion protection in different environments.

Type of copper alloy	Inhibitor compound	medium	Key findings and inhibition efficiency (IE)	Ref.
Organic compounds				
Copper	Different organic corrosion inhibitors and their derivatives that prevent copper corrosion	Chloride Environments (3.5 wt% NaCl)	Highlighted the unique copper corrosion mitigation abilities of various inhibitors, providing a foundation for future research and inhibitor selection.	[287]
copper	Expired linezolid and piperacillin	1.0 M HNO_3	Good corrosion resistance due to the formation of a complex between copper ions and the drug. Langmuir adsorption isotherm.	[288]
copper	N,N-bis(2-ethylhexyl)-4-methyl-1H-benzotriazol-1-methanamine (NBTAH) 2,5-bis(octyldithio)-1,3,4-thiadiazole (BTDA),	Oil-in-water (O/W) emulsions	Formation of multilayer inhibitor films which significantly reduced the wettability of the O/W emulsions on the copper surface, thus isolating copper from the corrosive medium	[289]
Pure copper (99.9%)	2-mercaptobenzothiazole and 2-amino benzothiazole	Artificial seawater	Very good corrosion performance with IE of 90 % at 0.5 mg/L at room temperature. Reduction in IE to approximately 70% revealed physisorption.	[290]
Copper rod, 99.9% purity	Ionic liquid - (1,4- (Divinyl-imidazolium bromide) butane	0.5 M HCl	Excellent corrosion performance with IE 99% at 2 mM.	[291]
Copper rod, 99.9% purity	Imidazole derivatives (4-methyl-5-hydroxylmetylimidazole, 1-phenyl-4methylimidazole, 1-(p -tolyl)-4-methylimidazole	0.5 M H_2SO_4	Corrosion resistance is structure-sensitive. The best inhibition efficiency (93%) was obtained by adding a phenyl ring to the imidazole structure	[292]
copper	Thiazolyl-based ionic liquids (3, 3′-Diethylthiadicarbocyanine iodide and Thioflavin	0.1 M HCl	Formation of a protective oxide film which increases with the addition of halides. As anticipated, iodide offered the best-enhanced adsorption. Both chemisorption and physisorption.	[293]
Plant extracts (Biomass inhibitors)				
Copper pipes	Palm oil	3.5% NaCl	Excellent corrosion resistance with IE of 99.60% at 150 ppm.	[294]
copper	Acteoside (ACT) isolated from A. orientalis L.	1.0 M HNO_3	Formation of a protective layer that alters the copper dissolution, which improves with increasing concentration.	[295]
copper	Lotus Leaf	Saline water	Formation of a hydrophobic film on the copper surface, which blocks the active sites on the Cu surface. The blocking degree improves with the higher number of layers of the film	[296]
Copper	Lady Finger Caps	0.5 M NaCl	Potent inhibitor with IE of 89%, which increased to 96% on the synergistic effect of NiO nanoparticles.	[297]
copper	*Pyracantha fortuneana*	0.5 H_2SO_4 media	Excellent inhibition efficiency exceeding 95 % at 600 mg/L.	[293]
copper	*Rhododendron simsii* leaf extract	0.5 H_2SO_4	Excellent corrosion resistance with 92.6% at 500 mg/L.	[298]
copper	*Capsicum annuum* L. leaf extract	0.5 M H_2SO_4	Excellent corrosion potential with IE 94 % at 500 mg/L.	[299]
copper	*Lycium barbarum* leaf extract	0.5 M H_2SO_4	Excellent corrosion performance with IE of 92.9%, 92.8%, and 94.1% at 298 K, 303 K, and 308 K, respectively at 400 mg/L.	[299]
Copper	*Morinda tinctoria*	1 M HCl	Potent inhibitor with maximum IE of 80%.	[300]
copper	*Davidia involucrata* leaf extract	0.5 M H_2SO_4	Good corrosion resistance with IE of 90% at different temperatures	[300]
copper	Oleuropein from *Olea europaea* leaves	1.0 M H_2SO_4	Mixed-type inhibitor with excellent IE, peaking at 98.92% on addition of 100 mg/L	[280]
Polymers				
copper	4-((1H-indol-3-yl)methyl)phenol (IMP) and 4-(di (1Hindol-3-yl)methyl)phenol (DIMP) based copolymer	0.5 M H_2SO_4	Excellent corrosion protection performance reaching staggering IE of 99.3 %	[301]
copper	*Alginate biopolymer* (SA)	1 M HCl	Good corrosion resistance which peaks at IE of 83% on addition 0.1mg L^{-1}	[302]
copper	Chitosan polymer	Polluted synthetic seawater (SSW) containing 20 ppm of sulfide	Physical adsorption with IE of 89% at 800 ppm.	[303]
copper	Polyacrylic Acid (PAM) and Polyacrylamide Polymers (PAA)	1.0 M HNO_3	PAM displayed a slightly better copper protection tendency in nitric acid than PAA, IE of 88% and 84% in the presence of 250 mg/L at 298 K.	[304]
copper	Sulfonated aromatic polyamide (SAP)	1M HCl	IE of 92%, making it an effective anti-corrosion compound for copper protection	[305]

barriers. Furthermore, the conductivity difference facilitates the movement of electrons from the metal surfaces to the conductive polymer layers, creating an electrical barrier that hinders the flow of charges during corrosion. The conductive polymers commonly used for corrosion prevention are polythiophene (PTh), polypyrrole (PPy), polyindole (PIN), and polyaniline (PANi). Their chemical structures are illustrated in Fig. 14 (b). There is a significant body of literature on the use of conductive polymers for copper substrates and their impact on corrosion resistance [308–318].

Annibaldi et al. [319] reported the consistent electrodeposition of uniform and adherent polypyrrole on copper via a salicylate solution. Shabani-Nooshabadi and colleagues [320] conducted an electrodeposition of a PANi/zeolite nanocomposite onto a copper electrode submerged in a solution of sodium oxalate, achieving enhanced corrosion resistance relative to unmodified PANi. The study identified the optimal current density for the synthesis of the nanocomposite coatings, which led to a remarkable reduction in the corrosion rate by around 130 times in NaCl solution, in contrast to a coating-free copper. Additionally, Jafari and his team effectively produced a PANi/graphene nanocomposite film on a copper surface, and the electrochemical assessments demonstrated a remarkable corrosion inhibition efficiency of 98% in aqueous NaCl solution due to the protective properties of the composite film [321]. Other studies have also demonstrated that the PPy/PANI bilayer coating is considerably more effective in inhibiting the ingress of corrosive agents into underlying copper substrates. Pan et al. developed a bilayer coating approach, comprising a PPy layer on the inside and a PANi layer on the outside. Electrochemical evaluations indicated that both the bilayer PPy/PANi coating and the single PPy coating offered

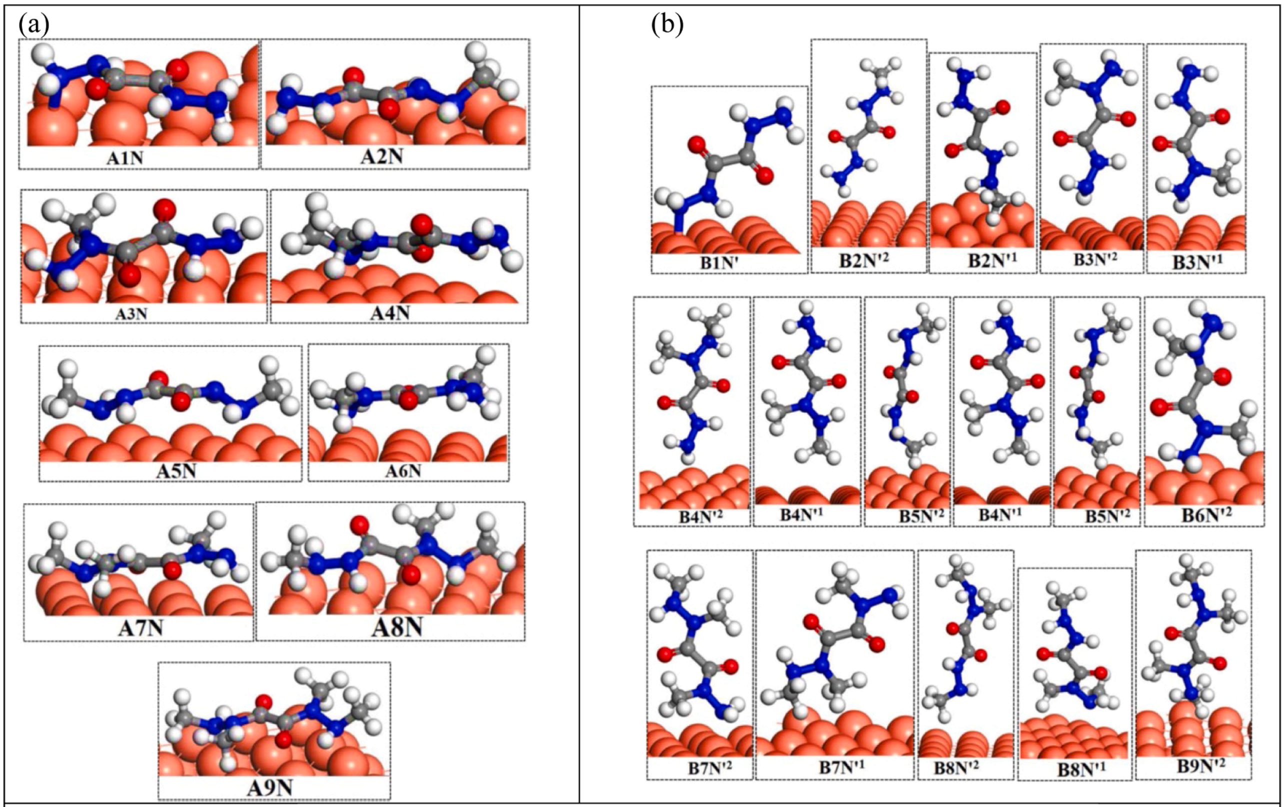

System	E_{ads}	E_{int}	System	E_{ads}	E_{int}
A1N	−31.4	−43.4	$\mathrm{B1N}'^{1}$	−10.7	−25.0
A2N	−37.9	−50.3	$\mathrm{B2N}'^{2}$	−13.9	−24.4
A3N	−36.9	−50.9	$\mathrm{B2N}'^{1}$	−38.0	−48.5
A4N	−42.8	−54.6	$\mathrm{B3N}'^{2}$	−27.0	−47.3
A5N	−43.8	−56.9	$\mathrm{B3N}'^{1}$	−19.8	–
A6N	−47.8	−53.7	$\mathrm{B4N}'^{2}$	−14.9	−25.0
A7N	−47.8	−59.7	$\mathrm{B4N}'^{1}$	−16.5	–
A8N	−45.7	−57.8	$\mathrm{B5N}'^{1}$	−8.44	−24.8
A9N	−49.8	−61.0	$\mathrm{B6N}'^{2}$	−32.4	−37.8
			$\mathrm{B6N}'^{1}$	−25.1	–
–	–	–	$\mathrm{B7N}'^{2}$	−27.4	−39.1
–	–	–	$\mathrm{B7N}'^{1}$	−25.1	35.6
–	–	–	$\mathrm{B8N}'^{2}$	−15.7	−26.3
–	–	–	$\mathrm{B8N}'^{1}$	−19.8	−21.9
–	–	–	$\mathrm{B9N}'^{2}$	−21.0	−30.5

(c)

Fig, 13. Orientation of the absorption of different derivatives of oxalohydrazide and the computed (a) the most stable and parallel derivatives on Cu(III) surface, (b) the most stable adsorption orientation of derivative adsorbed perpendicularly to Cu (111), (c) The corresponding $\Delta E_{adsorption}$ and interaction energy of the inhibitors in the gas phase (all in kcal mol^{-1}) [281].

comparable corrosion protection in acidic conditions at the initial period, effectively decreasing the corrosion rate by a factor of ten relative to a coating-free copper. Additionally, the bilayer coating demonstrated enhanced long-term corrosion protection, which was due to its enhanced barrier properties, hindering the ingress of corrosive agents.

Conducting polymers and their composites have shown significant potentials for the prevention of copper corrosion; however, certain challenges remain. Generally, anticorrosion coatings based on conducting polymers are more effective in less harsh corrosive systems, as they tend to decompose when exposed to high temperatures. Additionally, these coatings demonstrate limited effectiveness when applied as shields against corrosive gases (e.g. CO_2 and H_2S), especially under high-pressure conditions. Moreover, there is still a lack of broad understanding regarding the anticorrosion mechanisms of conducting polymers. In particular, the impact of their redox processes on the passivation of metal surfaces and the diffusion of aggressive species requires further investigation.

Graphene, recognized for its inertness and impermeability, presents significant potential for enhancing corrosion resistance. This material exhibits a range of advantageous electrochemical properties, and its exceptional thermal conductivity, substantial inherent capacity, and extensive specific surface area enable it to surpass many alternative materials. Additionally, graphene is characterized by remarkable strength, ductility, and notable chemical inertness, except when subjected to extreme reaction conditions [322]. It also offers resistance to oxidation, while its hydrophobic nature inhibits the formation of hydrogen bonds with water [323]. Given its numerous promising attributes, graphene is currently the subject of extensive research across various disciplines; however, the exploration of ultrathin graphene coatings as a protective barrier against corrosion remains insufficiently

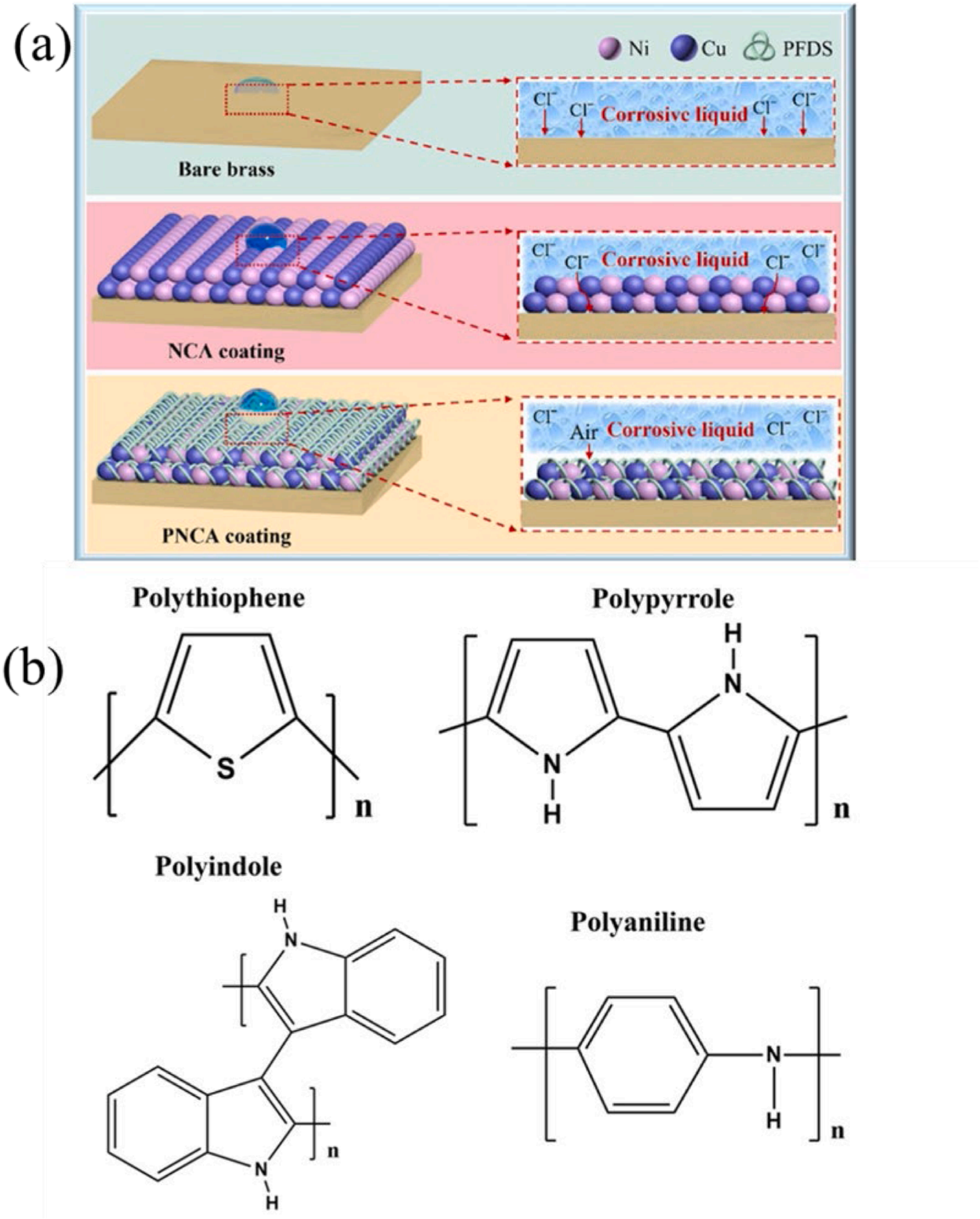

Fig. 14. (a) A critical interface outlook for the anticorrosion behavior of NCA coating and PNCA coating on bare brass exposed to a chloride environment [307]; (b) Some conductive polymers commonly used for anticorrosion coatings [308–318].

addressed. Zhu et al. successfully mitigated the local corrosion at defect locations on a copper substrate and reduced the galvanic corrosion between graphene and the metal by the deposition of a fluorocarbon polymer film onto the copper substrate which was pre-coated with a single layer of graphene in a Plasma-Enhanced Chemical Vapor Deposition system [324]. Zheng et al. produced polydopamine-graphene composites on a copper substrate, resulting in a remarkable corrosion resistance with a protection efficacy of 99.8%, and this enhanced protection was ascribed to the π-π interrelations between graphene and polydopamine [325]. Wu et al. proposed an innovative fluorination approach to develop a graphene-based anticorrosion coating [326]. The incorporation of fluorine atoms was believed to form bonds with carbon atoms at defect locations, thereby decreasing the corrosion rates by significantly raising the diffusion energy barriers for aggressive agents. Beyond pure graphene anti-corrosion layers, a graphene-based composite coating has attracted numerous research interests.

As with graphene, significant potentials have been demonstrated for other two-dimensional nanosheets as materials for the next generation. One of such is hexagonal boron nitride (hBN). hBN ranks as the second most utilized two-dimensional material, renowned for its exceptional chemical and thermal stability, as well as its potential applications in ultrathin coatings. Nevertheless, in contrast to graphene, its anticorrosion properties have received relatively limited attention. hBN possesses numerous characteristics that could enhance its effectiveness as an important nanofiller in anticorrosion coatings [344]. Due to the polar B-N bonds impeding electron transfer, BN does not conduct electricity [345]. Consequently, hBN is not anticipated to elevate corrosion rates, unlike graphene, which is a conductor of electricity. Moreover, its electrically insulating properties are effective in mitigating the risks associated with galvanic corrosion, which is observed for graphene coatings. Additionally, boron can undergo oxidation in environments rich in oxygen, leading to the formation of heat-stable interface

Table 5
Some anticorrosion coatings on copper-based substrates.

Anticorrosion coating	Test environment	Protection efficiency (%)	Ref.
Graphene	0.1 M Na_2SO_4	86	[327]
3-layer graphene	0.1 M NaCl	99.1	[328]
Melamine-treated graphene oxide	3.5 wt% NaCl	90.83	[329]
Fluorinated graphene	3.5 wt% NaCl	97	[326]
Fluorocarbon polymer/single-layer graphene	3.5 wt% NaCl	99.98	[326]
Polydopamine/graphene	3.5 wt% NaCl	99.8	[325]
Silane-graphene oxide	1 M NaCl	99.18	[330]
BTA-silane-graphene oxide	1 M NaCl	99.97	[330]
Acetone-based graphene	3.5 wt% NaCl	99	[331]
Monolayer hexagonal boron nitride	0.1 M NaOH	96	[332]
< 4 layers hexagonal boron nitride	0.5 M H_2SO_4	93	[333]
20 layers hexagonal boron nitride	3.5 wt% NaCl	99.5	[334]
Al_2O_3/monolayer hexagonal boron nitride	3.5 wt% NaCl	99.9	[335]
Al_2O_3/monolayer graphene	3.5 wt% NaCl	99	[335]
Graphene-ODA/TiO2	0.5 M H_2SO_4	93.6	[336]
S-N-C-doped TiO_2	3.5 wt% NaCl	99.6	[337]
Silane/Ti3C2T*x*	3.5 wt% NaCl	99.91	[338]
PNEA/sodium silicate	3.5 wt% NaCl	94.84	[318]
PENA-Mo	0.5 M H_2SO_4	91.72	[310]
BTA/silica-doped PPy	5 wt% NaCl	98	[339]
PPy-tartrate/ PPy-dodecylbenzene sulfonate	0.1 M NaCl	93.8	[340]
PNMA/phosphate	3.5 wt% NaCl	97	[318]
Polyeugenol-gum arabic/graphene oxide	3.5 wt% NaCl	72.12	[341]
Fluorographene/epoxy (coating)	3.5 wt% NaCl	99.95	[342]
benzaldehyde-derived molecules/ mesoporous silica/graphene oxide	3.5 wt% NaCl	99.85	[343]

compounds, such as boron oxide [346]. This oxide can provide protection by preventing direct contact and/or by facilitating the repair of any damage to coatings. Hwang et al showed that that hBN creates a monolayer that inhibits oxygen diffusion in an oxidizing environment, even at elevated temperatures [347]. Further research studies have shown that coatings of 15–20 layers of hBN nanosheets can enhance open circuit potential and mitigate metallic oxidation, including the oxidation of copper foils. Two-dimensional hBN thin coatings exhibit resilience against microbes, harsh chemicals, and high temperatures, and these are attributed to their chemical inertness and low environmental coupling [334].

6. Recent application of copper-based alloys

copper and copper-based alloys have continued to find relevant multi-faceted applications (Fig. 15) in several areas including antimicrobial homewares, shape memory alloys (SMAs), electrical cables, valves, high-speed railway contact wires, pipelines, boilers, heat exchangers, ship turbines, propellers and gears, amongst others [348]. Additionally, in today's world of cutting-edge technologies and microelectronics, the use of Cu is such a pivotal one including fundamental role of joining material within computer chips and integrated circuits (ICs) [349,350]. Moreover, copper and its alloys are well placed as nanowires (NWs) where they find good applications as current collectors in batteries and in the production of transparent conducting membranes for displays and solar panels cells [351,352]. Perhaps most notably, copper nanoparticles (CuNPs) have emerged as widely utilized and cost-effective substitutes for precious metals like silver (Ag), gold (Au), platinum (Pt), and across a range of fields, including spectroscopy, sensors, flexible devices, environmental science, catalysis, energy research, biomedicine, and biology [353–357].

6.1. *Copper-based alloys as shape-memory alloys (SMAs)*

Copper-based shape-memory alloys represent a unique category of functional alloys characterized by their ability to undergo a shape memory effect and super-elastic behavior, attributed to their reversible martensitic transformation. These properties make them particularly suitable for applications in sensors, microcontrollers, and actuators [358]. This class of alloys is distinguished by two notable functional characteristics: the shape memory effect, which allows them to return to their original shape after being deformed, and super-elasticity property, also known as pseudoelasticity, which enables them to recover from significant non-linear deformations during loading and unloading cycles [359,360].

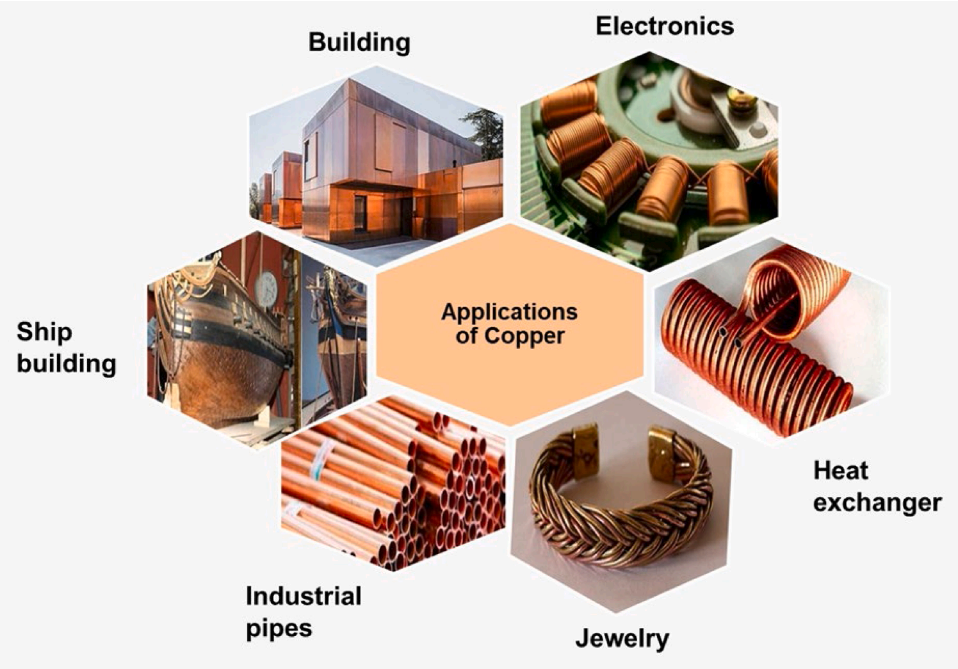

Fig. 15. Multi-faceted applications of copper-based alloys.

6.2. Copper-based alloy as an anti-microbial agent

Cu has demonstrated significant efficacy against microorganisms, and its incorporation markedly reduces bacterial adhesion and growth on various surfaces. The antimicrobial action of copper is attributed to several mechanisms: the release of Cu ions from Cu-containing alloys, the infiltration of these ions into bacterial cell membranes resulting in cell lysis, and the subsequent production of reactive oxygen species, which leads to protein oxidation and DNA damage within the bacterial cells, ultimately resulting in their demise. This mechanism highlights the essential role of Cu in successfully diminishing bacterial colonization across a wide range of surfaces, including household items and equipment, offering substantial advantages over many conventional antibacterial agents [361].

6.3. Copper-based alloy as an excellent electrical and thermal conductor

Cu stands out among common metals as having the highest levels of both electrical and thermal conductivity. Nevertheless, the electrical conductivity of copper-based alloys can differ significantly depending on the specific alloying elements used. For instance, high Cu alloys that incorporate iron, zirconium, magnesium, chromium, and tellurium demonstrate improved strength while maintaining conductivity levels between 75% and 90%. In contrast, another category of copper-based alloys, which includes combinations of zinc, cobalt, tin, and phosphorus, offers relatively lower yet still commendable strength, with conductivity ranging from 50% to 75%. Furthermore, these characteristics can be optimized by selecting appropriate alloying elements and applying suitable heat treatment methods, such as work-hardening, tempering, and annealing.

6.4. Copper as current collectors

The increasing demand for electric vehicles (EVs) and portable electronics has created a significant requirement for advanced energy storage systems characterized by high energy density, particularly in lithium-ion batteries (LIBs). Consequently, the utilization of Cu as a current collector, which encompasses structures such as Cu mesh, Cu foil, as well as 3D Cu frameworks (such as copper-based foams, coated Cu, and other innovative 3D copper-based structures, has emerged as a contemporary trend. In the design and fabrication of these systems, Cu foil, typically with a thickness ranging from 5 to 12 μm, is commonly employed as anode current collectors for LIBs. This preference is attributed to the low resistivity of the material (approximately 1.68×10^{-8} Ω m at 20°C), relatively low tensile strength (around 325 MPa), excellent electrochemical stability within the voltage range of 0 to 3 V versus Li/Li^{+} in $LiPF_6$ electrolyte, cost-effectiveness (approximately USD $640/m^2$), and widespread availability [362]. The choice of Cu for this application is primarily due to its inherent properties, which include high electrical conductivity, chemical resistance, flexibility, lightweight nature, affordability, and ease of processing.

6.5. Copper-based alloys in marine, offshore and chemical application

The primary use of copper and copper-based alloys in these sectors is largely attributed to their exceptional resistance to corrosion and oxidation in aqueous environments. Specifically, CuNi alloys that include iron are highly regarded materials in the construction of heat exchangers, marine vessels, power plants as well as serving as tubing and condenser materials in desalination facilities [363]. The corrosion resistance exhibited by these alloys is primarily due to the development of a stable and robust oxide layer on their surface, which is a result of the incorporated alloying elements. Alloys containing approximately 10–30% by weight of Ni demonstrate commendable resistance, even in hot seawater and under high flow speeds. In the chemical processing industry, CuNi alloys are utilized in the form of tubes, sheets, and cast products for applications in oil production, as well as in the manufacturing of pumps, valves, fittings, and propeller wheels, along with piping systems designed to handle salt and other highly corrosive substances. Additionally, these alloys are employed in various structures, including cooling systems, autoclaves, mixers, heat exchangers, agitators, pressure vessels, and other related equipment [364].

7. Challenges and Future Perspectives

Copper and its alloys are widely recognized for their sufficient strength, outstanding thermal and electrical conductivity, high ductility, excellent fabricability, and notable resistance to corrosion. Copper easily combines, either singly or in combination, with a number of well-known metallic elements, chiefly Zn, as well as Ni, Al, Si, Mn, Fe, Co, and Cr. The main aim of alloying other elements into Cu is to improve its strength and resistance to softening while maintaining its fundamental properties of fabricability, electrical conductivity, and corrosion resistance. These attributes facilitate the broad utilization of copper and its alloys across multiple industries, as illustrated in Fig. 16.

While copper and copper-based alloys exhibit superior properties and offer a wide range of applications, their utilization is not without significant challenges. These challenges stem from their physical, chemical, and economic characteristics, as well as limitations related to specific applications. Notable issues include high material costs, mechanical constraints, and limitations in thermal and electrical performance, manufacturing difficulties, compatibility concerns, industry-specific requirements, and vulnerability to corrosion in particular environments. For instance, the industrial use of copper-based alloys in extremely high-temperature environments, such as in electrical and thermal systems, aerospace applications, nuclear power plants, and bearings and bushings, poses significant challenges for these industries. It is important to note that the established corrosion inhibitors and anti-corrosion coatings materials have proven to be more effective at lower temperatures. This situation has opened up new research opportunities for developing high-temperature anti-corrosion materials specifically designed for copper-based alloys used in high-temperature applications.

The future of copper-based alloys appears highly promising, driven by technological advancements, sustainability objectives, and the increasing demand for high-performance materials. Different industries are expected to capitalize on these innovations, allowing copper-based alloys to remain crucial in high-tech, energy, and sustainable applications. This trend will ensure their ongoing relevance in future technological developments. Some of the key perspectives on the applications of copper and copper-based alloys are highlighted below:

1. They are essential for the development of miniaturized electronic components, including microprocessors and connectors, due to their excellent mechanical characteristics and electrical conductivity. As the implementation of 5G technology and future communication systems expands, the importance of copper alloys with enhanced conductivity and minimized signal loss will become increasingly critical.
2. They are expected to be integral to the functionality of electric vehicle (EV) motors, battery systems, charging stations, and power electronics, owing to their superior conductivity and thermal characteristics. Furthermore, copper alloys that exhibit enhanced corrosion resistance will continue to be vital for renewable energy infrastructure, particularly in applications such as inverters and generators
3. Current research initiatives are concentrating on the fabrication of coatings, corrosion inhibitors, and surface treatments designed to enhance the resistance of copper and its alloys against harsh environments, including those found in deep-sea and high-temperature scenarios. Future studies may investigate the potential for developing copper alloys with self-healing capabilities, or self-healing anticorrosion materials which could prove to be a significant

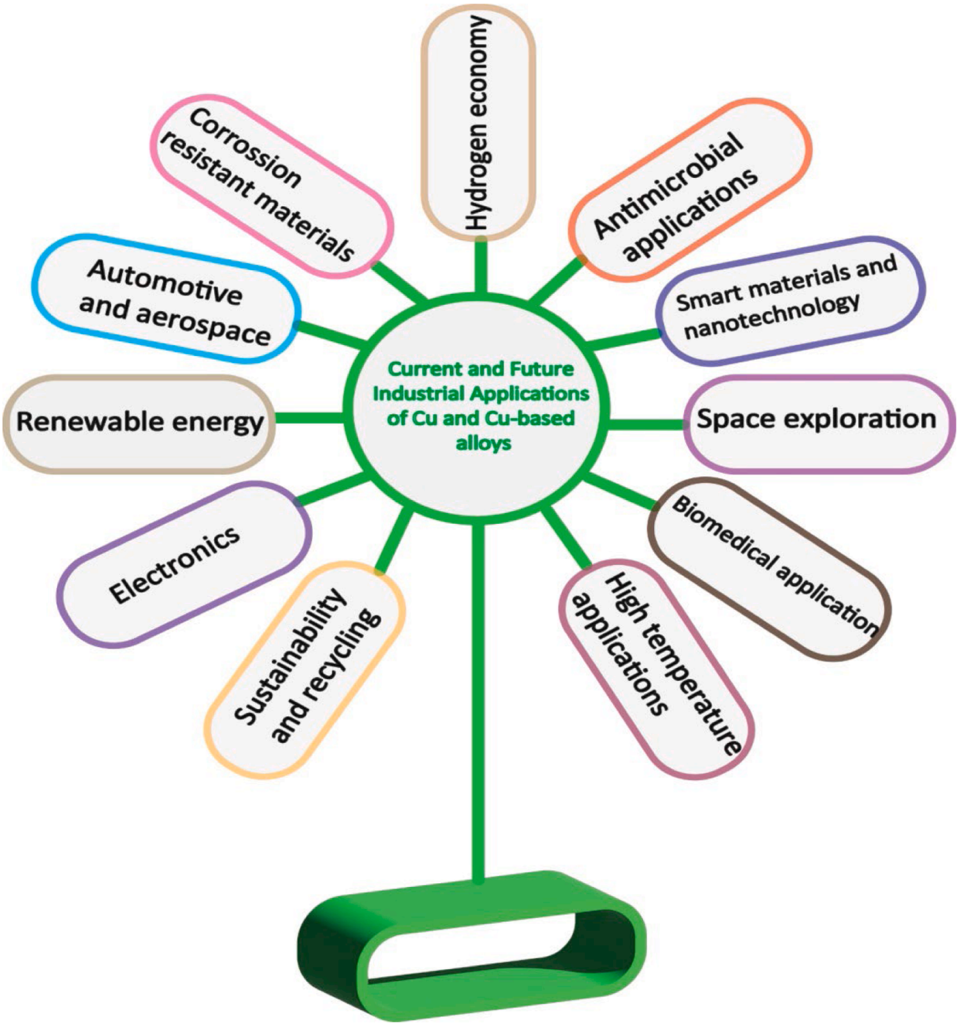

Fig, 16. Current and future industrial applications of copper and copper-based alloys.

advancement for essential applications in the aerospace, marine sectors and other high temperature applications.

4. Efforts are directed toward the development of lighter and stronger copper alloys for use in components such as bearings, bushings, and structural elements. The integration of copper alloys with composite materials may facilitate an optimal balance between weight reduction and performance.
5. Cu alloys with improved high-temperature performance are promising for next-generation power plants, rockets, and turbines.
6. These alloys are expected to be instrumental in the hydrogen economy, especially in their utilization in heat exchangers and hydrogen storage systems, which are essential for advancing the shift towards a low-carbon economy.

8. Conclusions

Copper and its alloys are extensively utilized in numerous industries owing to their superior corrosion resistance, high strength, exceptional fatigue resistance, and excellent electrical and thermal conductivity, along with their visual appeal. Nevertheless, these materials remain vulnerable to corrosion, which can result in premature failures when subjected to severe environmental conditions. The corrosion behavior of copper and its alloys is influenced by a range of factors, which can be categorized into material and environmental factors. Material factors encompass macrostructural attributes such as size and grain orientation, phases, inclusions, as well as the presence of alloying elements and manufacturing processes. Conversely, environmental factors pertain to the effects of interfaces, the presence of chloride ions, humidity levels, and contaminants such as ammonia and sulfides. Various mitigation strategies have been investigated for the protection of copper and its alloys against corrosion. These strategies include alloying, surface treatments, cathodic protection, the use of corrosion inhibitors, and anticorrosion coatings. Although these approaches have proven effective in mitigating Cu corrosion to some degree, the emergence of advanced self-healing materials presents promising prospects for enhanced protection. Such advancements are anticipated to significantly bolster the performance of copper-based materials in demanding environments, including high-temperature and deep-sea conditions. This thorough review provides essential insights into the corrosion mechanisms affecting copper and its alloys, effective protection methods, and potential future applications of these materials.

CRediT authorship contribution statement

Okpo O. Ekerenam: Writing – review & editing, Writing – original draft, Conceptualization. **Alexander I. Ikeuba:** Writing – review & editing, Writing – original draft, Conceptualization. **Chigoziri N. Njoku:** Writing – review & editing, Writing – original draft. **Demian I. Njoku:** Writing – review & editing, Writing – original draft. **Wilfred Emori:** Writing – review & editing, Writing – original draft, Conceptualization. **Izuchukwu K. Nwokolo:** Writing – review & editing, Writing – original draft. **Ini-Ibehe N. Etim:** Writing – review & editing, Writing –

original draft. **Bright O. Okonkwo:** Writing – review & editing, Writing – original draft. **Inime I. Udoh:** Writing – review & editing, Writing – original draft, Formal analysis. **Enobong F. Daniel:** Writing – review & editing, Writing – original draft. **Paul C. Uzoma:** Writing – review & editing, Writing – original draft. **Bukola O. Awonusi:** Writing – review & editing, Writing – original draft. **Sharafadeen K. Kolawole:** Writing – review & editing, Writing – original draft. **Iniobong P. Etim:** Writing – review & editing, Writing – original draft. **Olajire S. Olanrele:** Writing – review & editing, Writing – original draft.

Declaration of competing interest

The authors declare that they have no known competing financial interests or personal relationships that could have appeared to influence the work reported in this paper.

Data availability

No data was used for the research described in the article.

References

[1] P. Zhou, K. Ogle, The Corrosion of Copper and Copper Alloys, Encyclopedia of Interfacial Chemistry (2020) 478–489.

[2] M.R. World, Advanced Copper Alloy Market Trends: Size, Share, Substantial Growth, and Highest CAGR to 2031, in, 2024.

[3] W. Schleich, Typical failures of CuNi 90/10 seawater tubing systems and how to avoid them. Eurocorr 2004, NACE, 2004, pp. 1–10.

[4] L. Wu, A. Ma, L. Zhang, Y. Zheng, Intergranular erosion corrosion of pure copper tube in flowing NaCl solution, Corros. Sci. 201 (2022).

[5] G. Zhang, T. Wang, Z. Ma, H. Zhou, L. Cui, K.Y. Yu, Comparison of cracking behavior of nanocrystalline Cu film on substrates of different plastic deformation mechanisms, Mater. Today Commun. 31 (2022).

[6] K. Chandra, V. Kain, S.K. Sinha, H.G. Gujar, Metallurgical investigation of a heat-exchanger tube of 70/30 cupronickel failed by fretting corrosion, Eng. Fail. Anal. 116 (2020).

[7] S. Hu, L. Liu, Y. Cui, Y. Li, F. Wang, Influence of hydrostatic pressure on the corrosion behavior of 90/10 copper-nickel alloy tube under alternating dry and wet condition, Corros. Sci. 146 (2019) 202–212.

[8] A. Fateh, M. Aliofkhazraei, A.R. Rezvanian, Review of corrosive environments for copper and its corrosion inhibitors, Arabian Journal of Chemistry 13 (2020) 482–544.

[9] K.D. Efird, D.B. Anderson, Sea water corrosion of 90–10 and 70–30 Cu–Ni: 14 year exposures, Materials Perfomance 14 (1975).

[10] O.O. Ekerenam, A.L. Ma, Y.G. Zheng, W. Emori, Electrochemical Behavior of Three 90Cu-10Ni Tubes from Different Manufacturers after Immersion in 3.5% NaCl Solution, Journal of Materials Engineering and Performance 26 (2017) 1701–1716.

[11] O.O. Ekerenam, A.L. Ma, Y.G. Zheng, S.Y. He, P.C. Okafor, Evolution of the Corrosion Product film and its effect on the Erosion-corrosion Behavior of two Commercial 90Cu-10Ni tubes immersed in Seawater, Acta Metallugica Sinica (English Letter) 31 (2018) 1148–1170.

[12] C. Leygraf, I. Odnevall Wallinder, J. Tidblad, T. Graedel, Atmospheric corrosion, John Wiley & Sons, New York, 2016.

[13] W.A. Badawy, M.M. El-Rabiei, H. Nady, Synergistic effects of alloying elements in Cu-ternary alloys in chloride solutions, Electrochim Acta 120 (2014).

[14] A.L. Ma, S.L. Jiang, Y.G. Zheng, W. Ke, Corrosion product film formed on the 90/10 copper–nickel tube in natural seawater: Composition/structure and formation mechanism, Corrosion Science 91 (2015) 245–261.

[15] T.D. Burleigh, D.H. Waldeck, Effect of alloying on the resistance of Cu-10% Ni alloys to seawater impingement, Corrosion 55 (1999) 800–804.

[16] K.M. Ismail, A.M. Fathi, W.A. Badaway, The influence of Ni content on the stability of copper–nickel alloys in alkaline sulphate solutions, Journal of Applied Electrochemistry 34 (2004) 823–831.

[17] A. Ma, S. Jiang, Y. Zheng, Z. Yao, W. Ke, S. Xia, Correlation Between Microstructure and Corrosion Behavior of Two 90Cu10Ni Alloy Tubes, Acta Metall. Sin. (Engl. Lett.) 27 (2014) 730–738.

[18] X. Zhu, T. Lei, Characteristics and formation of corrosion product films of 70Cu–30Ni alloy in seawater, Corros Sci 44 (2002) 67–79.

[19] O.O. Ekerenam, W. Emori, A. Ma, A.I. Obike, Corrosion studies of 90Cu-10Ni alloy tubes in simulated sulfide-polluted seawater under dynamic flow conditions, Safety in Extreme Environments 5 (2023) 221–242.

[20] W. Schleich, Application of copper–nickel alloy UNS C70600 for seawater service, in: CORROSION/2005 Annual Conference and Exhibition, Houston, NACE International, 2005, pp. 1–14.

[21] B.C. Syrett, Erosion-Corrosion of Copper-Nickel Alloys in Seawater and Other Aqueous Environments -A Literature Review, Corrosion NACE 32 (1976) 242–252.

[22] I. Hamidah, A. Solehudin, A. Hamdani, L. Hasanah, K. Khairurrijal, T. Kurniawan, R. Mamat, B. Hammouti, Corrosion of copper alloys in KOH, NaOH, NaCl, and HCl electrolyte solutions and its impact to the mechanical properties, Alex. Eng. J. 60 (2021) 2235–2243.

[23] W.S. Tait, Electrochemical corrosion basics. In Handbook of environmental degradation of materials, William Andrew Publishing, 2018, pp. 97–115.

[24] H.Y. Li, C.F. Dong, K. Xiao, X.G. Li, P. Zhong, Effects of chloride ion concentration and pH values on the corrosion behavior of Cr12Ni3Co12Mo4W ultra-high-strength martensitic stainless steel, Int. J. Miner. Metall. Mater. 23 (2016) 1286–1293.

[25] Y. Zhao, R. Mirzaeifar, Investigating the flow induced corrosion of copper in chloride-containing solution at the atomistic scale, Appl. Surf. Sci. 538 (2021).

[26] W. Emori, R. Zhanga, P.C. Okafor, X. Zheng, T. He, K. Wei, X. Lin, C. Cheng, Adsorption and corrosion inhibition performance of multi-phytoconstituents from Dioscorea septemloba on carbon steel in acidic media: Characterization, experimental and theoretical studies, Colloids and Surfaces A 590 (2020).

[27] M. Rezaei, Z. Mahidashti, S. Eftekhari, E. Abdi, A corrosion failure analysis of heat exchanger tubes operating in petrochemical refinery, Eng. Fail. Anal. 119 (2021) 105011.

[28] M. Pourbaix, Establishment and interpretation of potential – pH equilibrium diagrams, (1974).

[29] G. Bianchi, P. Longhi, Copper in sea-water, potential-pH diagramsCopper in Sea-Water, Potential-pH Diagrams, Corrosion Science 13 (1973) 853–864.

[30] A. Fateh, M. Aliofkhazraei, A.R. Rezvanian, Review of corrosive environments for copper and its corrosion inhibitors, Arab, J. Chem. 13 (2020) 481–544.

[31] X. She, J. Peng, Y. Qiang, Y. Zhou, S. Zhang, Recent advances in protective technologies against copper corrosion, J. Mater. Sci. Technol. 201 (2024) 75–94.

[32] R.L. Frost, Raman spectroscopy of selected copper minerals of significance in corrosion, Spectrochim, Acta Part A Mol. Biomol. Spectrosc. 59 (2003) 1195–1204.

[33] X. Xia, C. Xie, S. Cai, Z. Yang, X. Yang, Corrosion characteristics of copper microparticles and copper nanoparticles in distilled water, Corros. Sci. 48 (2006) 3924–3932.

[34] F.M. Galleguillos Madrid, A. Soliz, L. Cáceres, M. Bergendahl, S. Leiva-Guajardo, C. Portillo, D. Olivares, N. Toro, V. Jimenez-Arevalo, M. Páez, Green Corrosion Inhibitors for Metal and Alloys Protection in Contact with Aqueous Saline, Materials (Basel) 17 (2024).

[35] C. Verma, E.E. Ebenso, M.A. Quraishi, Corrosion inhibitors for ferrous and non-ferrous metals and alloys in ionic sodium chloride solutions: A review, J. Mol. Liq. 248 (2017) 927–942.

[36] S. Kumar, D. Li, K. Kaiyang Li, G. J, Y. Liu, C. Qin, J. Li, Y. Li, W. Wei Cao, Y. Zhai, G. Huang, tress Corrosion Cracking of Copper–Nickel Alloys: A Review, Coatings 13 (2023).

[37] B. Bobić, B. Jegdić, B. Jugović, J. Stevanović, B. Gligorijević, A.C. Murariu, Failures of brass condenser tubes, Structural Integrity and Life 16 (2016) 19–23.

[38] D. Arguelles, C. Campechano, R. Galván-Martínez, T. Jimenez, R. Orozco-Cruz, Corrosion Protection Behavior of Patinas on Copper Alloys in Historical Metal Heritage: Electrochemical Study, in: AiMES 2018 Meeting ECS, 2018.

[39] J. López, L. Veleva, D. López-Sauri, Multifractal detrended analysis of the corrosion potential fluctuations during copper patina formation on its first stages in sea water, Int. J. Electrochem. Sci 9 (2014) 1637–1649.

[40] H. Ren, Y. Liu, Z. Gong, B. Tan, H. Deng, J. Xiong, P. Shao, Q. Dai, J. Cao, R. Marzouki, Pumpkin leaf extract crop waste as a new degradable and environmentally friendly corrosion inhibitor, Langmuir 40 (2024) 5738–5752.

[41] S. Wan, H. Chen, B. Liao, X. Guo, Adsorption and anticorrosion mechanism of glucose-based functionalized carbon dots for copper in neutral solution, J. Taiwan Inst. Chem. Eng. 129 (2021) 289–298.

[42] L. Wu, A. Ma, L. Zhang, Y. Zheng, Intergranular erosion corrosion of pure copper tube in flowing NaCl solution, Corros. Sci. 201 (2022).

[43] D. Zhang, R. Liu, Y. Liu, S. Xing, L. Yang, E. Wei, X. Dou, Multiscale characterization of seawater pipe erosion of B10 copper–nickel alloy welded joints, Scientifc Reports 12 (2022) 2164.

[44] N.W. Farro, L. Veleva, A. P, Copper Marine Corrosion: I. Corrosion Rates in Atmospheric and Seawater Environments of Peruvian Port, The Open Corrosion Journal 2 (2009) 130–138.

[45] L. Wu, A. Ma, L. Zhang, G. Li, L. Hu, Z. Wang, Erosion–Corrosion Behavior of 90/10 and 70/30 Copper–Nickel Tubes in 1 wt%, NaCl Solution Metals 13 (2023).

[46] Y. Cai, Y. Xu, Y. Zhao, W. Zhang, J. Yao, M. Wei, K. Zhou, X. Ma, Quantitative Understanding of the Environmental Effect on B10 Copper Alloy Corrosion in Seawater Metals 11 (2021).

[47] A. Khalifeh, Stress Corrosion Cracking Damages (Eds.) (Ed.), in: Z.-M. Huang, S. Hemeda (Eds.), Failure Analysis, IntechOpen., 2019.

[48] M. Karthik, J. Abhinav, K.V. Shankar, Morphological and Mechanical Behaviour of Cu–Sn Alloys—A review, Metals and Materials International 27 (2021) 1915–1946.

[49] A. Taher, Corrosion Behavior of Copper-Nickel Alloy in Marine Environment (Review Paper), Applied Mechanics and Materials 799–800 (2015) 222–231.

[50] X. Zhang, Y. Zhang, B.-H. Tian, K. Song, P. Liu, Y. Jia, X. Chen, J. An, Z. Zhao, Y. Liu, X. Li, T. Yin, Review of nano-phase effects in high strength and conductivity copper alloys, Nanotechnology Reviews 8 (2019) 383–395.

[51] G. Duscher, M. Chisholm, U. Alber, M. Rühle, Bismuth Induced Embrittlement of Copper Grain Boundaries, Nature Materials 3 (2004) 621–626.

[52] K.W. Gao, W.Y. Chu, H.L. Li, Y.P. Liu, L.J. Qiao, Correspondence between hydrogen enhancing dezincification layer-induced stress and susceptibility to SCC of brass, Materials Science and Engineering: A 37 (2004) 51–56.

[53] F.-H. Liu, C.-T. Li, X. Zhang, Y. Li, A. Ren, Lead-induced stress corrosion behavior of Alloy 690., Beijing Keji Daxue Xuebao/, Journal of University of Science and Technology Beijing 35 (2013) 1034–1039.

[54] S.S. Anargh, S. Alok, M.P. Yadukrishnan, R.K. Arun, K.A. Anirudh, V.S. Karthik, in: Study of Stress Corrosion Cracking Resistance Of Copper Based Spinodal Alloys-Part 1 Materials Today: Proceedings 24, 2020, pp. 2185–2192.

[55] T. Asabe, M. Rifai, M. Yuasa, H. Miyamoto, Effect of Grain Size on the Stress Corrosion Cracking of Ultrafine Grained Cu-10 wt% Zn Alloy in Ammonia, International Journal of Corrosion (2017) 1–8.

[56] S.P. Knight, N. Birbilis, B.C. Muddle, A.R. Trueman, S.P. Lynch, Correlations between intergranular stress corrosion cracking, grain-boundary microchemistry, and grain-boundary electrochemistry for Al–Zn–Mg–Cu alloys, Corrosion Science 52 (2010) 4073–4080.

[57] X. Fan, D. Jiang, L. Zhong, T. Wang, S. Ren, Influence of microstructure on the crack propagation and corrosion resistance of AL-Zn-Mg-Cu alloy 7150, Materials Characterization - mater charact 58 (2007) 24–28.

[58] A. Khalifeh, Stress Corrosion Cracking Behavior of Materials (Ed.) (Ed.), in: Thanapalan (Ed.), Engineering Failure Analysis, IntechOpen, 2020.

[59] H. Chen, T. Zhang, Y. Wang, J. Zheng, Analysis on Stress Corrosion Cracking of Brass Connecting Nut Utilized in Pneumatic Mechanism for 500kV Tank Circuit Breaker, Journal of Physics: Conference Series 1676 (2020) 012240.

[60] S.A. Fernández, M.G. Alvarez, Passivity breakdown and stress corrosion cracking of α-brass in sodium nitrate solutions, Corrosion Science 58 (2011) 82–88.

[61] S. Sun, H. Wang, L. Zhang, Y. Hao, C. Li, S. Hu, Intergranular-stress corrosion cracking mechanism of brass in H2S environment: A DFT study, Computational Materials Science 170 (2019) 109193.

[62] L.J. Qiao, J.L. Luo, Effect of ammonia concentrations on SCC of α-brass under mode III loading, Scripta Materialia 35 (1996) 1475–1480.

[63] R. Davalos-Monteiro, Observations of Corrosion Product Formation and Stress Corrosion Cracking on Brass Samples Exposed to Ammonia Environments, Materials Research 22 (2018) e20180077.

[64] K. Habib, A. Husain, Stress corrosion cracking of copper-nickel alloys in sulphide polluted natural seawater at moderate temperatures, Desalination 97 (1994) 29–34.

[65] L.E. Eiselstein, R.D. Caligiuri, S.S. WING, B.C. Syrett, Mechanisms of Corrosion of copper-nickel alloys in Sulfide-polluted Seawater, in: Office of Naval Research, Arlington, Virginia, 1980.

[66] F. Al-Kharafi, A. Abdel nazeer, R. Abdullah, A. Galal, Effect of Sulfide-Containing Solutions on the Corrosion of Cu-Ni Alloys; Electrochemical and Surface Studies, in: ECS Meeting Abstracts, MA2014-02, 2014, p. 727.

[67] S. Torchio, Stress corrosion cracking of aluminium brass in acidic chloride solutions, Corrosion Science 21 (1981) 59–68.

[68] L. Lin, Y. Zhao, Stress corrosion cracking of aluminium brass induced by marine organism fouling (Eds.) (Ed.), in: R.H.J.S.A. Shipilov, J.-M. Olive, R.B. Rebak (Eds.), Environment-Induced Cracking of Materials, Elsevier., 2008, pp. 369–373.

[69] Y. Liu, M.A. Arenas, S.J. Garcia-Vergara, T. Hashimoto, P. Skeldon, G. E. Thompson, H. Habazaki, P. Bailey, T.C.Q. Noakes, Behaviour of copper during alkaline corrosion of Al–Cu alloys, Corrosion Science 50 (2008) 1475–1480.

[70] R. Nishimura, T. Yoshida, Stress corrosion cracking of Cu–30% Zn alloy in: Mattsson's solutions at pH 7.0 and 10.0 using constant load method – A proposal of SCC mechanism, Corrosion Science (2008) 1205–1213.

[71] R. Amendola, A. Acharjee, Microbiologically Influenced Corrosion of Copper and Its Alloys in Anaerobic Aqueous Environments: A Review, Front Microbiol 13 (2022) 1–10.

[72] C. Li, J. Wu, P. Wang, D. Zhang, L. Zhu, Y. Gao, W. Wang, Corrosion of Pseudomonas aeruginosa toward a Cu–Zn–Ni alloy inhibited by the simulative tidal region, Environmental Science and Pollution Research 31 (2024) 3628–3640.

[73] D. Mitra, E.-T. Kang, K.G. Neoh, Antimicrobial Copper-Based Materials and Coatings: Potential Multifaceted Biomedical Applications, ACS Appl Mater Interfaces 12 (2020) 21159–21182.

[74] J.S. de Andrade, M.R.S. Vieira, S.H. Oliveira, S.K. de Melo Santos, S.L. Urtiga Filho, Study of microbiologically induced corrosion of 5052 aluminum alloy by sulfate-reducing bacteria in seawater, Mater Chem Phys 241 (2020) 122296.

[75] M. Lavanya, A Brief Insight into Microbial Corrosion and its Mitigation with Eco-friendly Inhibitors, J Bio Tribocorros 7 (2021) 125.

[76] I.N. Etim, D.I. Njoku, P.C. Uzoma, S.K. Kolawole, O.S. Olanrele, O.O. Ekarenem, B.O. Okonkwo, A.I. Ikeuba, I.I. Udoh, C.N. Njoku, P. IEtim, W. Emori, Microbiologically Influenced Corrosion: A Concern for Oil and Gas Sector in Africa, Chemistry Africa 6 (2023).

[77] I.N. Etim, J. Wei, J. Dong, D. Xu, N. Chen, X. Wei, M. Su, W. Ke, Mitigation of the corrosion-causing Desulfovibrio desulfuricans biofilm using an organic silicon quaternary ammonium salt in alkaline media simulated concrete pore solutions, Biofouling 34 (2018).

[78] I.I.N. Etim, J. Dong, J. Wei, C. Nan, E.F. Daniel, D.B. Subedi, D. Xu, A. Prasad Yadav, M. Su, W. Ke, Mitigation of sulphate-reducing bacteria attack on the corrosion of 20SiMn steel rebar in sulphoaluminate concrete using organic silicon quaternary ammonium salt, Constr Build Mater 257 (2020).

[79] I.N. Etim, J. Dong, J. Wei, C. Nan, D.B. Pokharel, A.J. Umoh, D. Xu, M. Su, W. Ke, Effect of organic silicon quaternary ammonium salts on mitigating corrosion of reinforced steel induced by SRB in mild alkaline simulated concrete pore solution, J Mater Sci Technol (2020).

[80] J. Li, D. Zhang, X. Chen, D. Xu, D. Qiu, F. Wang, M. Easton, Laser directed energy deposited, ultrafine-grained functional titanium-copper alloys tailored for marine environments: Antibacterial and anti-microbial corrosion studies, J Mater Sci Technol 166 (2023) 21–33.

[81] A.M. Orta-Rivera, Y. Meléndez-Contés, N. Medina-Berríos, A.M. Gómez-Cardona, A. Ramos-Rodríguez, C. Cruz-Santiago, C. González-Dumeng, J. López, J. Escribano, J.J. Rivera-Otero, J. Díaz-Rivera, S.C. Díaz-Vélez, Z. Feliciano-Delgado, A.D. Tinoco, Copper-Based Antibiotic Strategies: Exploring Applications in the Hospital Setting and the Targeting of Cu Regulatory Pathways and Current Drug Design Trends, Inorganics (Basel) 11 (2023).

[82] J. Cheng, Y. Wu, J. Duan, G. Polat, S. Hong, J. Cheng, The influence of SRB on corrosion behavior of Cu-based medium-entropy alloy coating sprayed by HVOF, Bioelectrochemistry 156 (2024) 108633.

[83] S. Cao, Z.-M. Zhang, J.-Q. Zhang, R.-X. Wang, X.-Y. Wang, L. Yang, D.-F. Chen, G.-W. Qin, E.-L. Zhang, Improvement in antibacterial ability and cell cytotoxicity of Ti–Cu alloy by anodic oxidation, Rare Metals 41 (2022) 594–609.

[84] T. Chang, K. Butina, G. Herting, G.K. Rajarao, A. Richter-Dahlfors, E. Blomberg, I. Odnevall Wallinder, C. Leygraf, The interplay between atmospheric corrosion and antimicrobial efficiency of Cu and Cu5Zn5Al1Sn during simulated high-touch conditions, Corros Sci 185 (2021) 109433.

[85] G.M. Ingo, C. Riccucci, G. Guida, M. Pascucci, C. Giuliani, E. Messina, G. Fierro, G. Di Carlo, Micro-chemical investigation of corrosion products naturally grown on archaeological Cu-based artefacts retrieved from the Mediterranean sea, Appl Surf Sci 470 (2019) 695–706.

[86] C. Xin, N. Wang, Y. Chen, B. He, Q. Zhao, L. Chen, Y. Tang, B. Luo, Y. Zhao, X. Yang, Biological corrosion behaviour and antibacterial properties of Ti-Cu alloy with different Ti2Cu morphologies for dental applications, Mater Des 215 (2022) 110540.

[87] N. Boulay, M. Edwards, Role of Temperature, Chlorine, and Organic Matter in Copper Corrosion by-Product Release in Soft Water, Water Research 35 (2001) 683–690.

[88] Z. Peng, K. Ogle, The Corrosion of Copper and Copper Alloys, in: Encyclopedia of Interfacial Chemistry: Surface Science and Electrochemistry, 2017.

[89] Z. Zhao, W. Xu, H. Xin, F. Yu, Microstructure, corrosion and anti-bacterial investigation of novel Ti-xNb-yCu alloy for biomedical implant application, Journal of Materials Research and Technology 18 (2022) 5212–5225.

[90] S. Al-Saadi, R.K.S. Raman, M.R. Anisur, S. Ahmed, J. Crosswell, M. Alnuwaiser, C. Panter, Graphene coating on a nickel-copper alloy (Monel 400) for microbial corrosion resistance: Electrochemical and surface characterizations, Corros Sci 182 (2021) 109299.

[91] C. García-Mintegui, L.C. Córdoba, J. Buxadera-Palomero, A. Marquina, E. Jiménez-Piqué, M.P. Ginebra, J.L. Cortina, M. Pegueroles, Zn-Mg and Zn-Cu alloys for stenting applications: From nanoscale mechanical characterization to in vitro degradation and biocompatibility, Bioact Mater 6 (2020) 4430–4446.

[92] Y. Hu, B. Liao, L. Chen, B. Wei, J. Xu, C. Sun, Mitigating Sulfate-Reducing Bacteria-Induced Corrosion of Pure Copper in Simulated Oilfield-Produced Water Using Cetylpyridinium Chloride, Coatings 15 (2025).

[93] G.G. Guerini, M.H.R. Suenaga, V.G. Vital, M.R. Silva, V.T. Santos, F.G. Lobo, M. A. Cardoso, F.R. Simões, D.S. Pellosi, S.P. Vasconcellos, Effectiveness of a CuZnNi alloy in preventing microbial growth and biofilm architecture, Journal of Materials Research and Technology (2025).

[94] W. Dou, R. Jia, P. Jin, J. Liu, S. Chen, T. Gu, Investigation of the mechanism and characteristics of copper corrosion by sulfate reducing bacteria, Corros Sci 144 (2018) 237–248.

[95] E.-T.K.D. Mitra, K.G. Neoh, Antimicrobial copper-based materials and coatings: potential multifaceted biomedical applications, ACS Appl Mater Interfaces 12 (2019) 21159–21182.

[96] Z. Qiu, R. Qiu, Y. Xiao, J. Zheng, C. Lin, Slippery liquid-infused porous surface fabricated on CuZn: A barrier to abiotic seawater corrosion and microbiologically induced corrosion, Appl Surf Sci 457 (2018) 468–476.

[97] K. Rahmani, R. Jadidian, S. Haghtalab, Evaluation of inhibitors and biocides on the corrosion, scaling and biofouling control of carbon steel and copper–nickel alloys in a power plant cooling water system, Desalination 393 (2016) 174–185.

[98] D. Xu, E. Zhou, Y. Zhao, H.L. Li, Z. Liu, D. Zhang, C. Yang, H. Lin, X. Li, K. Yang, Enhanced resistance of 2205 Cu-bearing duplex stainless steel towards microbiologically influenced corrosion by marine aerobic Pseudomonas aeruginosa biofilms, J Mater Sci Technol 34 (2018) 1325–1336.

[99] M. Arroussi, J. Zhao, C. Bai, S. Zhang, Z. Xia, Q. Jia, K. Yang, R. Yang, Evaluation of inhibition effect on microbiologically influenced corrosion of Ti-5Cu alloy against marine Bacillus vietnamensis biofilm, Bioelectrochemistry 149 (2023) 108265.

[100] J. Wang, H. Li, M. Du, M.X. Sun, L. Ma, Study on mechanism underlying the acceleration of pitting corrosion of B30 copper–nickel alloy by sulfate-reducing bacteria in seawater, Science of The Total Environment 928 (2024).

[101] M. Li, Z. Hu, D. Liu, Y. Liang, S. Liu, B. Wang, C. Niu, D. Xu, J. Li, B. Han, Efficient antibacterial and microbial corrosion resistant photocatalytic coating: Enhancing performance with S-type heterojunction and Cu synergy, Chemical Engineering Journal 495 (2024).

[102] X. Shi, W. Yan, D. Xu, M. Yan, C. Yang, Y. Shan, K. Yang, Microbial corrosion resistance of a novel Cu-bearing pipeline steel, J Mater Sci Technol 34 (2018) 2480–2491.

[103] M. Chen, X. Wang, X. Hou, J. Qiu, E. Zhang, J. Hu, Enhanced mechanical, bio-corrosion, and antibacterial properties of Ti-Cu alloy by forming a gradient nanostructured surface layer, Surf Coat Technol 465 (2023).

[104] J. Liu, Y. Ouyang, R. Qiu, B. Ma, Y. Zhang, S. Hu, Compositing fluid infused in superhydrophobic Cu (OH) 2 nanoneedle matrix to inhibit abiotic and microbiologically induced corrosion of Cu in seawater environment, Prog Org Coat 142 (2020).

[105] L. Wang, H. Chu, J. Xie, M. Guo, L. Jiang, X. Xi, Y. Fang, W. Zhao, Comparative study on the microbial corrosion resistance of mortars with Cu-Ti amorphous alloys and TiO2 nanoparticles, Constr Build Mater 448 (2024).

[106] H. Huang, S. Singh, A. Juhasz, A. Roccisano, A.S.M. Ang, N. Stanford, Influence of copper distribution in thermally sprayed Cu-bearing coatings on corrosion and microbial activity, Surf Coat Technol 478 (2024).

[107] P. Marcus, Corrosion Mechanisms in Theory and Practice, Taylor & Francis, 2011.

[108] V. Krivy, M. Kubzova, K. Kreislova, V. Urban, Characterization of Corrosion Products on Weathering Steel Bridges Influenced by Chloride Deposition, Metals (Basel) 7 (2017).

[109] D. de la Fuente, J.G. Castaño, M. Morcillo, Long-Term Atmospheric Corrosion of Zinc, Corros Sci 49 (2007) 1420–1436.

[110] M. Morcillo, B. Chico, D. de la Fuente, J. Simancas, Looking Back on Contributions in the Field of Atmospheric Corrosion Offered by the MICAT Ibero-American Testing Network, International Journal of Corrosion (2012) 824365.

[111] S. Syed, Atmospheric Corrosion of Materials, Emirates Journal for Engineering Research 11 (2006) 1–24.

[112] Y. Lu, H. Xu, J. Wang, X. Kong, Oxygen Reduction Mechanism on Copper in a 0.5M H2SO4, Electrochim Acta 54 (2009) 3972–3978, 2009.

[113] P. Zhou, M.J. Hutchison, J.R. Scully, K. Ogle, The Anodic Dissolution of Copper Alloys: Pure Copper in Synthetic Tap Water, Electrochim Acta 191 (2016) 548–557, 2009.

[114] G. Hultquist, P. Szakalos, M. Graham, A. Belonoshko, G. Sproule, L. Gråsjö, P. Dorogokupets, B. Danilov, T. Aastrup, G. Wikmark, G.-K. Chuah, J.-C. Eriksson, A. Rosengren, Water Corrodes Copper, Catal Letters 132 (2009) 311–316, 2009.

[115] D.J.G. Ives, A.E. Rawson, Copper Corrosion: I . Thermodynamic Aspects, J Electrochem Soc 109 (1962) 447.

[116] T.H. Merkel, S.O. Pehkonen, General Corrosion of Copper in Domestic Drinking Water Installations: Scientific Background and Mechanistic Understanding, Corrosion Engineering, Science and Technology 41 (2006) 21–37.

[117] M.J. Hutchison, P. Zhou, K. Ogle, J.R. Scully, Enhanced Electrochemical Cu Release from Commercial Cu-Sn Alloys: Fate of the Alloying Elements in Artificial Perspiration, Electrochim Acta 241 (2017) 73–88.

[118] L. Robbiola, J.-M. Blengino, C. Fiaud, Morphology and Mechanisms of Formation of Natural Patinas on Archaeological Cu–Sn Alloys, Corros Sci 40 (1998) 2083–2111.

[119] F. Seuss, N. Gaag, S. Virtanen, Corrosion Mechanism of CuZn21Si3P in Aggressive Tap Water, Materials and Corrosion 68 (2017) 42–49.

[120] Q. Liu, H. Luo, C. Dong, K. Xiao, X. Li, The Electrochemical Behaviour of Brass in NaHSO3 Solution Without and With Cl-, Int J Electrochem Sci 7 (2012) 11123–11136.

[121] A.V. Polunin, A.P. Pchelnikov, V.V. Losev, I.K. Marshakov, Electrochemical Studies of the Kinetics and Mechanism of Brass Dezincification, Electrochim Acta 27 (1982) 467–475.

[122] A.P. Pchelnikov, A.D. Sitnikov, I.K. Marshakov, V.V.A. Losev, Study of the Kinetics and Mechanism of Brass Dezincification by Radiotracer and Electrochemical Methods, Electrochim Acta 26 (1981) 591–600.

[123] B.O. Okonkwo, H. Ming, J. Wang, F. Meng, X. Xu, E.-H. Han, Microstructural characterization of low alloy steel A508 –309/308L stainless steel dissimilar weld metals, International J. Press Vessel & Pipings 190 (2021) 104297.

[124] B.O. Okonkwo, H. Ming, Z. Zhang, J. Wang, E. Rahimi, S. Hosseinpour, A. Davoodi, Microscale investigation of the correlation between microstructure and galvanic corrosion of low alloy steel A508 and its welded 309/308L stainless steel overlayer, Corros. Sci. 154 (2019) 49–58.

[125] B.O. Okonkwo, H. Ming, J. Wang, E.-H. Han, E. Rahimi, A. Davoodi, S. Hosseinpour, A new method to determine the synergistic effects of area ratio and microstructure on the galvanic corrosion of LAS 508/309L/308L SS dissimilar metals weld, J. Mater. Sci. Technol. 78 (2021) 38–50.

[126] T. Mineta, Analysis of indentation stress-strain response of copper by in-situ observation using optical indentation microscopy, Results in Engineering 15 (2022).

[127] M.C. Lucchetta, P. Ramasamy, F. Saporiti, J. Eckert, F. Audebert, Influence of the 1% Ti content on microstructure, friction coefficient and contribution to the strengthening mechanisms in the Al20Sn1Cu alloy, Results in Engineering 15 (2022).

[128] T. Kosec, J. Voglar, P. Močnik, A. Legat, Effect of the microstructural properties of copper on corrosion performance, Corros. Eng. Sci. & Technol. 56 (2021) 728–735.

[129] P. Gao, Y. Ren, S. Qian, Y. He, D.S. hen, Evolution of microstructure and electrochemical corrosion behavior of CuZn-based alloys induced by cold rolling, J. Mater. Research & Technol. (2021) 360–368.

[130] B. De Filippo, A. Brotzu, S. Natali, Corrosion behavior of Cu-Zn-Al shape memory alloy in controlled environments, in: AIP Conf. Proc, 2020 020013.

[131] T. Chang, I.O. Wallinder, D. de la Fuente, B. Chico, M. Morcillo, J. Welter, L. C, Analysis of Historic Copper Patinas. Influence of Inclusions on Patina Uniformity, Materials 10 (2017) 298.

[132] K. Samvatsar, V. Rao, Corrosion aspects of Ni–Cu alloy (UNS N04400) and its surface improvement: a review, Emergent Mater 4 (2021).

[133] L. Yang, X. Jiang, H. Sun, Z. Shao, Y. Fang, R. Shu, Effects of alloying, heat treatment and nanoreinforcement on mechanical properties and damping performances of Cu–Al-based alloys: A review, Nanotechnol Rev 10 (2021).

[134] V.G. Pushin, N.N. Kuranova, A.E. Svirid, A.N. Uksusnikov, Y.M. Ustyugov, Design and Development of High-Strength and Ductile Ternary and Multicomponent Eutectoid Cu-Based Shape Memory Alloys: Problems and Perspectives, Metals (Basel) 12 (2022).

[135] A. Jamwal, P. Mittal, R. Agrawal, S. Gupta, D. Kumar, K.K. Sadasivuni, P. Gupta, Towards sustainable copper matrix composites: Manufacturing routes with structural, mechanical, electrical and corrosion behaviour, J Compos Mater 54 (2020).

[136] S. Huang, W. Long, B. Huang, S. Zhong, L. Bao, A Review on Corrosion Resistant of Cu-Al Joints, in: IOP Conf Ser Mater Sci Eng, 2018.

[137] R. Wang, D. Wang, H. Nagaumi, Z. Wu, X. Zhang, X. Li, Effect of Zn content on corrosion resistance of as-cast Al-6Si-3Cu alloy, Mater Lett 312 (2022).

[138] D. Kong, C. Dong, X. Ni, C. Man, K. Xiao, X. Li, Insight into the mechanism of alloying elements (Sn, Be) effect on copper corrosion during long-term degradation in harsh marine environment, Appl Surf Sci 455 (2018).

[139] R. Su, K. Wang, Y. Yang, Y. Qu, R. Li, Effect of Mg Content on the Microstructure and Corrosion Properties of Al-Cu-Mn Alloy, J Mater Eng Perform 2 (2020).

[140] H. Nady, M.M. El-Rabiei, G.M. Abd El-Hafez, Electrochemical Stability of Cu–10Al–10Zn, Cu–10Al–10Ni, and Cu–10Ni–10Zn Ternary Alloys in Simulated Physiological Solutions, J Bio Tribo Corros 2 (2016).

[141] J. Wang, Z. Liu, S. Bai, J. Cao, J. Zhao, D. Zeng, Combined Effect of Ag and Mg Additions on Localized Corrosion Behavior of Al-Cu Alloys with High Cu Content, J Mater Eng Perform 29 (2020).

[142] X. Zhang, L. Zhang, L. Han, J. Bai, Z. Huang, C. Guo, F. Xue, P.K. Chu, C. Chu, Effects of Dynamic Flow Rates on the In Vitro Bio-Corrosion Behavior of Zn-Cu Alloy, Coatings 14 (2024) 711.

[143] L. Wu, Y. Zhang, Z. Zheng, Z. Tang, S. Chen, Comprehensive corrosion failure analysis of HAl77-2 alloy tubes serving in a low temperature multi-effect distillation plant: From feature analysis to corrosion mechanisms, Engineering Failure Analysis 163 (2024) 108590.

[144] M.M. Stack, S. Zhou, R.C. Newman, Identification of transitions in erosion-corrosion regimes in aqueous environments, Wear 186-187 (1995) 523–532.

[145] R.J.K. Wood, Erosion–corrosion interactions and their effect on marine and offshore materials, Wear 261 (2006) 1012–1023.

[146] Z.B. Wang, Y.G. Zheng, Critical flow velocity phenomenon in erosion-corrosion of pipelines: determination methods, mechanisms and applications, Journal of Pipeline Science and Engineering 1 (2021) 63–73.

[147] J. Zhou, L. Yan, J. Tang, Z. Sun, L. Ma, Interactive effect of ant nest corrosion and stress corrosion on the failure of copper tubes, Engineering Failure Analysis 83 (2018) 9–16.

[148] L. Wu, A. Ma, L. Zhang, Y. Zheng, Intergranular erosion corrosion of pure copper tube in flowing NaCl solution, Corrosion Science 201 (2022) 110304.

[149] Y. Luo, Q. Li, S. Song, Corrosion behavior of ZHMn55-3-1 copper alloy in stagnant and flowing seawater with entrained sediment, Anti-Corrosion Methods and Materials 61 (2014) 96–103.

[150] J. Wang, C.E. Smith, J. Sankar, Y. Yun, N. Huang, Absorbable magnesium-based stent: physiological factors to consider for in vitro degradation assessments, Regenerative Biomaterials 2 (2015) 59–69.

[151] J.L. Schenk, F. Wallner, W.L. Kepplinger, M.K. Shin, M.Y. Cho, I.O. Lee, Technology for an increased portion of fine ore in the COREX® process, Scandinavian Journal of Metallurgy 29 (2000) 81–91.

[152] Z.B. Zheng, Y.G. Zheng, X. Zhou, S.Y. He, W.H. Sun, J.Q. Wang, Determination of the critical flow velocities for erosion–corrosion of passive materials under impingement by NaCl solution containing sand, Corrosion Science 88 (2014) 187–196.

[153] D.D. MACDONALD, B.C. SYRETT, S.S. WING, The Corrosion of Copper-Nickel Alloys 706 and 715 in Flowing Sea Water. I—Effect of Oxygen, Corrosion 34 (2013) 289–301.

[154] J.Z. Yi, H.X. Hu, Z.B. Wang, Y.G. Zheng, On the critical flow velocity for erosion-corrosion of Ni-based alloys in a saline-sand solution, Wear 458-459 (2020) 203417.

[155] Z.B. Wang, Y.G. Zheng, J.Z. Yi, The role of surface film on the critical flow velocity for erosion-corrosion of pure titanium, Tribology International 133 (2019) 67–72.

[156] J.Z. Yi, H.X. Hu, Z.B. Wang, Y.G. Zheng, Comparison of critical flow velocity for erosion-corrosion of six stainless steels in 3.5 wt% NaCl solution containing 2 wt % silica sand particles, Wear 416-417 (2018) 62–71.

[157] N.-F.F. Society, Copper Development Association, Copper Casting Alloys, (1994.).

[158] R. Konen, F. S, Copper and Copper Alloys: Casting, Classification and Characteristic Microstructures, Copp. Alloy, Early Appl. Curr. Perform. - Enhancing Process. (2012) 3–31.

[159] S.V. S, Corrosion of permanent mould cast copper alloys in aqueous solutions, Corros Eng Sci Technol 40 (2005) 65–68.

[160] O. Papadopoulou, P. V, The Influence of Archaeometallurgical Copper Alloy Castings Microstructure towards Corrosion Evolution in Various Corrosive Media, Corros Mater Degrad 2 (2021) 227–247.

[161] Y. Zeng, F. Yang, Z. Chen, E. Guo, M. Gao, X. Wang, H. Kang, T. Wang, Enhancing mechanical properties and corrosion resistance of nickel-aluminum bronze via hot rolling process, J Mater Sci Technol 61 (2021) 186–196.

[162] A.M. Alfantazi, T.M. Ahmed, T. D, Corrosion behavior of copper alloys in chloride media, Materials and Design 30 (2009) 2425–2430.

[163] B.G. Ateya, E.A. Ashour, S.M. Sayed, Stress corrosion behavior of a-aluminum bronze in saline water, Corrosion 50 (1994) 20–25.

[164] J. Morales, G.T. Fernandez, S. Gonzalez, P. Esparza, R.C. Salvarezza, A.J. Arvia, A comparative study of the passivation of a-brass and b-brass in borate buffer solutions containing sodium chloride: III. The effect of temperature, Corrosion Science 40 (1998) 177–190.

[165] A.M. Sham El-Din, J.M. Abd El-Kader, M.M. Badran, Galvanic corrosion in the copper/zinc system: I. Potential distribution in relation to the nature of the cathode and to the type of anion in solution, Br Corros J 16 (1981) 32–37.

[166] I.M. Milošev, Passive films on 90Cu–10Ni alloy: the mechanism of breakdown in chloride containing solutions, J Electrochem Soc 138 (1991), 161–137.

[167] A.I. Ikeuba, Bimetallic corrosion evaluation of the π-Al8Mg3FeSi6 phase/Al couple in acidic, neutral and alkaline aqueous solutions using the scanning vibrating electrode technique, Electrochimica Acta (2023).

[168] A.I. Ikeuba, B. Zhang, Electrochemical investigation of the anodic hydrogen evolution on MgZn2, Mg2Si, and Al4Cu2Mg8Si7 intermetallic phases, Journal of Solid State Electrochemistry (2023).

[169] A.I. Ikeuba, TOF-SIMS and AFM analysis of pH effect on the interfacial films on η-phase in aqueous salt solutions, Surface Science 15 (2023) 100410.

[170] A.I. Ikeuba, B. Zhang, J. Wang, E.-H. Han, W. Ke, Electrochemical, TOF-SIMS and XPS studies on the corrosion behavior of the Q-phase, Applied Surface Science 490 (2019) 535–545.

[171] A.I. Ikeuba, P.C. Okafor, B.I. Ita, A.I. Obike, F.E. Abeng, A.A. Bamigbola, U. B. Essien, Insitu SVET studies on the current density distribution on dissolving of Mg, Mg2Si, Al4Cu2Mg8Si7 and MgZn2 surfaces in sodium chloride solutions, Anti-corrosion Methods and Materials (2021).

[172] P. Cristiani, G. Perbonib, A. Debenedetti, Effect of chlorination on the corrosion of Cu/Ni 70/30 condenser tubing, Electrochimica Acta 54 (2008) 100–107.

[173] A.F. Khan, A.P. Patil, Combined Effect Of Chloride And pH On Corrosion Resistance Of Cu-10Ni Alloy Trans. Indian Inst. Met., 61.

[174] Z. Y, X. Yuan, H. Huang, X. Zuo, Y. Cheng, Influence of chloride ion concentration and temperature on the corrosion of Cu–Al composite plates in salt fog, Journal of Alloys and Compounds 821 (2020) 153249.

[175] V. L, I. Ivanić, D. Čudina, L. Lokas, S. Kožuh, M. Gojić, The Influence Of Chloride Ion Concentration On The Corrosion Behavior Of The Cu Al Ni Alloy, Technical Journal 11 (2017) 67–72.

[176] A.I. Ikeuba, F. Kou, H. Duan, B. Zhang, J. Wang, E.-H. Han, W. Ke, Understanding the Electrochemical behavior of MgZn2 as a function of pH, Journal of Solid State Electrochemistry 23 (2019) 1165–1177.

[177] A.I. Ikeuba, B. Zhang, J. Wang, E.-H. Han, K. W, Understanding the galvanic corrosion of the Q-phase/Al couple using SVET and SIET, Journal of Materials Science and Technology 35 (2019) 1444–1454.

[178] A.I. Ikeuba, B. Zhang, J. Wang, E.-H. Han, W. Ke, P.C. Okafor, SVET and SIET Study of Galvanic Corrosion of Al/MgZn2 in Aqueous Solutions at Different pH, Journal of The Electrochemical Society 165 (2018) C180–C194.

[179] A.I. Ikeuba, B. Zhang, B.I. Ita, SVET and ToF-SIMS Studies on the Galvanic Corrosion of β-phase/Aluminum Couple in Aqueous Solutions as a Function of pH, Journal of The Electrochemical Society 167 (2020) 2.

[180] B.C. Syrett, Sulfide attack in steam surface condensers. Conf on environmental degradation of engineering materials in an aggressive environment, Virginia Polytechnic Institute, 1981.

[181] A.M. Beccaria, G. Poggi, P. Traverso, A study of 70Cu30Ni commercial alloy in sulphide polluted and un polluted sea water, Corrosion Science 32 (1991).

[182] J.N. Al-hajji, M.R. Reda, The corrosion of copper nickel alloys in sulfide polluted sea water: the effect of sulfide concentration, Corrosion science 34 (1993).

[183] D.R. Lenard, R.R. Welland, Corrosion problems with copper nickel components in sea water systems Corrosion (1998) 599.

[184] D.R. Lenard, The effect of decaying organisms on the corrosion of copper nickel alloys in sea water, Corrosion (2002).

[185] R.M. Kain, B.E. Weber, Effect of alternating sea water flow and stagnant layup conditions on the general and localized corrosion resistance of CuNi and NiCu alloys in marine service, Corrosion (1997).

[186] O. Aylor, R.A. Hays, R.M. Kain, Crevice performance of candidate naval ship sea water valve materials, Corrosion (1999).

[187] H. Hoffmeister, J. Ullrich, Quantitative effect of transient potentials and temperature on crevice corrosion of Naval Cast CuNiAl Valve bronze in natural seawater, Corrosion (2000).

[188] G. Joseph, R. Peret, M. Ossio, Copper and Al Cu Stress Corrosion in artificial sea water, in: 10th international congress on metallic corrosion Vol V Madras India, 1989, pp. 185–197.

[189] X. Gao, H.B. Wu, M. Liu, Y.X. Zhang, F. Gao, Corrosion Behavior of High Strength C71500 Cu-Ni Alloy Pipe in Simulated High Sulfide Polluted Seawater at Different Temperatures, Int. J. Electrochem. Sci. 16 (2021).

[190] G.X. Li, H.Y. Xing, M. Du, M.X. Sun, M. Li, Accelerated corrosion of 70/30 copper-nickel alloys in sulfide-polluted seawater environment by sulfide, Journal of Materials Research and Technology 30 (2024) 8620–8634.

[191] B. Ash, V.S. Nalajala, A.K. Popuri, T. Subbaiah, M. Minakshi, Perspectives on Nickel Hydroxide Electrodes Suitable for Rechargeable Batteries: Electrolytic vs. Chemical Synthesis Routes, Nanomaterials 10 (2020).

[192] E.A. Ashour, Effect of sulfide on the stress corrosion behaviour of a copper-aluminium alloy in saline water, Joural of material Science 36 (2001) 201–205.

[193] N. Taniguchi, M. Kawasaki, Influence of sulfide concentration on the corrosion behavior of pure copper in synthetic seawater, Journal of Nuclear Materials 379 (2008) 154–161.

[194] K. Ding, S. Liu, W. Cheng, J. Du, L. Fan, J. Hou, L. Xu, Corrosion behavior of T2 and B30 Cu-Ni alloy at diferent seawater depths of the south China sea, J Mater Eng Perform 30 (2021) 6027–6038.

[195] X. Gao, H. Wu, M. Liu, X. Zhou, Y. Zhang, Analysis of the infuence of sulfur on the hot tensile fracture of C71500 Cu-Ni alloy, J Mater Eng Perform 30 (2021) 312–319.

[196] M. Reda, J. Alhajji, Deleterious role of complexing agents in corrosion of copper-nickel alloys in sulphide polluted sea water, Br Corros J 30 (1995) 56–62.

[197] M. Reda, J.N. Alhajji, Comparison of current reversal chronopotentiometry (CRC) and small amplitude cyclic voltammetry (SACV) method to determine the long-term corrosion tendency of copper-nickel alloys in polluted and unpolluted seawater under jet-impingement conditions, ASTM Special Technical Publication 1300 (1997) 143–158.

[198] A.E. Domiaty, J.N. Alhajji, The susceptibility of 90Cu-10Ni alloy to stress corrosion cracking in seawater polluted by sulfide ions, J. Mater. Eng Perform. 6 (1997).

[199] C. Nila, I. González, The role of pH and Cu(II) concentration in the electrodeposition of Cu(II) in NH4Cl solutions Author links open overlay panel, Journal of Electroanalytical Chemistry 401 (1996).

[200] H.E. Johnson, J. Leja, On the Potential/pH Diagrams of the Cu - NH 3 - H 2 O and Zn - NH 3 - H 2 O Systems, Journal of The Electrochemical Society, 112 (9651).

[201] T.P. Hoar, G.P. Rothwell, The potential/pH diagram for a copper-water-ammonia system: its significance in the stress-corrosion cracking of brass in ammoniacal solutions, Electrochim. Acta 15 (1970).

[202] R. Bartonicek, M. Lukasovska, A potential pH diagram for the system G1-NH3-CI-H2O, Corrosion Science 9 (1969) 35–42.

[203] E. Mattsson, Stress corrosion in brass considered against the background of potential/pH diagrams, Electrochim. Acta 3 (1961).

[204] D. Tromans, Copper and zinc equilibria in concentrated ammonia solutions: Relevance to stress corrosion cracking of alpha-brass, Corrosion Science 39 (1997) 1307–1319.

[205] J. Halpern, Kinetics of the Dissolution of Copper in Aqueous Ammonia, Journal of the Electrochemical Society 100 (1953).

[206] J. Sedzimir, M. Bujanska, The corrosion of copper in copper (II)-Ammonium sulphate solutions: the influences of ammonia concentration, of temperature and of the substitution of sulphates, Corros. Sci. 20 (1980) 1029.

[207] E.B. Khobotova, V.N. Baumer, Russ, J. Electrochem. 29 (1993).

[208] E.B. Khobotova, V.I. Glushko, Russ, J. Electrochem 30 (1994).

[209] E.B. Khobotova, A.P. Krasnoperova, Russ, J. Electrochem 32 (1996).

[210] G. Gizer, U. Önal, M. Ram, N. Şahiner, Biofouling and mitigation methods: A review, Biointerface Research in Applied Chemistry 13 (2023).

[211] L. Vedaprakash, R. Dineshram, K. Ratnam, K. Lakshmi, K. Jayaraj, S.M. Babu, R. Venkatesan, A. Shanmugam, Experimental studies on the effect of different metallic substrates on marine biofouling, Colloids and Surfaces B: Biointerfaces 106 (2013) 101–110.

[212] K.A. Dafforn, J.A. Lewis, E.L. Johnston, Antifouling strategies: history and regulation, ecological impacts and mitigation, Marine pollution bulletin 62 (2011) 453–465.

[213] U. Von Ammon, S.A. Wood, O. Laroche, A. Zaiko, L. Tait, S. Lavery, I. Graeme, X. Pochon, The impact of artificial surfaces on marine bacterial and eukaryotic biofouling assemblages: A high-throughput sequencing analysis, Marine Environmental Research 133 (2018) 57–66.

[214] D. Peters, Review of Copper-Nickel Alloy Sheathing of Ship Hulls and Offshore Structures. The Application of Copper-Nickel Alloys in Marine Systems, in: Technical report 7044-1919, Greenwich, CT, Copper Development Association (CDA), 1991.

[215] C. Bulow, Corrosion and Biofouling of Copper-Base Alloys in Sea Water, Transactions of The Electrochemical Society 87 (1945) 127.

[216] D.S.A. P, H. Seta, J. H, K. VV, S.E. G, Antifouling alternatives for aquaculture in tropical waters of the Atlantic Ocean, Aquaculture reports (2020) 100477 in.

[217] S. Campbell, R. Fletcher, P. C, Long-term Exposure Trials Evaluating the Biofouling and Corrosion Resistance of Copper-nickel Alloy Sheathing Materials, in: The 12th International Congress on Marine Corrosion & Fouling, University of Southampton, UK, 2004.

[218] C.N. Haas, G.A. Burlingame, A.K. Camper, R.M. Clark, Drinking water distribution systems: Assessing and reducing risks, National Academies Press, 2007.

[219] G. Grass, C. Rensing, M. Solioz, Metallic copper as an antimicrobial surface, Applied and environmental microbiology 77 (2011) 1541–1547.

[220] A. Morvay, M. Decun, M. Scurtu, C. Sala, M. A, M. Sarandan, Biofilm formation on materials commonly used in household drinking water systems, Water Science and Technology: Water Supply 11 (2011) 2.

[221] M.J. Lehtola, I.T. Miettinen, M.M. Keinänen, T.K. Kekki, O. Laine, A. Hirvonen, T. Vartiainen, M.P. J, Microbiology, chemistry and biofilm development in a pilot drinking water distribution system with copper and plastic pipes, Water research 38 (2004) 3769–3779.

[222] C. Jungfer, F. Friedrich, J. Varela Villarreal, K. Brändle, H.-J. Gross, U. Obst, T. Schwartz, Drinking water biofilms on copper and stainless steel exhibit specific molecular responses towards different disinfection regimes at waterworks, Biofouling 29 (8) (2013) 891–907.

[223] I.B. Gomes, L.C. Simões, M. Simões, The role of surface copper content on biofilm formation by drinking water bacteria, RSC Adv 9 (2019).

[224] J. Silhan, C.B. Corfitzen, H.J. Albrechtsen, Effect of temperature and pipe material on biofilm formation and survival of Escherichia coli in used drinking water pipes: a laboratory-based study, Water Science and Technology 5 (2006) 49–56.

[225] I.B. Gomes, M. Simões, L.C. Simões, Copper surfaces in biofilm control, Nanomaterials 10 (2020).

[226] H. Liu, Y. Tang, S. Zhang, H. Liu, Z. Wang, Y. Li, X. Wang, L. Ren, Y. K, L.L. Qin, Anti-infection mechanism of a novel dental implant made of titanium-copper (TiCu) alloy and its mechanism associated with oral microbiology, Bioactive Materials 8 (2022) 1–95.

[227] R. Liu, K. Memarzadeh, B. Chang, Y. Zhang, Z. Ma, R.P. Allaker, L. Ren, Y. K, Antibacterial effect of copper-bearing titanium alloy (Ti-Cu) against Streptococcus mutans and Porphyromonas gingivalis, Scientific reports 6 (2016).

[228] C. Bergemann, S. Zaatreh, K. Wegner, K. Arndt, A. Podbielski, R. Bader, C. Prinz, U. Lembke, J.N. Nebe, Copper as an alternative antimicrobial coating for implants-An in vitro study, World journal of transplantation 7 (2017).

[229] L.E. Ghasemian, H. Jahangirian, M. Dashti, E. Khajehali, S. S, R.-M. R, T. J. Webste, Antimicrobial double-layer wound dressing based on chitosan/polyvinyl alcohol/copper: in vitro and in vivo assessment, International journal of nanomedicine (2021) 223–235.
[230] M. Mohammady, M. Radmehr, H. Taherian, A. Tahmourespour, S.T. Hashemi, Effect of copper-coated surfaces on the bacterial burden in the intensive care unit, Iranian Red Crescent Medical Science 24 (2022).
[231] F.H. C, Biofouling and me: My Stockholm syndrome with biofilms, Water research 173 (2020).
[232] X.L. Li, J. Narenkumar, A. Rajasekar, Y.P. Ting, Biocorrosion of mild steel and copper used in cooling tower water and its control, Biotech 3 (2018) 1–11, 8.
[233] S. Vanithakumari, P. Yadavalli, R. George, C. Mallika, Development of hydrophobic cupronickel surface with biofouling resistance by sandblasting, Surface and Coatings Technology 345 (2018) 389–395.
[234] V. Vishwakarma, J. Josephine, R. George, R. Krishnan, S. Dash, K. Kamruddin M, K. Sridhar, N. Manoharan, A.K. Tyagi, R.K. Dayal, Antibacterial copper–nickel bilayers and multilayer coatings by pulsed laser deposition on titanium, Biofouling 25 (2009) 705–710.
[235] M.G. Fontana, Corrosion Engineering McGraw-Hill, 1987.
[236] H.H. Uhlig, R.W. Revie, Corrosion and Corrosion Control: An Introduction to Corrosion Science and Engineering, John Wiley & Sons., 2008.
[237] A. International, ASM Handbook, ASM International., 1992.
[238] P.R. Roberge, Handbook of Corrosion Engineering, McGraw-Hill., 2000.
[239] J.R. Davis, Corrosion: Understanding the Basics, ASM International., 2000.
[240] L.L. Shreir, R.A. Jarman, G.T. Burstein, Corrosion: Metal/Environment Reactions, 3rd ed., Butterworth-Heinemann., 1994.
[241] E. McCafferty, Introduction to Corrosion Science, Springer., 2010.
[242] P.A. Schweitzer, Fundamentals of Metallic Corrosion: Atmospheric and Media Corrosion of Metals, CRC Press., 2007.
[243] R. Heidersbach, Metallurgy and Corrosion Control in Oil and Gas Production, John Wiley & Sons., 2018.
[244] R.A. Jones, Corrosion Control in the Oil and Gas Industry, Gulf Professional Publishing., 2011.
[245] W.D. Callister, D.G. Rethwisch, Materials Science and Engineering: An Introduction, John Wiley & Sons., 2008.
[246] M. Pourbaix, Atlas of Electrochemical Equilibria in Aqueous Solutions, National Association of Corrosion Engineers., 1974.
[247] R. Baboian, Corrosion Tests and Standards: Application and Interpretation, ASTM International., 1990.
[248] K.R. Trethewey, J. Chamberlain, Corrosion for Science and Engineering, 2nd . ed., Longman, 1995.
[249] S. Suhartini, N.A. Rohma, A.P.A. Pratama, N.M.S. Sunyoto, E. Mardawati, A.M. Sulaiman Kasbawati, A. Harmayanti, F. Gapsari, Sustainable corrosion protection: Chitosan/reduced graphene oxide nanocomposite coating derived from palm oil empty fruit bunches on low carbon steel, Case Studies in Chemical and Environmental Engineering 11 (2025).
[250] F. Gapsari, S. Sharma, S. Hadisaputra, C.W. Lai, A.M. Sulaiman, D.B. Darmadi, A. Kumar, Assessing the newly synthesized bio-based amylase-chitosan/cellulose nanocrystals- ZnO composite for enhanced corrosion protection of carbon steel in acidic medium, Material Today Communication 44 (2025).
[251] F. Gapsari, P. Setyarini, K. Anam, S. Hadisaputra, S. Hidayatullah, Purnami, A. M. Sulaiman, C.W. Lai, Efficacy of Andrographis paniculata leaf extract as a green corrosion inhibitor for mild steel in concentrated sulfuric acid: Experimental and computational insights, Results in Surfaces and Interfaces 18 (2025).
[252] b., E. F. Gapsari, S. Hadisaputr, A.M. Sulaiman, A. Thakur, A. Kumar, Eco-friendly corrosion inhibition of copper in NaCl media using Perseana americana extract: Insights from quantum and electrochemical studies Results in Surfaces and Interfaces 17 (2024).
[253] C.N. Njoku, B.N. Enendu, S.J. Okechukwu, N. Igboko, S.O. Anyikwa, A.I. Ikeuba, I.B. Onyeachu, I.N. Etim, D.I. Njoku, Review on anti-corrosion properties of expired antihypertensive drugs as benign corrosion inhibitors for metallic materials in various environments, Results in Engineering 18 (2023).
[254] F.E. Abeng, B.I. Ita, V.C. Anadebe, V.I. Chukwuike, K.M. Etiowo, P.Y. Nkom, O. O. Ekerenam, N.B. Iroha, I.J. Ikot, Multidimensional insight into the corrosion mitigation of clonazepam drug molecule on mild steel in chloride environment: Empirical and computer simulation explorations, Results in Engineering 17 (2023).
[255] M. Mouanga, L. Ricq, J. Douglade, Study of the Corrosion Inhibition of Copper in 3% NaCl by a Triazole Compound Using Electrochemical and Analytical Techniques, Corrosion Science 48 (2006) 2205–2221.
[256] S. Feliu, M. Morcillo, The Role of Surface Films on the Corrosion Resistance of Copper Alloys, Corrosion Science 50 (2008) 2959–2965.
[257] F. Mansfeld, The Use of Electrochemical Techniques in Corrosion Control, Corrosion Science 16 (1976) 1–9.
[258] Y.X. Gan, Y. Chang, C. Chen, M. Li, J.B. Gan, J. Li, Seawater Corrosion of Copper and Its Alloy Coated withHydrothermal Carbon, Coatings 12 (2022).
[259] Ž.Z. Tasić, M.B. Petrović Mihajlović, M.B. Radovanović, M.M. Antonijević, New trends in corrosion protection of copper, Chem. Pap. 73 (2019) 2103–2132.
[260] M. Finšgar, I. Milošev, Inhibition of copper corrosion by 1,2,3-benzotriazole: A review, Corros. Sci. 52 (2010) 2737–2749.
[261] D.I. Njoku, A.C. Njoku, I.I. Udoh, P.C. Uzoma, I.I.N. Etim, B. Li, Y. Li, Understanding the multifunctional anticorrosion protective mechanism of epoxy-based coatings modified with hydrogel and benzotriazole conveying nanotubes for Q235 steel protection in 3.5 % NaCl, Surf. Coatings Technol. 484 (2024).
[262] D.I. Njoku, B. Li, M.S. Khan, U.P. Chinonso, C.N. Njoku, I.B. Onyeachu, Y. Li, Quadruple-action coatings provided by doping epoxy with inhibitor laden clay nanotubes functionalized with layer-by-layer of cross-bridged chitosan and anionic polyelectrolytes, Prog. Org. Coatings 157 (2021).
[263] D.I. Njoku, M. Cui, H. Xiao, B. Shang, Y. Li, Understanding the anticorrosive protective mechanisms of modified epoxy coatings with improved barrier, active and self-healing functionalities: EIS and spectroscopic techniques, Sci. Rep. 7 (2017).
[264] D.I. Njoku, Y. Li, H. Lgaz, E.E. Oguzie, Dispersive adsorption of Xylopia aethiopica constituents on carbon steel in acid-chloride medium: A combined experimental and theoretical approach, J. Mol. Liq. 249 (2018) 371–388.
[265] D.I. Njoku, I. Ukaga, O.B. Ikenna, E.E. Oguzie, K.L. Oguzie, N. Ibisi, Natural products for materials protection: Corrosion protection of aluminium in hydrochloric acid by Kola nitida extract, J. Mol. Liq. 219 (2016) 417–424.
[266] D.I. Njoku, C.N. Njoku, H. Lgaz, P.C. Okafor, E.E. Oguzie, Y. Li, Corrosion protection of Q235 steel in acidic-chloride media using seed extracts of Piper guineense, J. Mol. Liq. 330 (2021).
[267] Z.Z. Tasic, M.M. Antonijevic, Copper corrosion behaviour in acidic sulphate media in the presence of 5-methyl-lH-benzotriazole and 5-chloro-lH-benzotriazole, Journal of Chemical papers 70 (2016) 620–634.
[268] P.F. Khan, V. Shanthi, R.K. Babu, S. Muralidharan, R.C. Barik, Effect of benzotriazole on corrosion inhibition of copper under flow conditions, J. Environ. Chem. Eng. 3 (2015) 10–19.
[269] Y. Qiang, S. Zhang, S. Xu, W. Li, Experimental and theoretical studies on the corrosion inhibition of copper by two indazole derivatives in 3.0% NaCl solution, J. Colloid Interface Sci. (2016) 52–59.
[270] D. Yin, L. Yang, B. Tan, T. Ma, S. Zhang, Y. Wang, L. Guo, B. Gao, Y. He, Theoretical and electrochemical analysis on inhibition effects of benzotriazole derivatives (un- and methyl) on copper surface, J. Mol. Struct. 1243 (2021).
[271] K.F. Khaled, S.A. Fadl-Allah, B. Hammouti, Some benzotriazole derivatives as corrosion inhibitors for copper in acidic medium: Experimental and quantum chemical molecular dynamics approach, Mater. Chem. Phys. 117 (2009) 148–155.
[272] B.V. Appa Rao, K. Chaitanya Kumar, 5-(3-Aminophenyl)tetrazole – A new corrosion inhibitor for Cu–Ni (90/10) alloy in seawater and sulphide containing seawater, Arab. J. Chem. 10 (2017) S2245–S2259.
[273] B. Tan, S. Zhang, H. Liu, Y. Qiang, W. Li, L. Guo, S. Chen, Insights into the inhibition mechanism of three 5-phenyltetrazole derivatives for copper corrosion in sulfuric acid medium via experimental and DFT methods, J. Taiwan Inst. Chem. Eng. 102 (2019) 424–437.
[274] N. Benzbiria, S. Echihi, M.E. Belghiti, A. Thoume, A. Elmakssoudi, A. Zarrouk, M. Zertoubi, M. Azzi, Novel synthetized benzodiazepine as efficient corrosion inhibitor for copper in 3.5% NaCl solution, Mater. Today Proc. 37 (2021) 3932–3939.
[275] N. Kovačević, I. Milošev, A. Kokalj, The roles of mercapto, benzene, and methyl groups in the corrosion inhibition of imidazoles on copper: II. Inhibitor–copper bonding, Corros. Sci. 98 (2015) 457–470.
[276] S. Zeng, F. Zhang, Y. Liu, S. Ouyang, Y.W. Ye, H. Chen, Synthesis of Ce, N co–doped carbon dots as green and effective corrosion inhibitor for copper in acid environment, J. Taiwan Inst. Chem. Eng. (2022) 141.
[277] K.W. Shinato, A.A. Zewde, Y. Jin, Corrosion protection of copper and copper alloys in different corrosive medium using environmentally friendly Corrosion inhibitors, Corros Rev 38 (2020) 101–109.
[278] N. Chaubey, S.A. Qurashi, D.S. Chauhan, M.A. Quraishi, Frontiers and advances in green and sustainable inhibitors for corrosion applications: A critical review, J. Mol. Liq. 321 (2021).
[279] R.M. Nair, B. Bindhu, N.T. Manikandanath, R.S. Rimal Isaac, An eco-friendly green biopolymer blend for copper corrosion inhibition, Polym. Bull. 79 (2022) 121–136.
[280] M.A. Deyab, Q. Mohsen, E. Bloise, M.R. Lazzoi, G. Mele, Experimental and theoretical evaluations on Oleuropein as a natural origin corrosion inhibitor for copper in acidic environment, Sci. Rep. 12 (2022) 1–12.
[281] S. Rahimi, A. Najafi Chermahini, H. Farrokhpour, A.R. Hajipour, Corrosion inhibition of copper by oxalohydrazide and its methylated derivatives: A theoretical study, J. Mol. Graph. Model. 138 (2025).
[282] M. El Mahamdi, W. Daoudi, I.A. Naguib, L. Benhadi, O. Dagdag, A. Berisha, H. Kim, B. Noureddine, A. El Aatiaoui, Enhanced corrosion protection of copper in saline environments using bio-nanocomposite coatings based on chitosan and chitosan Schiff base, Int. J. Biol. Macromol. (2024) 282.
[283] F. Chiter, D. Costa, V. Maurice, P. Marcus, Corrosion inhibition of locally de-passivated surfaces by DFT study of 2-mercaptobenzothiazole on copper, Npj Mater. Degrad. 5 (2021) 52.
[284] J. Liu, X. Niu, Y. Jia, N. Zhan, Y. Zou, Y. Shi, J. Zhou, Corrosion inhibition mechanisms of triazole derivatives on copper chemical mechanical polishing: Combined experiment and DFT study, Appl. Surf. Sci. 654 (2024) 159469.
[285] F. Chiter, D. Costa, V. Maurice, P. Marcus, Atomic Scale Insight into Corrosion Inhibition: DFT Study of 2-Mercaptobenzimidazole on Locally De-Passivated Copper Surfaces, J. Electrochem. Soc. 168 (2021).
[286] D. Kumar, V. Jain, B. Rai, Imidazole derivatives as corrosion inhibitors for copper: A DFT and reactive force field study, Corros. Sci. 171 (2020).
[287] M. Lasri, A. Ait-karra, O. Zakir, R. Idouhli, B. Dikici, M.E. hadiri, A. Abouelfida, Copper Corrosion in Chloride Environments: Key Inhibitors and Strategies, J. Bio-Tribo-Corrosion 11 (2025).
[288] A.-J. M. Abdallah, A. Majda, G. Nizar, F. Rasha, N. Salih, S. Fatima, A.H. Sobhi, Appraisal of expired linezolid and piperacillin as potent and harmless inhibitors for mitigation of copper corrosion in 1.0 M HNO3 Green Chem. Lett. Rev. 18 (2025).

[289] X. Yan, W. Liu, Y. Xu, S. Xiong, Enhancing the corrosion inhibition of copper sheets in oil-in-water (O/W) emulsions by combining two organic heterocyclic derivatives, RSC Adv 1 (4) (2024) 31825–31836.

[290] Z. Liu, B. Fan, J. Zhao, B. Yang, X. Zheng, Benzothiazole derivatives-based supramolecular assemblies as efficient corrosion inhibitors for copper in artificial seawater: Formation, interfacial release and protective mechanisms, Corros. Sci. 212 (2023) 110957.

[291] M. HosseinpourRokni, R. Naderi, M. Soleimani, E. Kowsari, M. Pourfath, Indirect interactions between the ionic liquid and Cu surface in 0.5 M HCl: a novel mechanism explaining cathodic corrosion inhibition, Corros. Sci. 216 (2023).

[292] E. Stupnišek-Lisac, A. Gazivoda, M. Madžarac, E v aluation of non-toxic corrosion inhibitors for copper in sulphuric acid, Electrochimica Acta 47 (2002) 4189–4194.

[293] B. Tan, Y. Liu, Z. Gong, X. Zhang, J.W. Chen, L. Guo, J. Xiong, J. Liu, R. Marzouki, W. Li, Pyracantha fortuneana alcohol extracts as biodegradable corrosion inhibitors for copper in H2SO4 media, J. Mol. Liq. (2024) 397.

[294] M.P.S. Barbosa, C.C.F. do Nascimento, D.de M.L. dos Santos, C.de J. C. Pereira Junior, Evaluation of Palm Oil Corrosion Inhibition Through Image Analysis in Copper Pipes Used in Air Conditioning Systems, J. Bio- Tribo-Corrosion 11 (2025).

[295] M.A. Al-qudah, T.T. Bataineh, M.A. Orabi, S.T. Abu, RSC Advances of copper in 1 . 0 M HNO 3 solution : experimental and theoretical investigation, RSC Adv (2025) 9335–9347.

[296] V.K. Jha, S. Jana, S. Pal, G. Ji, R. Prakash, Thin-Film Coating of the Hydrophobic Lotus Leaf on Copper by the Floating Film Transfer Method and Investigation on the Corrosion Behavior of Coated Copper in Saline Water, Ind. Eng. Chem. Res 62 (2023).

[297] I. Pandey, A.V. Ullas, C.K. Rastogi, M.K. Singh, V. Kumar, B. Mangi, G. Ji, Extract Preparation of Waste Lady Finger Caps Using Ethanol, Generation of Extract's Layers on Copper Through Drop Casting Without and with NiO Nanoparticles, and Study of their Corrosion Performances in Saline Water, Waste and Biomass Valorization 16 (2025) 971–985.

[298] Q. Wang, C. Zhao, R. Wang, R. Aslam, X. Zhou, Q. Zhang, Z. Yan, Y. Sun, X. Li, H. Zheng, Rhododendron simsii leaf extract as a corrosion inhibitor for Cu in 0.5 M H2SO4: Experimental and theoretical studies, Colloids Surfaces A Physicochem. Eng. Asp. 682 (2024).

[299] T. Gu, Z. Xu, X. Zheng, A. Fu, F. Zhang, N. Al-Zaqri, J.W. Chen, B. Tan, W. Li, Lycium barbarum leaf extract as biodegradable corrosion inhibitor for copper in sulfuric acid medium, Ind. Crops Prod. 203 (2023).

[300] X. Zhang, W. Li, X. Zuo, B. Tan, C. Xu, S. Zhang, Investigating the inhibitive effect of Davidia involucrata leaf extract as a biological eco-friendly inhibitor for copper in acidic medium, J. Mol. Liq. 325 (2021).

[301] L. Feng, S. Zhang, Y. Feng, X. Ren, H. Lu, B. Tan, S. Chen, Self-aggregate nanoscale copolymer of new synthesized compounds efficiently protecting copper corrosion in sulfuric acid solution, Chem. Eng. J. 394 (2020).

[302] A. Jmiai, B. El Ibrahimi, A. Tara, S. El Issami, O. Jbara, L. Bazzi, Alginate biopolymer as green corrosion inhibitor for copper in 1 M hydrochloric acid: Experimental and theoretical approaches, J. Mol. Struct. 1157 (2018) 408–417.

[303] K. El Mouaden, B. El Ibrahimi, R. Oukhrib, L. Bazzi, B. Hammouti, O. Jbara, A. Tara, D.S. Chauhan, M.A. Quraishi, Chitosan polymer as a green corrosion inhibitor for copper in sulfide-containing synthetic seawater, Int. J. Biol. Macromol. 119 (2018) 1311–1323.

[304] A. Toghan, A. Fawzy, A. Al Bahir, N. Alqarni, M.M.S. Sanad, M. Khairy, A. I. Alakhras, A.A. Farag, Computational Foretelling and Experimental Implementation of the Performance of Polyacrylic Acid and Polyacrylamide Polymers as Eco-Friendly Corrosion Inhibitors for Copper in Nitric Acid, Polymers (Basel) 14 (2022).

[305] R. Farahati, A. Ghaffarinejad, (Jafar) Rezania, S.M. Mousavi-Khoshdel, H. Behzadi, Sulfonated aromatic polyamide as water-soluble polymeric corrosion inhibitor of copper in HCl, Colloids Surfaces A Physicochem. Eng. Asp. 578 (2019).

[306] I.I. Udoh, O.O. Ekerenam, E.F. Daniel, A.I. Ikeuba, D.I. Njoku, S.K. Kolawole, I.-I. N. Etim, W. Emori, C.N. Njoku, I.P. Etim, P.C. Uzoma, Developments in anticorrosive organic coatings modulated by nano/microcontainers with porous matrices, Adv. Colloid Interface Sci. 330 (2024) 103209.

[307] C. Bai, C. Hu, X. Zhang, W. Zhang, B. Ma, T. Li, A rapid two-step method for fabrication of superhydrophobic-superoleophobic nickel/copper alloy coating with self-cleaning and anticorrosion properties, Colloids Surfaces A Physicochem Eng. Asp. 651 (2022).

[308] M. Menkuer, H. Ozkazanc, Electrodeposition of polypyrrole on copper surfaces in OXA-DBSA mix electrolyte and their corrosion behaviour, Prog. Org. Coatings. 130 (2019) 149–157.

[309] Y. Lei, N. Sheng, A. Hyono, M. Ueda, T. Ohtsuka, Electrochemical synthesis of polypyrrole films on copper from phytic solution for corrosion protection, Corros. Sci. 76 (2013) 302–309.

[310] Y. Ma, B. Fan, H. Liu, G. Fan, H. Hao, B. Yang, Enhanced corrosion inhibition of aniline derivatives electropolymerized coatings on copper: Preparation, characterization and mechanism modeling, Appl. Surf. Sci. 514 (2020).

[311] S.A. Umoren, M.M. Solomon, Protective polymeric films for industrial substrates: A critical review on past and recent applications with conducting polymers and polymer composites/nanocomposites, Prog. Mater. Sci. 104 (2019) 380–450.

[312] P. Sun, X. Shen, P. Xu, W. Huang, Q. Xu, Conductive polyaniline film synthesized through in-situ polymerization as a conductive seed layer for hole metallization of printed circuit boards, Appl. Surf. Sci. 655 (2024).

[313] Y. Dong, H. Yu, Y. Feng, W. Feng, Structure, properties and applications of multi-functional thermally conductive polymer composites, J. Mater. Sci. Technol. 200 (2024) 141–161.

[314] M. Goyal, K. Singh, N. Bhatnagar, Conductive polymers: A multipurpose material for protecting coating, Prog. Org. Coatings. 187 (2024).

[315] C.I. Idumah, Design, fabrication, characterization and properties of metallic and conductive smart polymeric textiles for multifunctional applications, Nano-Structures & Nano-Objects 35 (2023).

[316] L. Bazli, M. Yusuf, A. Farahani, M. Kiamarzi, Z. Seyedhosseini, M. Nezhadmansari, M. Aliasghari, M. Iranpoor, Application of composite conducting polymers for improving the corrosion behavior of various substrates: A Review, J. Compos. Compd., 2 (202) 228–240.

[317] F. Gao, J. Mu, Z. Bi, S. Wang, Z. Li, Recent advances of polyaniline composites in anticorrosive coatings: A review, Prog. Org. Coatings. 151 (2021).

[318] H. Liu, B. Fan, G. Fan, Y. Ma, H. Hao, W. Zhang, Anti-corrosive mechanism of poly (N-ethylaniline)/sodium silicate electrochemical composites for copper: Correlated experimental and in-silico studies, J. Mater. Sci. Technol. 72 (2021) 202–216.

[319] V. Annibaldi, A.D. Rooney, C.B. Breslin, Corrosion protection of copper using polypyrrole electrosynthesised from a salicylate solution, Corros. Sci. 59 (2012) 179–185.

[320] M. Shabani-Nooshabadi, F. Karimian-Taheri, Electrosynthesis of a polyaniline/zeolite nanocomposite coating on copper in a three-step process and the effect of current density on its corrosion protection performance, RSC Adv 5 (2015) 96601–96610.

[321] Y. Jafari, S.M. Ghoreishi, M. Shabani-Nooshabadi, Polyaniline/Graphene nanocomposite coatings on copper: Electropolymerization, characterization, and evaluation of corrosion protection performance, Synth. Met. 217 (2016) 220–230.

[322] V. Mišković-Stanković, I. Jevremović, I. Jung, K. Rhee, Electrochemical study of corrosion behavior of graphene coatings on copper and aluminum in a chloride solution, Carbon N. Y. 75 (2014) 335–344.

[323] Z. Chen, W. Ren, D. Gao, B. Liu, S. Pei, H.-M. Cheng, Three-dimensional flexible and conductive interconnected graphene networks grown by chemical vapour deposition, Nat. Mater. 10 (2011) 424–428.

[324] X. Zhu, W. Yinghao, W. Zhao, J. Pu, D. Yang, Q. Xue, Large-area preparation of defect-repaired fluorocarbon polymer coatings on graphene for long-term corrosion resistance, Prog. Org. Coatings. 134 (2019) 234–243.

[325] Z. Zheng, L. Xiao, P. Huang, F. Wang, Polydopamine improved anticorrosion of graphene on copper: Inhibiting galvanic corrosion and healing structure defects, Appl. Mater. Today 24 (2021).

[326] Y. Wu, W. Zhao, Z. Lu, L. Wang, Fluorinated graphene film for corrosion control on copper: Experimental and theoretical studies, Carbon N. Y. 179 (2021) 445–457.

[327] D. Prasai, J.C. Tuberquia, R.R. Harl, G.K. Jennings, K.I. Bolotin, Graphene: Corrosion-Inhibiting Coating, ACS Nano 6 (2012) 1102–1108.

[328] H. Zhang, Q. Ma, Y. Wang, B. Xu, J. Guo, Improved corrosion resistance of copper coated by graphene, Carbon N. Y. 150 (2019) 550–551.

[329] Y. Li, H. Yang, F. Wang, Y. Huang, Fabrication and anti-corrosion properties of melamine-treated graphene oxide adsorbed on copper, Prog. Org. Coatings. 141 (2020).

[330] Y. Chen, Y.W. Liu, Y. Xie, H.H. Zhang, X.Q. Du, Z. Zhang, Preparation of hydrophobic silane/graphene oxide composite coating implanted with benzotriazole to improve the anti-corrosion performance of copper, J. Alloys Compd. 893 (2022).

[331] J.-H. Huh, S.H. Kim, J.H. Chu, S.Y. Kim, J.H. Kim, S.-Y. Kwon, Enhancement of seawater corrosion resistance in copper using acetone-derived graphene coating, Nanoscale 6 (2014) 4379–4386.

[332] F. Mahvash, S. Eissa, T. Bordjiba, A.C. Tavares, T. Szkopek, M. Siaj, Corrosion resistance of monolayer hexagonal boron nitride on copper, Sci. Rep. 7 (2017).

[333] G. Chilkoor, K. Jawaharraj, B. Vemuri, A. Kutana, M. Tripathi, D. Kota, T. Arif, T. Filleter, A.B. Dalton, B.I. Yakobson, M. Meyyappan, M.M. Rahman, P. M. Ajayan, V. Gadhamshetty, Hexagonal Boron Nitride for Sulfur Corrosion Inhibition, ACS Nano 14 (2020) 14809–14819.

[334] S. Ren, M. Cui, J. Pu, Q. Xue, L. Wang, Multilayer Regulation of Atomic Boron Nitride Films to Improve Oxidation and Corrosion Resistance of Cu, ACS Appl. Mater. Interfaces. 9 (2017) 27152–27165.

[335] S. Ren, Y. Hao, M. Cui, J. Pu, L.-F. Huang, L. Wang, Correlated morphological and chemical mechanisms for the superior corrosion resistance of alumina-deposited 2D nanofilms on copper, Materialia 11 (2020) 100697.

[336] Z. Sadeghian, M.R. Hadidi, D. Salehzadeh, A. Nemati, Hydrophobic octadecylamine-functionalized graphene/TiO2 hybrid coating for corrosion protection of copper bipolar plates in simulated proton exchange membrane fuel cell environment, Int. J. Hydrogen Energy. 45 (2020) 15380–15389.

[337] F. Razavi, M. Shabani-Nooshabadi, M. Behpour, Sol-gel synthesis, characterization and electrochemical corrosion behavior of S-N-C-doped TiO2 nano coating on copper, J. Mol. Liq. 266 (2018) 99–105.

[338] H. Cao, M. Fang, W. Jia, X. Liu, Q. Xu, Remarkable improvement of corrosion resistance of silane composite coating with Ti3C2Tx MXene on copper, Compos. Part B Eng. 228 (2022).

[339] S. Wan, C.-H. Miao, R.-M. Wang, Z.-F. Zhang, Z.-H. Dong, Enhanced corrosion resistance of copper by synergetic effects of silica and BTA codoped in polypyrrole film, Prog. Org. Coatings 129 (2019) 187–198.

[340] U. Carragher, C.B. Breslin, Polypyrrole doped with dodecylbenzene sulfonate as a protective coating for copper, Electrochim. Acta. 291 (2018) 362–372.

[341] N.B.A. Prasetya, M.R. Putri, N. Gunawan, Polyeugenol-gum arabic/graphene oxide composite coating for high performance anticorrosion material, Case Study, Chem. Environ. Eng. 9 (2024) (2024).

[342] Z. Yang, L. Wang, W. Sun, S. Li, T. Zhu, W. Liu, G. Liu, Superhydrophobic epoxy coating modified by fluorographene used for anti-corrosion and self-cleaning, Appl. Surf. Sci. 401 (2017).

[343] M. Lasri, M. Fawzi, A. Bimoussa, R. Idouhli, M.Eddine Khadiri, B. El Ibrahimi, M. Youssef Ait Itto, A. Abouelfida, Doped STR@mSiO2-GO nanocomposite coatings for enhanced anticorrosion protection of copper, Inorg. Chem. Commun. 167 (2024).

[344] K. Zhang, Y. Feng, F. Wang, Z. Yang, J. Wang, Two dimensional hexagonal boron nitride (2D-hBN): synthesis, properties and applications, J. Mater. Chem. C. 5 (2017) 11992–12022.

[345] M. Rafiq, X. Hu, Z. Ye, A. Qayum, H. Xia, L. Hu, F. Lu, P.K. Chu, Recent advances in structural engineering of 2D hexagonal boron nitride electrocatalysts, Nano Energy. 91 (2022) 106661.

[346] C. Verma, S. Dubey, I. Barsoum, A. Alfantazi, E.E. Ebenso, M.A. Quraishi, Hexagonal boron nitride as a cutting-edge 2D material for additive application in anticorrosive coatings: Recent progress, challenges and opportunities, Mater. Today Commun. 35 (2023).

[347] J.H. Hwang, B.K. Shrestha, J.H. Kim, T.H. Seo, C.H. Park, M.J. Kim, Nanoscale layer of a minimized defect area of graphene and hexagonal boron nitride on copper for excellent anti-corrosion activity, Nanotechnology 33 (2021) 55601.

[348] Q. Xiang, R. Navik, H. Huijun Tan, Y. Zhao, Synthesis of oxidation-resistance copper nanowires-formate for high-performance transparent conductive electrodes, J. Alloys Compd. 914 (2022) 165265.

[349] X. Zeng, P. He, M. Hu, W. Zhao, H. Chen, L. Liu, J. Sun, J. Yang, Copper inks for printed electronics: a review, Nanoscale 14 (2022) 16003–16032.

[350] C. Yin, Q. Li, J. Zheng, Y. Ni, H. Wu, A.L. Kjøniksen, C. Liu, Y. Lei, Y. Zhang, Progress in regulating electronic structure strategies on Cu-based bimetallic catalysts for CO2 reduction reaction, Adv. Powder Mater. 1 (2022).

[351] Y. Jia, F. Li, K. Fan, L. Sun, Cu-based bimetallic electrocatalysts for CO2 reduction, Adv. Powder Mater. 1 (2022).

[352] Y. Yang, S. Louisia, S. Yu, J. Jin, I. Roh, C.R. Chen, M.V.F. Guzman, J. Feijóo, P. C. Chen, H. Wang, C.J. Pollock, X. Huang, Y.T. Shao, C. Wang, D.A. Muller, H. D. Abruña, P. Yang, Operando studies reveal active Cu nanograins for CO2 electroreduction, Nature 614 (2023) 262–269.

[353] L.Y. Chen, J.S. Yu, T. Fujita, M.W. Chen, Nanoporous copper with tunable nanoporosity for SERS applications, Adv. Funct. Mater. 19 (2009) 1221–1226.

[354] J. Chapman, L.L. Nor, R. Brown, E. Kitteringham, S. Russell, T. Sullivan, F. Regan, Antifouling performances of macro-to micro-to nano-copper materials for the inhibition of biofouling in its early stages, A J. Mater. Chem. B 1 (2013) 6194–6200.

[355] X. Ren, H. Wang, J. Chen, W. Xu, Q. He, H. Wang, F. Zhan, S. Chen, L. Chen, Emerging 2D Copper-Based Materials for Energy Storage and Conversion: A Review and Perspective, Small 19 (2023).

[356] J. Yang, J. Chen, Y. Zhou, K. Wu, Sensors and actuators B : chemical a nano-copper electrochemical sensor for sensitive detection of chemical oxygen demand, Sensors Actuators B Chem 153 (2011) 78–82.

[357] B.D. Harishchandra, M. Pappuswamy, A.P. Shama, G.A. Pragatheesh, V. A. Arumugam, T. Periyaswamy, R.G. Sundaram, Copper Nanoparticles: A Review on Synthesis, Characterization and Applications, Asian Pac, J. Cancer Biol. 5 (2020) 201–210.

[358] E.M. Mazzer, M.R. da Silva, P. Gargarella, Revisiting Cu-based shape memory alloys: Recent developments and new perspectives, J. Mater. Res. 37 (2022) 162–182.

[359] K. Otsuka, X. Ren, Recent developments in the research of shape memory alloys, Intermetallics 41 (1999) 511–528.

[360] K. Otsuka, C.M. Wayman, Shape Memory Materials, Cambridge University Press, Cambridge, 1998.

[361] S.K. Kolawole, W. Hai, S. Zhang, Z. Sun, M.A. Siddiqui, I. Ullah, W. Song, F. Witte, K. Yang, Preliminary study of microstructure, mechanical properties and corrosion resistance of antibacterial Ti-15Zr-xCu alloy for dental application, J. Mater Sci. Technol. 50 (2020) 31–43.

[362] S. Luo, K. Pei, Lithium Batt.: Recent Adv. & Emerg. Topics, 2024.

[363] A. Klassert, L. Tikana, Corros. Behaviour and Protection of Cu & Al Alloys in Seawater, in: EFC Series, 2007, pp. 47–61.

[364] C.A. Powell, H.T. Michels, Corrosion/2000, NACE International, Houston, Texas, 2000.